Report no. 93/CE/61 December 1996

Assessment of MCFC technology using Indian coal

Submitted to
Central Mine Planning and Design Institute, Ranchi

Chemical and Hydrogen Energy
Tata Energy Research Institute

Members of the project team

Ajay Mathur

Sushant Maharana (till March 1996)

Sanjay Bali

Ramkumar Perumal

Malini Balakrishnan

To ascertain the availability of this report and the terms of supply, please write to

Chemical and Hydrogen Energy
Tata Energy Research Institute
Darbari Seth Block
Habitat Place, Lodhi Road
New Delhi – 110 003 / India

Telephone (+91 11) 462 2246, 460 1550
Fax (+91 11) 462 1770, 463 2609
Cable TERINST, New Delhi – 110 003
e-mail mailbox@teri.ernet.in

Acknowledgments

The project team would, at the outset, like to thank the Central Mine Planning and Design Institute for entrusting the work of assessing the potential of molten carbonate fuel cell technology to use Indian coal to TERI. We are especially grateful for the vision and the initiatives of Mr R K Sachdev, then Advisor, Ministry of Coal, Government of India, that have promoted the introduction of clean coal technologies in this country. We are also thankful to Mr D K Jain and Mr N N Gautam of CMPDIL, for their interest in and continued support for this project.

The project team received help from various organizations during the collection of information on coal gasifiers, most valuable among these being the generous sharing of information by the Coal Research Group of Bharat Heavy Electricals Limited, Hyderabad. We deeply appreciate the help and hospitality provided by Mr K Basu, AGM during our two visits to BHEL R&D, as well as for the very useful discussions we had with him. Special thanks are due to Mr S Krishnamoorthi, Engineer, who showed us around BHEL's PEDU gasifier at their Maula Ali site. We also thank Mr N Krishnamurthy, AGM, BHEL-Tiruchirapalli for arranging a visit to their Combined Cycle Demonstration Plant (CCDP), as well as Mr T Manivannan, Dr S N Srivastava, Mr C Velayudham and others for useful discussions.

Finally, we would like to thank all those colleagues at TERI who had helped us at various stages during the project. In particular, we would like to thank our Purchase Section and the Computer Centre for meeting our requirements. The timely assistance provided by our administration in relocating our (heavy) furnace is also acknowledged. Special thanks are due to Mr R K Joshi, who did all the sketches amid a tight schedule. We appreciate the secretarial assistance provided by Ms Savitri Rawat and Ms Shruti Ghai and thank Mr Dhir Singh and Mr Bhagwat Singh for help with the laboratory activities.

Ajay Mathur
Malini Balakrishnan
Sanjay Bali
Ramkumar Perumal

Contents

List of Tables

List of Figures

Executive Summary

Power generation efficiencies of coal-based power plants in this country are only of the order of 30%. As the economic and environmental implications are becoming apparent, various agencies of the Government of India are attempting to find more efficient ways of using Indian coal, most of which is very high in ash content.

High temperature fuel cells (HTFCs), namely, the molten carbonate fuel cell (MCFC – operating temperature : 650°C) and the solid oxide fuel cell (SOFC, operating temperature around 1000°C) are being evaluated in several countries worldwide for large-scale, coal-based power generation at high overall efficiencies (60 – 70%). The major reasons are (1) fuel cells need hydrogen as the fuel, (2) HTFCs can, in addition, use carbon monoxide (CO) as a fuel – CO is not tolerated by low temperature fuel cells such as the phosphoric acid fuel cell (PAFC) and proton exchange membrane fuel cell (PEMFC), (3) hydrogen and CO are the major usable constituents of coal gas, and (4) the waste heat from HTFCs is available at temperatures high enough to raise steam for further power generation in a steam turbine bottoming cycle.

The Central Mine Planning and Design Institute (CMPDI), Ranchi appointed TERI to carry out an assessment of this technology for power generation using Indian coal. Some of the major findings of this study are :

1. MCFC technology appears to be nearing commercialization within the next five years or so.
2. As the development of SOFC to a commercial stage is expected to lag behind that of MCFC, it is felt that development of the MCFC technology is important, so as to integrate this with a coal gasification system.
3. Tests carried out in a laboratory-scale MCFC using simulated coal gas show that coal gas can be used in MCFC as a fuel; the drop in performance of the fuel cell when using simulated coal gas, as compared to that of pure hydrogen (the reference) is nominal.
4. Development of coal gasification technology indigenously appears necessary, as technologies developed elsewhere have been mainly designed to utilize superior quality coal.
5. Considerable amount of expertise exists in this country in the area of coal gasification, with the BHEL's Coal Research Group playing a major role in developing the pressurised fluidized bed gasifier (PFBG) technology, which seems to be better suited to use the high ash Indian coal.
6. The logical next step, therefore, is to develop an MCFC multi-cell stack in the kilowatt-level, and to couple it with a coal gasifier. This group has already initiated activities towards this objective.

CHAPTER 1

INTRODUCTION

As in several other developing countries, the demand for energy supply is growing fast in India. Though the per capita energy consumption would still be less than one-fifth of that of industrialized countries, the implications of this growth in energy consumption for a country with a population of nearly 900 million are rather severe, when viewed in terms of the prevailing economic, technological, social and environmental conditions. Among the various forms of end use of energy, electricity constitutes a significant portion of the total energy consumption. A fairly conservative estimate for the growth in the demand for electricity, assuming a 6% growth rate of GDP, still suggests a doubling of the demand within the next ten years. With limited oil and gas reserves, India is heavily dependent on conventional, coal-based power generation, though attempts are being made to increase the share of non-conventional means of power generation. At the present cost levels, these latter methods, such as wind and solar photovoltaic generation are yet to become viable on a large scale even in the more developed countries. Dependence on fossil fuels, therefore seems inevitable for the foreseeable future, despite growing environmental concerns. One direct consequence is the growth in the emissions level of various pollutants.

The impact of CO_2 on climate change is a matter of global concern, and one that calls for immediate steps to arrest the growth in the emission level globally, while longer-term strategies to reduce the emissions level can take effect. The emission of CO and hydrocarbons are primarily due to inefficient, i.e. incomplete combustion. The emission of nitrogen oxides (NO_x) is usually from combustion at high temperatures, and sulfur oxides (SO_x) are emitted from combustion of sulfur containing fuels. Desulfurization of fuels prior to use or removal of sulfur oxides after combustion seem to be the only alternatives for SO_x mitigation. The emission of CO, hydrocarbons and NO_x can, to some extent, be reduced by improved design of combustion processes, catalytic conversion, etc. As the magnitude of CO_2 emission is directly dependent on the amount of fossil fuel consumed, reduced consumption of fossil fuel, though not so practical at present, is the ultimate solution. In the present situation, a more practical, and immediately adaptable approach seems to be to employ more efficient and 'cleaner' means of power generation, while simultaneously increasing the efficiency at the end use level, such as by integrating heat and power requirements, reducing transmission and distribution (T&D) losses by dispersed power generation, etc. Thus, though the dependence on fossil fuels, such as coal and natural gas will continue well into the next century, one would be getting more out of each tonne of coal or gas, while hopefully limiting the emission of CO_2 at the present level. Fuel cells are a prime candidate for fulfilling these requirements, viz., power generation at higher efficiency and reduced emissions.

1.1 Coal for power generation

The demand for electricity is growing rapidly in India, with current generation capacity at around 84,000 MW. A shortfall of peak electric power of 11,247 MW (or 15.3% of the demand), and an energy deficit of around 9,757 million kWh (2.3%) are estimated for the year 1997. Of the total installed capacity, around 50,000 MW (or about 60%) of the installed capacity is from coal-based power plants. The average generation efficiency of these power plants is of the order of 30%. This clearly implies that electricity generation in India involves use of enormous quantities of coal and is accompanied by huge amounts of emissions. Even though most Indian coals are very high in ash content (of the order of 40%), this trend is expected to continue well into the next century as India still has vast reserves of coal and import of hydrocarbons for power generation involves an enormous outflow of foreign exchange. Any improvement in the power generation efficiency, therefore, would automatically lead to reduced consumption of coal per kWh of electricity produced, as well as a reduction in the emissions.

The Government of India and the various research organizations have been evaluating, and implementing to a limited extent, some technological options for more efficient power generation using coal. Among these, the use of coal gasification, particularly in the combined cycle mode appears to be a promising option. While gasification of coal substantially improves the combustion efficiency, the coal gas still has to be burnt in a gas turbine, whose efficiency is governed by the Carnot cycle limitations. A concept that is receiving increased attention worldwide is the use of coal gas in a high temperature fuel cell system, such as the molten carbonate fuel cell (MCFC).

1.2 Fuel cells

A fuel cell is an electrochemical device, much like a battery, with an anode, a cathode and an electrolyte which is typically in an immobilized form, contained in a thin, porous matrix. Fuel (hydrogen or hydrocarbons) is fed to the anode, and the oxidant (air) to the cathode. The higher efficiency of a fuel cell arises from the electrochemical route to oxidation, involving electron transfer between the electrodes, with an electromotive force (e.m.f.) dependent upon the free energy change of the oxidation reaction. Water, carbon dioxide (if pure hydrogen is not used), and the exothermic heat of oxidation are the main products from this reaction. Because the electrochemical process is not limited by the Carnot cycle efficiency levels that are encountered in the conventional turbine-route, typical electrical conversion efficiencies in

fuel cells are in the 40–55% range, with high temperature fuel cells like molten carbonate fuel cells (MCFC) and solid oxide fuel cell (SOFC) operating near the higher end.

1.3 Why high temperature fuel cells are attractive

The various types of fuel cells that are being developed towards commercialization are shown in Table 1. Among these, the high temperature fuel cells (HTFCs), particularly MCFC is of interest to us. While all fuel cells need hydrogen as the fuel, HTFCs can, in addition, use carbon monoxide (CO) as a fuel. CO is a poison for the electrocatalysts in low temperature fuel cells, whereas, HTFCs can produce electricity and heat from CO, either through direct oxidation of CO (which is very slow), or through the water-gas-shift reaction, which produces hydrogen. It is this feature that makes HTFCs a very attractive option, that can be coupled to a coal gasifier, as CO is a major component of coal gas. In addition, the exothermic heat of oxidation can be gainfully recovered for further use. For example, in an MCFC system which operates at 650°C, the waste heat can be used in a downstream bottoming cycle, thus leading to an overall efficiency in the range of 70%.

1.4 Environmental benefits

Apart from the high overall efficiencies, the other major driving force behind worldwide research and development activities in coal-based HTFCs are the environmental implications of using coal in a cleaner manner. Higher efficiencies directly lead to reduced emissions per unit of power produced. Because the electrochemical oxidation takes place at temperatures much lower than in conventional combustion, NO_x emissions are negligible. And since fuel has to be desulfurized prior to feeding into the fuel cell stack, sulfur oxide emissions are also practically eliminated.

1.5 Objectives of the project

With the above background, the Central Mine Planning and Design Institute (CMPDI) appointed TERI to carry out a study to assess and evaluate the use of Indian coal in MCFC for power generation. The objectives of this study were as follows:

a) Identification of state-of-the-art of MCFC technology;
b) Evaluation and identification of coal gasifiers appropriate for use with Indian

coals and MCFCs;

c) Data bank on Indian coal gas and performance of gasifiers using Indian coals;

d) Setting up of integrated mathematical frameworks for gasifier-MCFC system and evaluation of material and energy requirements;

e) Data bank on MCFC performance with various Indian coal gas compositions;

f) Evaluation of system; material and energy balances, overall efficiency, gas clean-up requirements.

g) Identification of R&D needs towards the development of MCFC components and stack engineering.

Apart from collection and review of information on the status of MCFC technology and coal gasification, a major aspect of the study was to fabricate MCFC single cells for the purpose of testing its performance with simulated coal gas. The results of the study are given in the following chapters.

Table 1.1 Fuel cell applications

Fuel cell type						
	AFC	PEMFC	PAFC	MCFC	SOFC†	DMFC†
Operating Temperature	60°–80°C	65°–100°C	150°–200°C	650°C	1000°C	100°C (?)
Rated power level (projected)	10–100 kW	1–1000 kW	100–5000 kW	1000–100,000 kW	100–100,000kW	1–100kW
Market Segments (projected)						
Electric utility			●	●		
Remote generation	●		●	●		
Dispersed	●	●	●	●	●	
On-site cogeneration		●	●	●	●	
Automotive	●	●	●			● (?)
Buses, trucks	●	●	●		●	
Railway	●	●				
Space	●	●	●			
Submersibles		●				
Portable, commercial	●					
Portable, military		●			●	
Portable, Mining	●	●				

AFC - alkaline fuel cell; PEMFC - polymer electrolyte fuel cell; PAFC - phosphoric acid fuel cell; MCFC - molten carbonate fuel cell; SOFC - solid oxide fuel cell; DMFC - direct methanol fuel cell

CHAPTER 2

MCFC - STATE-OF-THE-ART

The concept of the molten carbonate fuel cell evolved in the late 1940's and the first cells were demonstrated by Boers and Ketlaar in the 1950's. In spite of its several advantages viz. the possibility of using natural gas without external reforming, generation of high grade waste heat and the relative ease of cell-area scale-up without excessive mechanical stress, the first pressurized MCFC stacks were operated only in the early 1980's. This lack of rapid progress was primarily due to the constraints imposed by high temperature (600-700°C) operation, the extreme corrosivity of the molten salt and the rather complicated electrode processes of the MCFC. This has stimulated active research in the areas of :

- Materials development viz. electrode material selection and fabrication, as well as the development of the electrolyte matrix, and
- Stack engineering which includes design of separator plates, gas distribution system and effective utilization of the waste heat.

The following sections review the current status of MCFC technology, with particular emphasis on the developments in the last five years.

2.1 Materials Development

2.1.1 Cathode

2.1.1.1 Electrode fabrication

Molten carbonate is an extremely corrosive medium and the stability of specific metals and alloys depends upon the gas atmosphere. Under oxidizing conditions such as air or O_2-CO_2 mixtures, only a few noble metals are stable and thus semi-conducting oxides are the only practical cathode materials. Lithiated nickel oxide is the generally employed cathode material. The cathode can be fabricated by any one of the following methods (Antolini, 1992) :

- The fuel cell can be assembled with a porous metallic nickel cathode in the form of a plaque, which becomes oxidized and lithiated *in-situ* soon after the cell is brought to the operating temperature. The lithium is supplied by the electrolyte and the oxygen by the gas phase.
- The nickel plaque can be oxidized, or oxidized and lithiated, before it is assembled into a cell.
- The cathode can be fabricated directly from nickel oxide powder and incorporated into the cell as a porous sintered ceramic. The oxide powder can be lithiated either before the structure is formed, during sintering, or the cathode can be lithiated in the cell.

- Metallic nickel powder can be sintered in air so that oxidation and sintering occur in one process.

Of these, the preferred technique is the *in-situ* oxidation of pure porous nickel followed by lithiation. The method, however, has some drawbacks. The *in-situ* oxidation of the nickel plaque causes the original nickel microstructure to break into clusters of much smaller particles with no interconnections, leading to a cathode that is structurally weak and fragile. Secondly, the process involves a 30-40% volume expansion which would pose severe problems in a stack of several cells. Also, there is an early consumption and compositional variation of the electrolyte since the lithium for doping during the oxidation process is supplied by the Li_2CO_3-K_2CO_3 electrolyte. This probably results in a less than optimal lithium concentration in the final product. Finally, the sintered structure that is oxidized is expensive. To overcome these limitations, a modified *in-situ* cathode formation procedure using unsintered nickel plaques containing Li_2CO_3 and an organic binder has been proposed (Antolini, 1992). The cathode displayed good in-cell performance of 190mA/cm^2 with a limited current density decay of 18% after 3500h of operation. More details on the preparation and characteristics of porous lithium doped NiO are discussed in a recent comprehensive review by Antolini (1993).

2.1.1.2 Operational Constraints

The NiO cathode ranges in thickness from 0.4-0.8mm and exhibits a bimodal pore size distribution with a median pore diameter of 5-7μm. However, it is slightly soluble in the melt with estimated losses up to 35% of the cathode over 10,000 hours of operation (Pierce, 1982). The dissolution of the NiO at a time averaged value of 2-20 μg/cm^{2}h (Plomp et al., 1992; Ota et al., 1992a) results in decreasing cathode thickness which is accompanied by increasing polarization losses. The NiO dissolves into molten alkali metal carbonate M_2CO_3 (where M denotes Li, Na, K or Rb) in one of the following modes (Xie et al., 1990b) :

Acidic dissolution (at high CO_2 pressures) :

$$NiO + CO_2 \rightarrow NiCO_3$$

Basic dissolution (at low CO_2 pressures):

$$NiO + M_2CO_3 \rightarrow M_2NiO_2 + CO_2$$

Experimental observations also indicate the presence of a higher nickel oxide (Ni_2O_3) under cell operating conditions (Xie et al., 1990a). This species is formed at -400mV and is an unstable, surface-defect structure of NiO. Thus the degradation of the MCFC cathode is

possibly an indirect dissolution i.e. the NiO is first oxidized into Ni_2O_3 and then decomposed into NiO again while some of the newly formed NiO dissolves into the electrolyte. The phenomenon of NiO cathode dissolution has been the subject of much theoretical analysis as well (Kunz and Pandolfo, 1992).

In addition to the above mechanism, loss of cathode material can occur due to the conversion of NiO to metallic Ni according to one of the following reactions :

$$NiO + CO_2 \rightarrow Ni^{+2} + CO_3^{-2}$$

$$Ni^{+2} + H_2 + CO_3^{-2} \rightarrow Ni + H_2O + CO_2$$

The precipitation of nickel leads to an increase of ohmic losses in the electrolyte matrix and eventually to cell short-circuiting.

The loss of NiO from the cathode is a primary concern since it can substantially curtail the operating lifetime of the MCFC. The major parameters controlling this phenomenon are :

- Basicity of the electrolyte
- Partial pressure of CO_2 in the oxidant
- Matrix thickness and porosity
- Operating temperature
- Cathode potential and
- Period of operation.

Experimental data indicates that the minimum solubility of NiO in the Li-K carbonate eutectic at 650°C is 1 molar ppm at a partial pressure of 0.01 atm. CO_2 (Ota et al., 1990). The NiO dissolution can be suppressed to a great degree by increasing the basicity of the electrolyte within the cathode. This strategy is discussed further in sec. 2.1.3.1. The matrix thickness is also critical since cell short-circuiting via NiO dissolution is a strong function of this parameter. Thus, it has been observed that a 0.5 mm thick matrix under 0.3 atm. CO_2 shorted after 1000-2000 h while a 1 mm matrix did not visibly short even after 10,000 h (Urushibata and Murahashi, 1992). With a reduced CO_2 partial pressure of 0.1 atm., the same structure had an estimated lifetime of 20,000 h. Increasing the temperature increases the CO_2 partial pressure and consequently the NiO solubility. Under normal MCFC operation conditions, NiO dissolution is usually acidic and increases linearly with CO_2 partial pressure.

2.1.1.3 Recent Developments

Several measures can be taken to reduce the effects of cathode degradation viz. application of Li/Na instead of Li/K carbonate mixture, use of electrolyte additives and reduction of the CO_2 partial pressure. In addition, this has motivated the search for alternate cost effective cathode materials. These new materials must satisfy the following criteria :

- Chemical and morphological stability in both the electrolyte and the oxidant environment
- Ease of control of the pore size distribution and porosity
- Low solubility combined with resistance to precipitation under anodic conditions
- High electrocatalytic activity for oxygen reduction
- High electrical conductivity ($\sigma > 1$ S/cm) and
- Good wettability in the oxidant environment.

Most of the studies carried out on alternative materials have focused on electrical conductivity. Thus, very limited information is available on the physico-chemical and electrochemical characteristics related to the fabrication procedure. Because of this, results obtained by different groups are often contradictory. More than 50 ceramic compounds viz. ferrites, cobaltites, magnatites, doped metallic oxides, illmenites and spinels have been investigated as possible cathode materials.

One of the most promising new materials appears to be lithium doped metal oxides (Fe, Co, Mn). Pierce et al. (1987) considered several such replacements for the NiO cathode in the 1-10 atm. pressure range. The best stability was displayed by Mg doped $LiFeO_2$ and Mn doped Li_2MnO_3 . The conductivity levels were, however, unsatisfactory. Better results were obtained by Franke and Winnick (1989) using a perovskite type compound, $La_{0.8}Sr_{0.2}CoO_3$ displaying high porosity (65%), good conductivity (~1 ohm^{-1} cm^{-1}) and reasonable mechanical strength. Exchange current densities calculated on a superficial area basis were up to 20% higher compared to NiO. Masao et al. (1988) explored a Ni-Cr-Al-Y alloy coated SUS 316 and found this cathode material to be reasonably stable. Other choices have been nickel ferrite which is highly stable in molten carbonates (Ota et al., 1988a; 1990), unsintered nickel containing Li_2CO_3 and an organic binder (Antolini, 1992), doped cerium oxide (De Gurie et al., 1990) and yttrium iron garnet (YAG) (Khandar, 1992).

To date, the best performance, relative to that of lithium doped NiO has been obtained with lithium cobaltite. This material is being investigated by several researchers (Brown et al., 1992; Plomp et al., 1992; Bergman et al., 1992; Koch et al., 1992 and Lee et al., 1993) and the results indicate that the dissolution rate is about an order of magnitude lower than that for NiO (Veldhuis, 1992). For the same level of performance, the estimated lifetime of a $LiCoO_2$ cathode at 7 bar is 90,000h compared to 3500h for NiO (Plomp et al., 1992). More recently,

Giorgi et al. (1994) tested cathodes prepared by cold pressing and sintering Li_xCoO_2 (0.8 <x <1.1) powders with various pore-formers. The material was less soluble in the melt as compared to NiO and displayed porosities in the range of 10-65%, a bimodal pore-size distribution with a mean pore diameter of 0.15-8μm and surface areas between 2-12 m^2/g. Experiments indicated that the electrical conductivity was a strong function of the Li content. Also, the kinetics of the process was positively influenced by the partial pressure of O_2 but CO_2 has a smaller negative effect on mass transport than in the case of the NiO cathodes.

2.1.2 Anode

The MCFC anode, which consists of a porous substrate loaded with an electrocatalyst, mediates the electrochemical oxidation of the fuel (H_2 and CO). The porous geometry provides intimate 3-phase contact between the fuel gas, the electrolyte and the electrode. In addition, the anode serves as a reservoir for the electrolyte and provides structural support for the electrolyte tile and the cathode. A built-in layer of fine porosity at the anode-tile interface acts as a bubble pressure barrier (BPB) that prevents gas crossover in the cell.

The anode operates under a reducing atmosphere, at a potential typically 700-1000mV more negative than that of the cathode. Several transition metals are suitable as electrocatalysts for hydrogen oxidation under these conditions. Nickel, cobalt and copper are currently used as anode materials, often in the form of powdered alloys and composites with oxides. Typically, a porous nickel anode is 0.8-1mm thick and has a mean pore size of 3-7μm with a porosity of 50-70%. Usually, the nickel plaques are manufactured from gravity sintered nickel powder by a carbonyl process. Attempts have been made to prepare the anode by several other techniques as well. The noncarbonyl process based on the precipitation of nickel hydroxide from nickel salt was pioneered by ERC (Dharia et al., 1979). The method yields an uniform, inexpensive anode of large surface area; also, it permits the coprecipitation of other components.

There are two major limitations associated with the MCFC anode viz.

- Sintering, which results in increased particle size and hence decreased electrode porosity. This adversely affects the anode electrolyte holding capacity and thus the long term cell performance.
- Creep or micro-dimensional deformation under mechanical load which leads to decreased porosity, increased contact resistance and increased risk of anode to cathode gas leaks.

Studies on anode materials and methods of fabrication indicate that the deleterious effects of sintering can be overcome by (Iacovangelo, 1986b) :

- Alloying the nickel with chromium
- Dispersion of refractory oxides (Al_2O_3) and
- Electroless plating of nickel and/or copper onto refractory oxides of Al_2O_3, $SrTiO_3$ and $LiAlO_2$.

The use of Ni-Cr alloy (2-10% Cr) is very effective in arresting anode sintering. The chromium component segregates in a lithium chromite ($LiCrO_2$) phase which prevents the solid state diffusion leading to coarsening. Iacovangelo (1986b) has examined the influence of additive content (Cr and Al_2O_3), additive particle size and fabrication temperature on the degree of sintering. Since the MCFC operation is controlled by electrolyte-gas contact, any substantial change in the pore size distribution is unacceptable. It was observed for 6000h of sintering that addition of small amounts of Cr (3%) reduces the loss of anode porosity to less than 4% compared to a decrease of over 80% for the pure nickel plaque. However, this is at the expense of lower initial porosity and median pore size.This can be resolved using 2μm particle size Cr powder and raising the fabrication temperature to 1000°C (Ghosh, 1991).

Dispersion of refractory oxides like Al_2O_3 within the nickel plaque is another strategy to improve resistance to sintering. Preparation of nickel plaques with the addition of 1-5 vol.% of Al_2O_3 showed excellent resistance to sintering while maintaining 70% porosity with no perceptible change in the pore size distribution over the test duration. Similar studies have been conducted for copper as well (Ness et al., 1985).

Though Ni shows good performance as an anode material, it is expensive. Thus, more economic alternatives are being sought by different investigators. Energy Research Corporation has tested Ni -Co (10%) plaques prepared by coprecipitation and found improved sintering resistance (Dharia et al., 1979). In another study, Institute of Gas Technology (IGT) has advocated the use of copper anodes (Camara and Ong, 1983). Copper has several advantages over nickel viz. higher electrical and thermal conductivity, a better matched coefficient of thermal expansion with other cell materials and a lower cost combined with easier availability. From the technical viewpoint, it possesses a superior resistance to anodic oxidation thus permitting operation at higher current densities. Donald (1988) has patented the preparation of anodes from porous metals like Co, Ni and/or Al as well as $Li_2CrO_4$and $Li_2Cr_2O_7$. Attempts have also been made with tungsten (Ito et al., 1988), lanthanons (Furukawa et al., 1988) and tungsten/tungsten carbide (Yabe et al., 1988) along with porous Ni anodes. Xie et al. (1991) have suggested the surface modification of the nickel anode by electrodeposition of either tungsten or tungsten carbide from an LiCl-KCl eutectic melt containing K_2WO_4. Both the anode performance as well as its mechanical properties are considerably enhanced by this treatment. The possibility of employing electroless Ni and Cu

plated ceramics e.g. Al_2O_3, $SrTiO_3$ and $LiAlO_2$ as anode material has also been explored (Iacovangelo, 1986a). These materials offer a high degree of flexibility in achieving the desired electrode pore size, excellent stability and creep resistance and reliable cell performance. More recent studies (Takashima et al., 1992; Urushibata and Murahashi, 1992, Chun et al., 1994) advocate the use of Ni-Al alloy as a very effective creep resistant anode material with better performance as compared to Ni-$LiAlO_2$.

Apart from improving the anode material characteristics, the electrode configuration has also been a subject of interest. The porous gas-diffusion electrodes of the MCFC are in the shape of plates which are separated by a ceramic matrix containing electrolyte. To obtain high current densities, a gas diffusion electrode must be thin, porous and possess a large surface area to provide enough active reaction sites. In this aspect, three dimensional electrodes such as fluidized bed and fixed bed electrodes offer the advantages of large electrode area per unit volume and a high rate of mass transfer. In addition, from the fabrication viewpoint, their ease of construction and replacement make them attractive. Matsuno et al. (1995) performed studies using fixed bed anode of nickel coated alumina particles and fluidized bed anode of nickel particles. They observed that polarization was predominantly diffusion controlled in the fixed bed unlike in the fluidized bed which possessed a high mass transfer rate owing to forced convection. However, the increase in gas velocity decreased the electronic conduction of working-electrode particles in the fluidized bed electrode, resulting in an increase in polarization. Also, they advised the use of a larger current collector to reduce the contact resistance between itself and the electrode particles in the fixed-bed electrode.

2.1.3 Electrolyte Matrix

The electrolyte matrix or tile in a MCFC consists of a paste of alkali metal carbonate as the electrolyte along with ceramic particles as the inert support which are stable in the presence of CO_2 and water. The primary functions of the electrolyte matrix are :

- To provide the ionic path (CO_3^{-2}) with a minimum resistance between the anode and cathode
- To separate the fuel and oxidant gases with a minimum of crossover through voids or by diffusion of the dissolved gases and
- To effect electrolyte distribution within the cell as well as at the cell edge seal ("wet seal").

The electrolyte matrix varies in thickness between 0.5mm to 1.8mm depending upon whether it is hot-pressed or tape cast and possesses a support surface area of 0.1-12 m^2/g. The electrolyte currently used by most developers is a mixture of lithium carbonate (Li_2CO_3),

potassium carbonate (K_2CO_3) and possibly smaller amounts of sodium carbonate (Na_2CO_3) and carbonates of alkaline earth metals, with a melting point of approx. 500°C. A commonly used composition is 62 mole% Li_2CO_3 and 38 mole% K_2CO_3., though a ternary eutectic mixture of composition Li : K : Na :: 60 : 10: 30 is better since the addition of sodium results in higher electrical conductivity, lower coefficient of expansion and lower vapor pressure. The electrolyte support is usually finely divided submicron $LiAlO_2$ particles. Efforts are still being made to further improve the electrolyte composition and the corresponding operating temperature. Both these parameters have a strong effect upon the ohmic resistance of the cell and on factors determining cell polarization like solubility of various gases and the kinetics of oxygen reduction. In addition, the NiO cathode solubility which limits cell lifetime, is affected by the electrolyte composition.

The following sections review the three major aspects of an electrolyte matrix viz the composition, the fabrication technology and the electrolyte management strategies.

2.1.3.1 Matrix Composition

The MCFC electrolyte composition has a strong influence upon both the short term as well as the long term performance of the fuel cell. The short term performance i.e cell voltage at a given current density depends upon the ohmic resistance of the cell and the polarization of the electrodes. These, in turn, are determined by factors directly linked to the chemistry and the physical properties of the electrolyte. For instance, Li rich electrolytes have higher ionic conductivities and hence lower ohmic polarization, due to the relatively high ionic conductivity of Li_2CO_3 compared to Na_2CO_3 and K_2CO_3 . On the other hand, the solubility and diffusivity of reactant gases such as H_2, O_2, CO_2 and H_2O is lower in the Li_2CO_3 rich melts. Based on these observations, the region in the Li-Na-K ternary phase diagram having 60-70 mol% Li_2CO_3 and 0-20% Na_2CO_3 appears to be a promising composition to start with.

A more systematic approach to electrolyte optimization, however, also incorporate the effects of electrode kinetics and transport processes as well as the long term changes in structure and composition of the electrodes and electrolyte. The carbonate electrolyte undergoes dissociation and hydrolysis according to the following reactions :

$$CO_3^{-2} \rightarrow CO_2 + O^{-2}$$

$$CO_3^{-2} + H_2O \rightarrow CO_2 + 2OH^-$$

The cationic composition of the electrolyte melt strongly influences these processes which, in turn, contribute significantly to the cathode polarization and the overall cell performance.

The long-term performance issues governing electrolyte composition are endurance related parameters like cathode dissolution, hardware corrosion, $LiAlO_2$ matrix stability and electrolyte volatility. Several attempts have been made to optimize the carbonate composition in an effort to provide a milder environment for the NiO cathode. From a comprehensive study of several Li-K and Li-Na electrolyte compositions, Yuh and Piguead(1989) concluded that Li-Na in eutectic or off-eutectic composition is a viable alternative to Li-K eutectic since it yields superior performance with respect to NiO cathode dissolution, electrolyte creepage and volatilization, as well as conductivity and cathode polarization. In an independent study (Ota et al., 1992b), it was confirmed that NiO solubility is lower in the Li-Na than in the Li-K carbonate melt. Ota et al. (1988b) pointed out that the solubility of nickel oxide in $(Li_{0.52}Na_{0.48})_2CO_3$ was lower than in $(Li_{0.62}K_{0.38})_2CO_3$. In another work, Doyen et al. (1987) suggested that the presence of MgO, CaO and SrO in $(Li_{0.62}K_{0.38})_2CO_3$ reduced the solubility of NiO. The addition of alkaline earth carbonates to $(Li_{0.62}K_{0.38})_2CO_3$ also display similar behavior (Shores et al., 1989; Tanimoto et al., 1991). Laboratory scale cell testing corroborate these results and it has been observed that addition of even 1 mol% of an alkaline earth cation to $(Li_{0.62}K_{0.38})_2CO_3$ leads to almost 50% reduction in the amount of dissolved nickel (Kishida, 1990). More recent evaluations of cell performance indicate that 0-15 mol% of alkaline carbonate additives in the $(Li_{0.62}K_{0.38})_2CO_3$ / $(Li_{0.52}Na_{0.48})_2CO_3$ electrolyte material is optimum (Tanimoto et al., 1992a).

Apart from the electrolyte composition, the matrix support material is also crucial. Besides being chemically inert, the support must possess a stable morphological form and should display minimum propensity for particle growth. The size, shape and distribution of the support particles control the carbonate retention, mechanical properties and effective conductivity of the electrolyte tile. Magnesium oxide (MgO) was used by earlier investigators but now it has been largely replaced by $LiAlO_2$ since the latter is thermodynamically the most likely aluminate present in the particle mixture of all metal carbonates. But $LiAlO_2$ particles are unstable under the cell operating conditions and so attempts have been made to curtail the crystal growth by using more than one oxide. $SrTiO_3$ along with $LiAlO_2$, and gallium and iron additives were used by General Electric (1982) as it was observed that $SrTiO_3$ has a 100 times lower growth rate as compared to $LiAlO_2$. Yet another strategy to improve the mechanical stability of the electrolyte matrix in thermal cycling, for instance, involves the use of inert fibers or particles as "crack arresters" (Kakihara et al., 1991).

To achieve better performance through better electrolyte distribution, the support material should have a narrow pore size distribution with smaller mean pore size. The physical characteristics of the support material are largely determined by the method of preparation. Initially attempts were made to prepare β-$LiAlO_2$ but since it was thermodynamically

unstable, attention was diverted to the synthesis of γ-$LiAlO_2$. Kinoshita (1979) synthesized the γ form from a reactant mixture containing LiOH and $Al(OH)_3$; Piguead (1990) prepared the support by using a mixture of γ-Al_2O_3 and Li_2CO_3 . The search is also on for pure but cheaper alumina for producing γ-$LiAlO_2$ with a reasonable surface area.

2.1.3.2 Fabrication Technology

Though the basic electrolyte material has remained relatively unchanged except for some minor modifications, there have been significant developments in the matrix fabrication technology. Prior to the 80's, the electrolyte matrix was prepared by hot-pressing the components under pressure. The matrix thus obtained was relatively thick (1-2mm), had a high porosity (> 5%) and high ohmic resistance. Because of a lack of uniform microstructure, it was frequently prone to crack formation under stress. In addition, it was exceedingly difficult to produce tiles larger than 1m^2 with adequate dimensional and structural uniformity.

To overcome these process limitations, alternative techniques like tape-casting and electrophoretic deposition were explored in the early 1980s. Although the thin electrophoretic matrices developed by GE and ERC were less prone to cracking on thermal recycling, they were not completely devoid of this problem. Besides, it was not easy to incorporate large crack-arresting particles into them in a controlled manner. Thus, tape-casting has proved to be successful not only for preparing the electrolyte matrix, but the electrodes as well. This greatly helps in streamlining the fuel cell production process since the cell can be assembled from similarly produced tapes. Also, tape-casting is easily amenable to scale-up, besides being capable of producing very thin electrolyte structures (0.25-0.5 mm). A thin structure reduces ohmic resistance and hence improves short term performance. However, there is an increased risk of enhanced gas crossover by liquid phase diffusion as well as via opening of pores due to long term electrolyte loss. In addition, the thinner the cell, the greater is the likelihood of shorting due to cathode dissolution and nickel reprecipitation. As such, electrolyte matrices have a minimum thickness of at least 0.4mm in practice.

Another important development in MCFC matrix technology is the introduction of the bubble pressure barrier(BPB). It consists of a dense, fine pore-size metal (nickel) or ceramic ($LiAlO_2$) structure located between the anode and the electrolyte matrix . Due to its very fine pore size, it always remains filled with electrolyte thus preventing gas crossover from one electrode to another. At the same time, it reinforces the electrolyte matrix. To design an effective BPB requires careful matching of its pore-size distribution with those of the anode and the electrolyte matrix. For instance, if the median pore size of the anode is 4-8 µm and that of the electrolyte is 0.5-0.8 µm, then an appropriate size of the BPB pores would be 1-1.5 µm. Such a combination prevents drainage of electrolyte from the BPB part of the matrix and

would hence prevent gas crossover due to long term electrolyte loss or in the event of a crack in the matrix.

2.1.3.3 Electrolyte Management

Apart from the electrolyte composition, another critical aspect of MCFC performance relates to the electrolyte management which denotes the control over the quantity and distribution of molten carbonate electrolyte among different cell components. When a completely filled tile is first contacted with empty porous electrodes, part of the electrolyte wicks out of the tile into the electrodes until a dynamic equilibrium of capillary forces is established between the cathode, the anode and the electrolyte. Thus, to ensure that only a very small amount of the electrolyte wicks out of the electrolyte tile and the amount of electrolyte in each electrode is sufficient to yield the desired gas-liquid interface, it is essential to :

(a) make a proper choice of the pore-size distributions of the electrodes as well as the electrolyte matrix and

(b) partly prefill the porous electrodes.

During the lifetime of an MCFC, various processes occur which cause loss of a small part of the electrolyte and the subsequent redistribution of the remaining electrolyte. This can have a deleterious effect upon the long term cell performance particularly if the loss exceeds 20-25% of the initial content (Freni et al., 1994). The electrolyte is lost, slowly but continuously, due to:

- Consumption by corrosion processes
- Flow into or out of the cell via the wet seal due to capillary forces("creepage"), galvanic corrosion cells and migration i.e. ionic motion due to an electric field. In cell stacks, the electrolyte flows may be powerfully reinforced and the loss could become quite significant.
- Volatilization of the electrolyte (usually Li_2CO_3 and/or K_2CO_3) by either direct (carbonate) or indirect (hydroxide) evaporation

These processes take place either singly or in combination at varying rates during the lifetime of a MCFC. For instance, during the initial 500-2000 h of operation, the electrolyte loss is relatively steep and is predominantly due to hardware corrosion. Thereafter, the loss occurs at a constant rate due to the volatilization of the carbonate. Normally, in a properly operating cell, the migration losses and electrolyte creepage are not appreciable and become limiting only if corrosion protection of the wet seal breaks down. However, stacks with external manifolding are an exception where migration could be a major factor of electrolyte loss.

Since electrolyte loss is the prime cause of performance decay in a MCFC stack, this issue has been well investigated. The corrosion related loss for cells operating at 150 mA/cm^2 for a

variety of fuel gas compositions has been documented by Urushibata and Murahashi (1992). The carbonate electrolyte, by creepage and by evaporation and condensation, forms a film which covers the walls of the flow channels. Though stainless steel 316 and 310 are quite corrosion resistant, they are not adequately protected in the wet-seal area and in the area in contact with the anode. It was observed that the Li_2CO_3 loss due to corrosion is proportional to the square root of time and continues to increase well beyond 10,000h of operation. On the contrary, the K_2CO_3 loss is independent of time and occurs at a constant rate of 2 μmol/cm². In addition, the electrolyte is also lost by vaporization at a rate which is determined by the fuel gas composition and pressure. The greater the gas pressure, the lower is the vaporization rate.

Redistribution of the electrolyte component, even in the absence of electrolyte loss, is another continuously occurring phenomenon. This is due to the changes in the pore size distributions of the electrodes, which are quite pronounced in the early stages of cell operation but continue to occur throughout the life of the cell. Morphological changes in the porous nickel anode are primarily caused by sintering or creeping. In the case of the nickel oxide cathode, slow dissolution as well as progressive compression changes the electrode structure.

Thus, the persistent slow loss of electrolyte coupled with the changes in the electrode pore size distribution require electrolyte management. The frequently adopted strategy is to provide an initial excess charge of electrolyte to partially fill the porous electrodes. A more reliable method involves feeding of the carbonate charge accommodated adjacent to the electrode in a gas channel, or loaded in one of the electrodes or added as one or more separate carbonate tapes (fig. 2.1). The last cited technique is widely accepted for internally manifolded stacks. Intermittent additions are also possible, provided the cell and stack design permit it. In addition, the compression of the cell stack must be adjusted continually so as to compensate for the effect of structural changes.

In this context, it is also essential to consider the importance of electrolyte loading i.e ratio of the electrolyte volume to the void volume of the matrix. A low electrolyte fill level in the electrodes means the active area required for adequate electrochemical reaction can't be achieved. If *local* electrolyte filling falls below a certain crucial level, the larger pores, being unable to hold their electrolyte, become connected and gas crossover may occur between the electrodes. This is usually accompanied by intense local heating ("hot spots") and rapid performance deterioration. On the other hand, an extremely high electrolyte fill level disturbs the rapid diffusion of reactant gases to the reaction site. There are, however, contradictions in optimal electrolyte-loading ratio recommended by various investigators. For instance, Tanimoto et al. (1992b) report best cell performance at a loading ratio of 90% while Saito et al. (1991) suggest much higher values between 160-290% for stable cell performance.

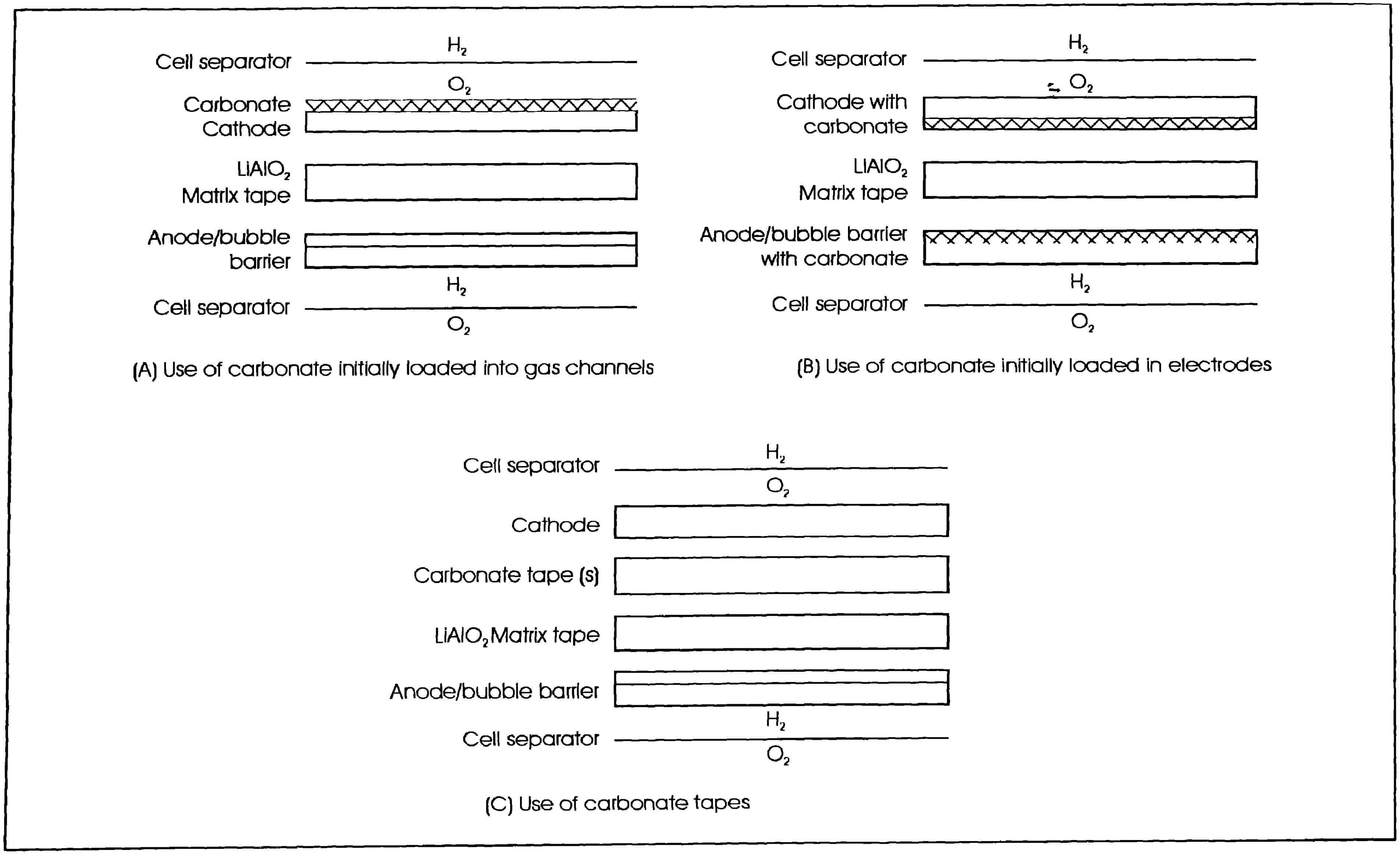


Figure 2.1. Carbonate loading methods

2.2 Stack Engineering

The MCFC stack consists of repeating units of a single cell viz. the electrolyte matrix, the electrodes and the corresponding current collectors (fig. 2.2). The separator plate (or bipolar plate) replaces the single-cell housing and provides cell-to-cell contact. Thus, the stack is essentially a collection of thin cells, each less than 0.5 cm thick with an area greater than 1 m^2/cell in large capacity stacks. Thus, the stack strongly retains the two-dimensional characteristics of the individual MCFC cell. Scale-up of stacks by increasing cell area is, however, limited by increasing non-uniformity of current and temperature distribution in the flow direction. The main technical problems in the design and operation of large scale stacks are :

- Ensuring uniform in-plane distribution of the gas flow, both within each cell as well as among the cells in the stack. This is essential to achieve stable performance without the formation of hot spots and excessive wetness of the fuel gas.
- Optimal design of the separator plate. This would include the issues like the choice of the material, structure and fabrication method.
- Ensuring adequate sealing between cells to prevent problems like escape of gas and the migration of electrolyte
- Efficient thermal management of the heat generated within the cell. Care must be taken to effectively convect away the heat so as to prevent excessive temperature rise in the cell hardware.

Each of these concerns will be addressed in detail in the following sections.

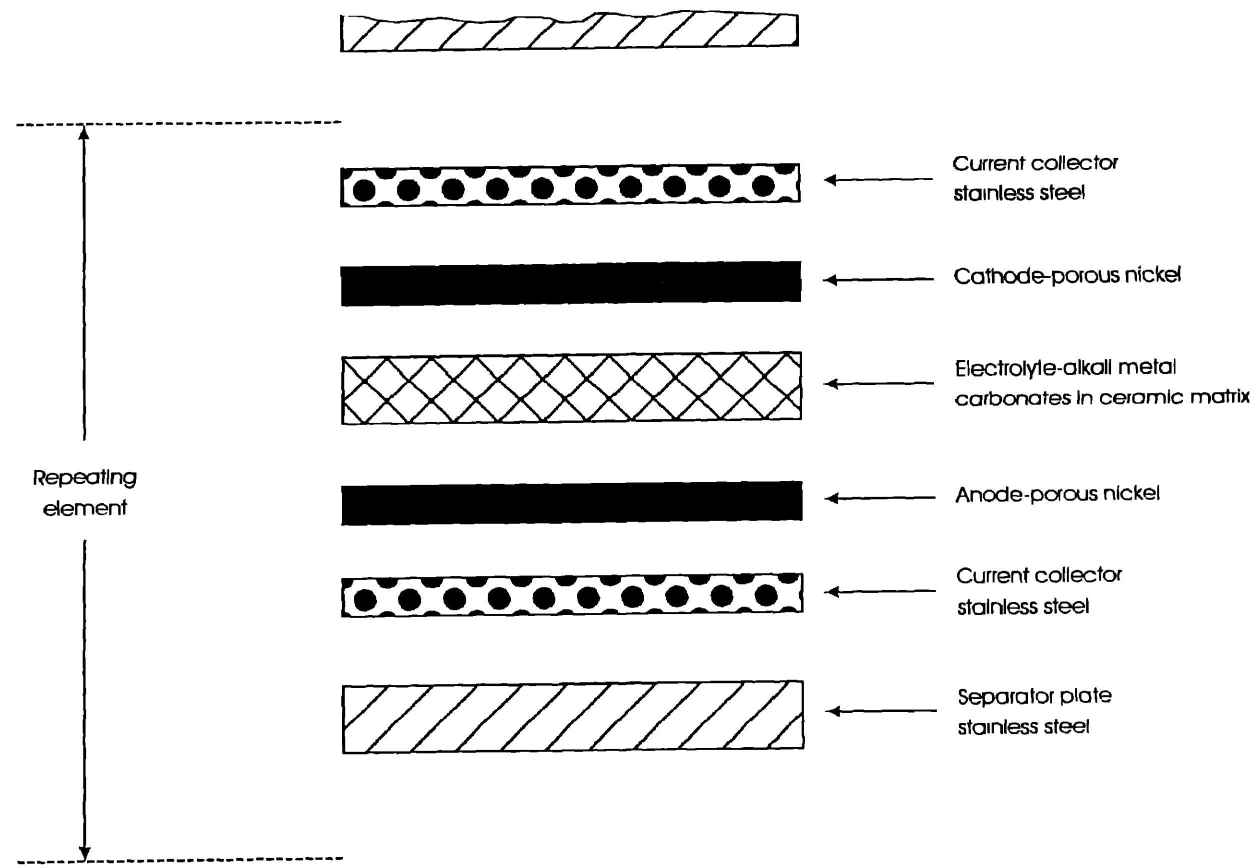


Figure 2.1 Repeating elements in MCFC stack.

Figure 2.2. Repeating elements in an MCFC stack

TERI REPORT NO. 93CE61(1996)

2.2.1 Stack Configuration

The gas flow distribution is primarily controlled by the manifolding design. Both internal and external manifolds are in use to feed the reactant gases in parallel to all the cells in the stack' (fig. 2.3). The salient features of each of these configurations is summarized in Table 2.1.

2.2.1.1 External Manifolding

In external manifolding, the reactant gas mixtures are supplied each from a central source to a large fuel and oxidant inlet and the exhaust gas removed via large outlet manifolds, each on the opposite side of the corresponding inlet. The flow configuration is necessarily crossflow. This design was pioneered by UTC and has been extensively used by several developers like ERC, Mitsubishi Electric and Sanyo. The main advantage of external manifolding is its simplicity, leading to symmetrical cell design with low projected manufacturing costs. Furthermore, large manifold cross-sectional areas are possible with a minimum amount of material. This maintains a low pressure drop and facilitates uniform gas distribution. However, this design suffers from gas leakage and electrolyte displacement by migration ("ion-pumping"); both are associated with the manifold gasket which seals the edges of the stack.

Each external manifold, covering one side of the stack, has an insulating gasket to form a seal with the edges of the stack and thus prevent shorting of cells via the metal manifold. In addition, the material should be elastic but stiff. The commonly used gasket material is a fibrous ceramic material like zirconia felt. Many variations have been tested by different manufacturers e.g. Fuji has used solid zirconia gaskets in small stacks constructed to high mechanical precision while Toshiba has employed zirconia felt filled with borate glasses. A favored scheme is the one pioneered by UTC employing zirconia felt filled with ceramics and a small amount of electrolyte ($< 1\%$ volume). This electrolyte column, though thin and fairly resistant, conducts current ("bipolar leak current" or "shunt current") from the positive to the negative end-plate of the stack. This migration manifests itself at start-up itself since there is a severe flooding of the electrolyte near the negative end of the stack and a corresponding electrolyte draining from the cell near the positive end. Experiments indicate that a leakage current of 1 mA is equivalent to an electrolyte displacement of the order of 1 mg/h. Thus, performance decline can be drastic with electrolyte losses as high as 60% within the first 1000h of operation (UTC report, 1985).

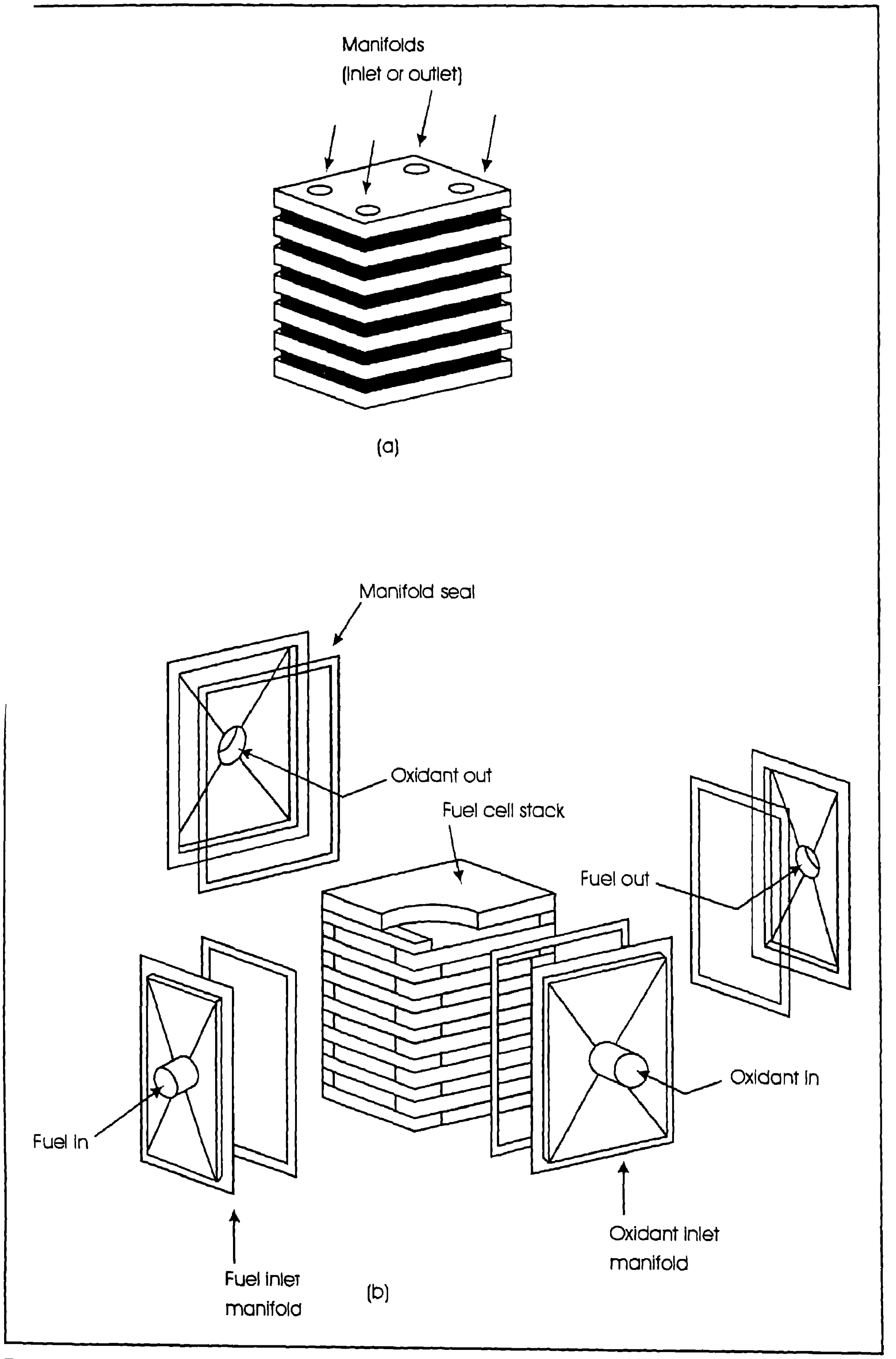


Figure 2.3. Manifolding concepts in MCFC

TABLE 2.1 : Comparison of external and internal manifolding (Sato, 1990)

	External	**Internal**
Flow configuration	Crossflow	Any flow
Flow distribution	Straightforward	Requires separator plate design
Stack compression	Triaxial	Uniaxial
Critical component in fabrication	Electrolyte matrix	Separator plate
Critical step in stack assembly	Manifold installation	
Electrolyte migration	Depends on gasket porosity	Practically zero
Gas leakage out of cell	Depends on accuracy of component dimensions	No major problem

The migration phenomena has been investigated, both theoretically as well as experimentally, by several workers (Kunz, 1987; Kunz and Bergoli, 1990; Kuroe at al., 1992). The mechanism appears to be electroosmotic in nature. The key parameter controlling migration is the difference in the mobility of the cations with respect to the common anion CO_3^{-2}. In the Li-K eutectic carbonate, the mobility of the K^+ ion is larger than that of the Li^+ ion. Thus, migration results in an enrichment in the K^+ ions and depletion in the Li^+ ions near the negative end-plate and *vice-versa* near the positive end-plate. Because the partial volumes of Li and K carbonate are different, this change in composition causes a displacement (net velocity) of the carbonate melt from the positive end to the negative end. The cells communicating with the low pressure positive end will lose electrolyte, while those communicating with the high pressure negative end will be flooded; both cases would lead to poor performance. Yet another mechanism which comes into play is the electrolysis of the carbonate at the end plates, since the stack voltage far exceeds that necessary for carbonate decomposition. This, in turn, results in net loss of electrolyte.

Attempts have been made to counter the migration effect by built-in electrolyte reservoirs (a: mentioned in sec. 2.1.3.3) but these are difficult to control once the large scale stack has started operating. One solution would be to employ a completely dense dielectric such as α-alumina as a manifold gasket but this is impractical from the structural viewpoint.

During the initial operation of the stack, the porous cell components shrink appreciably and the trend continues, albeit at a slower rate, under the compressive force exerted on the stack. Since the manifold and the relatively stiff gasket prevent the cells from accommodating this shrinkage, gas leakages start to occur. The ohmic resistance may also increase, due to loss of contact between the cell components. Though the gas leakages can be minimized by increasing the flexibility of the manifold gasket by using more fluid ceramic paste, it would increase the electrolyte displacement via the gasket.

The above discussion points to an urgent need to minimize migration. There are two strategies which can be adopted :

- Minimize bipolar leak currents by minimizing the electric field in the leakage path. This can be accomplished, for instance, by superimposing an electric field of the opposite sign over the entire height of the manifold gasket.
- Apply an electrolyte composition such that the main cations have equal mobility. In Li-K carbonate, this isomobility composition is rather high in Li. This is attractive from the viewpoint of ohmic resistance but not from that of the polarization because of decreasing gas solubility and inferior kinetics. A compromise can be obtained by working with various combinations of Li-Na or Li-Na-K carbonate melts. This aspect has been discussed earlier in Sec. 2.1.3.1.

Of these, the first option (which has been adopted from bipolar battery technology) has been observed to be quite effective in controlling migration.

2.2.1.2 Internal Manifolding

In internal manifolding, there is a duct inside the stack itself, penetrating the separator plates. This duct is formed by profiles in the stacked separator plates when the holes penetrating them are properly aligned. The separator plates are designed with profiles, corrugations or inserts, which besides forming the walls of the internal manifold, control the flow distribution over each plate. This design has been adopted by developers like MCPower, IHI, Hitachi and ECN.

The flow distribution in internal manifolding is governed by the separator plate between cells. Each plate is shaped to have four plenums (source-sink areas) and is supplied with a fuel gas from above and the oxidant gas from below. This configuration naturally leads to a parallel gas flow which could either be coflow or counterflow. However, crossflow is also an option. In the coflow mode, one side serves as the inlet for both the fuel and the oxidant while the opposite side is the outlet for both the gases. In the case of counterflow, the plenums on one side of the plate function as the fuel inlet/ oxidant outlet while the complementary set on the other side are the fuel outlet and oxidant inlet. Fig. 2.4 depicts various types of flow

configurations currently in use. Of all the available options, parallel flow especially coflow, is quite attractive since it provides the most uniform temperature distribution.

Another primary design issue in internal manifolding is the system of gas seal in the manifold area. One option is to utilize the penetrated electrolyte approach where the electrolyte matrix forms the wet seal as it surrounds the gas ducts in the manifold area. In this method, the entire periphery of the cell may be wet sealed. The other possibility is to use separate gaskets such as dry ring type gaskets for sealing. This is the non-penetrated electrolyte approach and the electrolyte matrix extends only over the active cell area i.e. the electrodes in this instance.

Internal manifolding was first developed by IGT to overcome the problems associated with external manifolding. This configuration offers considerable flexibility with respect to gas flow which can either be parallel (coflow/counterflow) or crossflow. Enlargement of stack capacity is much easier as compared to external manifolding where the manifolds become heavier with size. Also, the mechanics of stack construction and operation are relatively easier in this case since only uniaxial compression is required in contrast to externally manifolded stacks which require balanced compression along all three axes. The design does have limitations since the complexity and the higher fabrication cost of the separator plate should be accounted for.

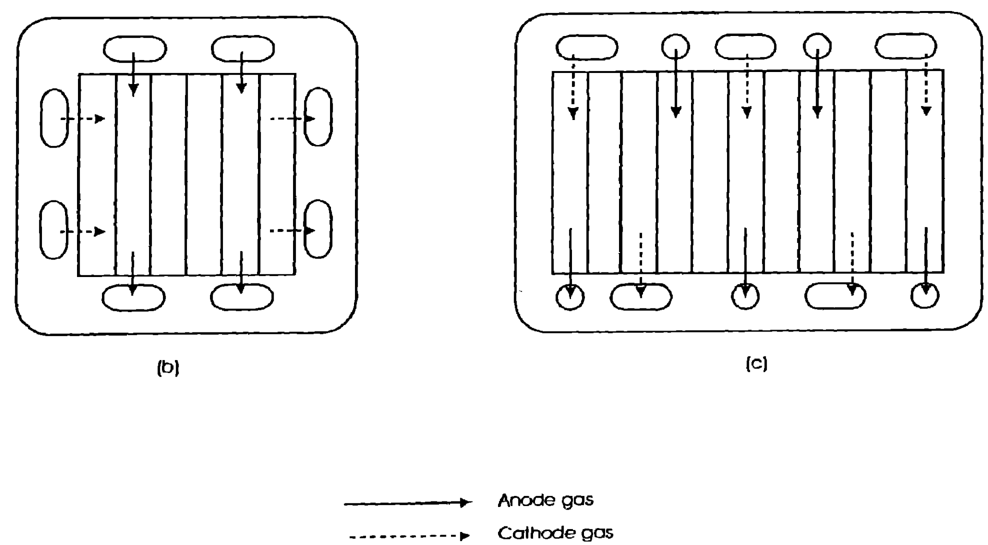


Figure 2.4. Flow configuration in internally manifolded stacks

2.2.2 *Separator plate*

2.2.2.1 Material

A key issue in the separator fabrication is the choice of the separator material. The separator plate contacts the fuel gas channel on one side and the oxidant on the other. Thus, it is imperative that the separator material be stable in both an oxidizing as well as a reducing environment. The challenge lies in identifying cost-effective material(s) /combination of materials which are not only inherently resistant but are also amenable to fabrication. In practice, commercially available Fe and Ni based alloys are generally employed. The potential separator material is conventionally tested by subjecting it to dual atmosphere test i.e. oxidant on one side and fuel gas on the other, specifically under high risk exposure conditions like high fuel concentration and low oxidant. Although the conditions are more severe on the anode side than on the oxidant side, especially near the fuel gas exit, the high hydrogen partial pressure near the fuel gas entrance can cause significant dissolution and diffusion of hydrogen in the plate. This may lead to carburization of the steel; it is also possible that hydrogen diffusion through the bipolar plate may prevent passivation on the oxidant side. The likelihood of this occurance depends upon both the gasflow configuration as well as the material itself.

It is a common but expensive practice to clad the anode side of the separator plate with Ni or Cu, especially near the fuel gas exit. This effectively prevents the carburization. Systematic screening of separator materials by several investigators indicates that stainless steel 310S, Avesta 600 (Fe-28Cr-4Ni-2 Mo) and Inconel 601 possess the best overall corrosion resistance (Machielse et al., 1992; Vesely, 1990 and Miyazaki et al., 1988). However, even these materials can corrode significantly near the wet seal areas, especially around the fuel gas outlets on the anode side. This can usually be contained by either by using Al rich or Cr rich alloys separator fabrication or by employing a coating of aluminum oxide. The latter can be performed by pack cementation or hot-dip coating in molten aluminium, especially for single cells. But both these techniques require high temperature and hence tend to deform the separator plate. Thus, other methods such as plasma spraying, physical vapor deposition, cermet coating, electroplating and spray painting have been explored for aluminizing the seal areas.

2.2.2.2 Design & Fabrication

The design of the separator plate is a primary concern since the cost of separator fabrication determines the overall stack cost to a large extent (George and Mayfield, 1990). In general, the design is much simpler in the case of external manifolding since the gas flow structure is straight throughout and a simple channel structure is sufficient. This can be accomplished by

using a corrugated separator plate or a flat plate with either ribbed electrodes or a separate ribbed insert (current collector) which gives good access to the electrode. Alternatively, a permeable insert with large void structure can be employed. In contrast, the internally manifolded separator has a much more complicated structure (fig. 2.4). One of the simpler designs is the type A separator which is applied in the IMHEX concept and is analogous to a flat plate heat exchanger. In this case, a one-piece separator plate functions simultaneously as a current collector and a flow guide. Though this is obviously advantageous for mass production, for large separators (> 1 m^2) the pressing process itself becomes a limitation. To avoid this constraint, one can either employ smaller separator plates joined together or stacks connected in series in gas flow. Yet another alternative is to use large scale plates with corrugated or shaped metal inserts to generate the flow field. Examples of this concept are the IHI separator and the FLEXSEP design by ECN. The choice between the corrugated plate or a pressed type flow guiding structure has important implications for separator corrosion. Though corrugated sheets possess a much simpler structure, they are more prone to corrosion, possibly because of differences in oxidant concentration (differential aeration) or due to residual stresses. Pressed separator plates are better in this regard; however they must still possess adequate mechanical strength and compliance.

There are two basic choices in separator types viz.

- The hard-rail concept in which the intercell separation is fixed by the height of the stiff rails or inserts and
- The soft-rail concept in which the inserts or masks, at the edge of the separator plate are folded back upon themselves.

The soft-rail concept is the more favored one since the separator is designed to accommodate the changes in the thickness of the electrolyte-electrode package during start-up as well as during the course of operation. In terms of manufacturing, it consumes less material as compared to the hard-rail design but finally requires more fabrication steps in terms of welding, annealing and pressing operations. This technique helps to maintain contact resistance as low as possible with the matrix filled at all times. However, in externally manifolded stacks, a certain level of rigidity is required since cell to cell distances are fixed. Too much sagging in the stack in this instance can result in leaky gas seals leading to gas crossover both to and from the ambient atmosphere as well as between the fuel and oxidant channels. Fixed dimensions in the hard-rail separator design demand stringent control over

(a) the amount of electrolyte in each cell (to prevent long term rise in ohmic resistance) and

(b) thermal expansion of cells (to prevent discrepancies in lateral expansion, which cannot be accommodated by stiff manifolds and gaskets, thus causing intercell gas leakage.)

Thus, the design and fabrication of externally manifolded stacks relies upon accurate thermal and mechanical stack models.

2.2.3 *Thermal Management*

2.2.3.1. Temperature Distribution

The structure and operating characteristics of an individual cell have a strong influence upon the ohmic resistance and polarization. This, in turn, affects the cell and consequently the stack performance in terms of the output voltage and the current density. For a good performance even in a small bench scale (100-300 cm^2) cell, it is imperative to ensure intimate contact of the fuel gas and oxidant with the electrodes. This is because the local current density across the thin electrode-electrolyte-electrode package depends upon the thermodynamic driving force i.e. the equilibrium cell voltage and the local resistance (both ohmic and polarization). The equilibrium voltage varies from point to point in the cell due to the concentration gradient created by the increasing utilization of fuel gas and the oxidant as they each flow from the inlet to the exit. The actual cell voltage i.e. the equilibrium voltage minus the losses due to ohmic potential drop and polarization, however, is invariant with position. This is due to the fact that the cell housing (or the separator plate in the case of a stack), is a good ohmic conductor and therefore at an uniform potential. The following potential balance must be satisfied at any point in the cell plane :

$$V = E - iR_t - iZ_{anode} - iZ_{cathode}$$

where V = actual cell voltage
E = local equilibrium cell voltage
i = local current density
R_t = ohmic resistance and
Z = polarization resistance at either electrode.

This potential balance concept is fundamental to the development of cell performance models. The polarization Z is quantified either using porous electrode models or empirical correlations based on measurements with small laboratory cells at negligible utilization (Yuh and Selman, 1992). As mathematical models are useful to understand and predict the distribution of the current density and the temperature in single cells / cell stacks, several groups have emphasized this aspect (e.g. Selman, 1981; Kobayashi, 1989; Takashima, 1990; Fujimura et al., 1992; Watanabe et al., 1992). These models are particularly useful in stack-design and scale-up.

Since a low polarization resistance is crucial to enhanced fuel cell output, it is essential to minimize this parameter. The cell temperature plays a crucial role in this context. This is

mainly due to the large activation energy of electrode kinetics reactions as well as the temperature dependence of transport processes. Both work to decrease polarization resistance. The ohmic resistance, which is mainly due to the electrolyte, also decreases with temperature. Therefore, the net temperature effect is positive. This has discouraged attempts to operate MCFCs at temperatures lower than 650°C which would be desirable from the corrosion viewpoint. However, it should also be noted that local heat generation increases more than linearly with the current density since the irreversible (ohmic) heat generation is proportional to the square of the current density. Therefore, if heat is not conducted or convected away from high current density areas, the current density will be amplified leading to "hot spots".

In most single cells, especially in small bench scale cells, a uniform temperature is established due to the large thermal capacity and thermal conductivity of the metal housing. Thus, the operation of such cells can be considered isothermal. However, in fuel cell stacks, where cells typically have a surface area of 0.1-1 m^2 and the separator is a 0.5mm thick plate, maintaining uniform temperature can be rather tricky. Since there is a complex interaction between the current and temperature distributions in such stacks, it becomes necessary to analyze the distributions in detail. This is usually accomplished by applying two mass balances i.e. on the fuel and oxidant gas and four energy balances viz. on the electrode-electrolyte-electrode package, the fuel gas, the oxidant gas and the separator. Additional equations for the water gas shift reaction and methanation should also be taken into account, if applicable (Freni et al., 1992). It is only in the case of in-cell reforming of CH_4 (direct reforming) that there is a strong thermal effect of the gas phase reaction upon the solid temperature. This issue is subsequently dealt with in detail.

Experimental as well as theoretical analyses demonstrate that the temperature distribution is dominated by the cathode gas stream and the current distribution by the concentration of hydrogen in the anode gas stream. Also, the oxidant on the cathode side acts as a cooling medium. Thus, a steep temperature gradient is found to occur in the direction of the cathode gas stream and a corresponding sharp current density gradient in the direction of the anode gas stream. In the case of a stack, significant deviations can occur from these single-cell patterns since the temperature distribution is strongly influenced by the thermal conductivity of the separator plates. A highly conductive separator will have a strong smoothing action on the temperature gradient. Also, the current collector, which conducts heat between the separator plate and the electrode-electrolyte-electrode bundle can also play a significant role with an effective cross-plane conductivity. Finally, the contact resistances between the cells as well as the massive end plates also affect the three-dimensional temperature distribution.

2.2.3.2 Reformer placement

A fuel cell system conventionally utilizes a carbonaceous fuel which is first steam-reformed to produce a mixture of H_2, H_2O, CO and CO_2 before being fed to the fuel cell. The reformers usually operate at 800-900°C achieving 95-99% conversion with a steam to carbon ratio of 2.5-3.0. The reforming reaction viz.

$$CH_4 + H_2O \rightleftharpoons CO + 3H_2$$

is strongly endothermic and thus it can provide a major sink for waste heat. There are three possible reformer configurations viz. external, direct internal and indirect internal (fig. 2.5). The implications of each of these designs is considered below.

In MCFC's with external reforming, reforming takes place outside the cell stack with the heat required for the reforming reaction being supplied by the burnout of the anode exhaust gas followed by heat exchange. The reformer is, however, located in close proximity to the cell so as to encourage effective heat transfer. This layout has the advantages of keeping stack design and manufacturing simple by isolating the reformer operation from the stack. This is particularly useful from the viewpoint of system upsets and maintenance. A primary concern in this design, however, is the need for continuous heat removal in order to maintain the stack operating temperature at 650°C. The cooling load is significant since the overall fuel cell reaction viz.

$$H_2 + 0.5\,O_2 \rightarrow H_2O$$

is strongly exothermic ($\Delta H_{650°C} = +225$ kJ/mol) which makes the net reaction of CH_4 oxidation

$$CH_4 + 2O_2 \rightarrow CO_2 + 2H_2O$$

much less exothermic. The heat effect can be expressed as a cell voltage (termed the thermoneutral voltage) E_{tn} which is defined as

$$E_{tn} = -\Delta H_r / nF$$

A cell operated at the thermoneutral voltage has a net heat effect of zero i.e. it operates adiabatically. For the reaction of CH_4 oxidation, the E_{tn} and the emf are practically equal whereas E_{tn} for hydrogen oxidation is substantially higher. This means that the exothermic heat effect of a fuel cell operating on CH_4 is much less than that of a H_2-fed fuel cell. The difference is equivalent to 244mV but the electric output of the two fuel cells differ by only 18mV.

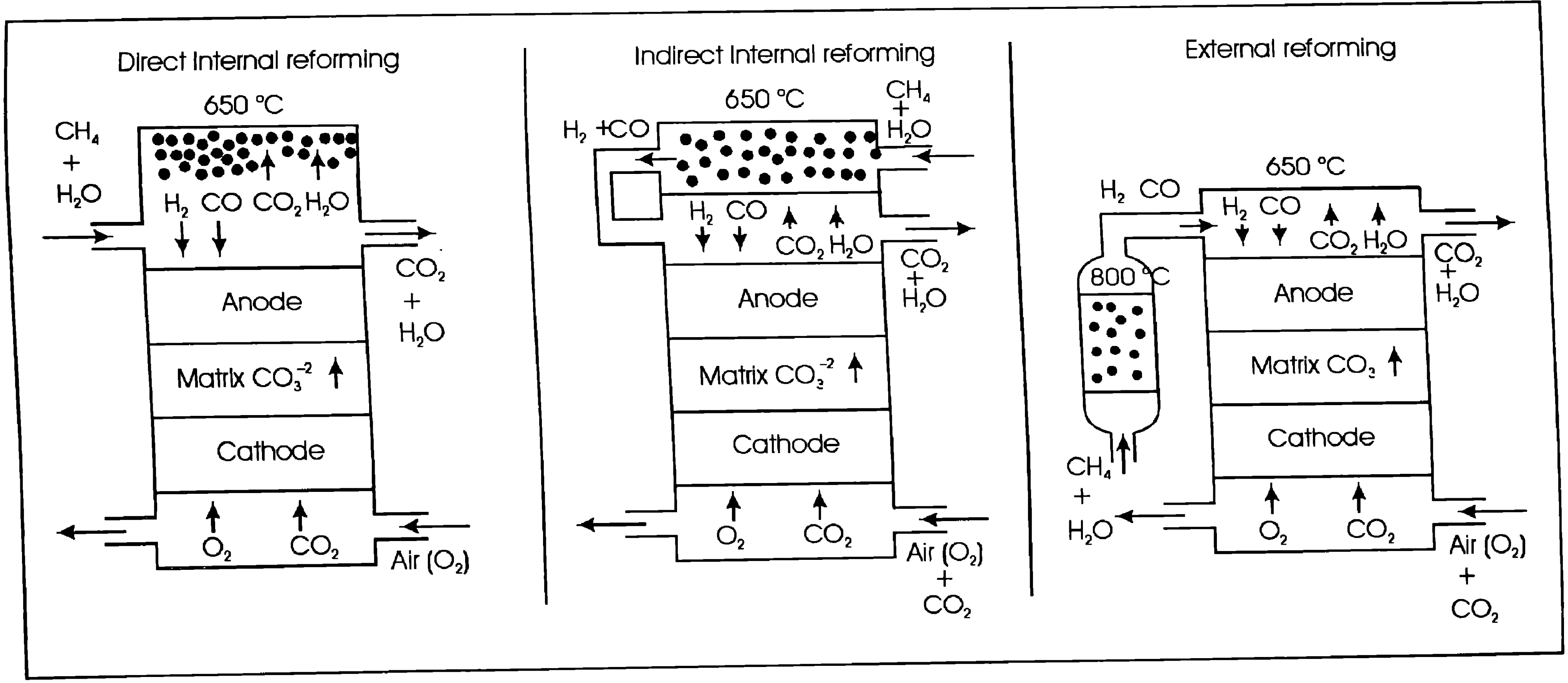


Figure 2.5. Reformer configurations

The concept of an internal reforming MCFC (IR-MCFC) involves the integration of the reforming reaction with the electrochemical oxidation within the fuel cell. This is feasible for high temperature fuel cells because using a catalyst (Ni supported on MgO or γ-$LiAlO_2$), the steam reforming reactions can be sustained by the continuous production of H_2O in the anodic oxidation of hydrogen. This can cutback on the cooling load by as much as 50% thus reducing the number and area of heat exchangers. This, in turn, translates to plant simplicity and reduced capital cost. There are two possible variations in this configuration viz. direct internal reforming (DIR) or indirect internal reforming (IIR). In DIR, the reaction takes place on catalyst loaded directly in the anode gas channel while in the IIR, reforming occurs in separate "reformer plates" adjacent to the fuel cell plates and in good contact with the anodes of the cells. The DIR concept has the advantages of the direct product and heat exchange. Because of the rapid exchange, the kinetics of the reforming reaction is fast and approaches the equilibrium limit. However, because of their close proximity to the anode, the catalyst particles are exposed to the electrolyte vapour which permeates the porous anode and condenses in the cooler parts of the channel. Electrolyte films which form by creepage can also cover the catalyst and its support. All this leads to a gradual loss of activity of the catalyst particles and thus has a deleterious effect upon the long-term performance of the IR-MCFC.

Extending the catalyst lifetime is a major challenge in the case of the IR-MCFC. The catalyst deactivation appears to occur because of (Tanaka et al., 1990) :

(a) Sintering of the catalyst particles which is accelerated by contact with electrolyte and

(b) Poisoning of the catalyst support by alkaline compounds and sulfur.

Experimental observations indicate that carbonate deposits exceeding 5% of the catalyst mass lead to the degradation of the latter (Camara and Ong, 1983). The carbonate resistance of the catalyst support also plays a role; MgO is considered the best choice though $LiAlO_2$ is also acceptable. But it is advisable to protect even these from direct exposure to the carbonate vapour (Cavallaro et al., 1992). This can be accomplished either by modification of the cell design to avoid condensation or to use an absorbent to scour the vapour before its contacts the catalyst. In addition, alternative support materials are also being explored since it would provide the flexibility to modify hardware surfaces (like the separator, current collector and flow guides) so as to render them catalytically active.

Apart from the electrolyte vapor, the presence of contaminants such as alkaline compounds and sulfur in the feed gas has a deleterious effect upon the catalyst activity. These chemicals attack the catalyst support and modify the catalyst-support interaction with consequent loss o activity. Sulphur and its compounds are particularly powerful poisons and the fuel gas must

contain less than 0.1ppm sulfur to ensure adequate performance (Appleby, 1988). This implies that fuels such as natural gas should undergo appropriate pretreatment to strip off any H_2S, mercaptans etc. before being fed into an IR-MCFC.

In the IIR concept, the fuel gas flows through a separate reformer chamber in thermal contact with the fuel cells before it contacts the electrolyte. The catalyst, is therefore not affected by the electrolyte vapour and catalyst poisoning does not occur. But since the reforming reaction is not driven by the local water partial pressure, the local temperature gradient supplying heat to the reformer chamber is not steep and so methane conversion is less. To overcome this limitation, either an cascaded IIR or a hybrid DIR-IIR combination can be employed. In the former, the residual CH_4 in the first stack is converted in the second stack so that the overall conversion approaches that in a DIR stack. The second option involves keeping the reforming load of the DIR intentionally low in order to stretch catalyst lifetime.

The reformer placement has a significant effect upon the choice of strategy for thermal management of a MCFC. Since the strongly endothermic reforming reaction leads to a sudden temperature drop at the anode inlet thus adversely affecting the cell performance, several ideas have been propounded to overcome this limitation. In a DIR-MCFC, the problem can be contained by :

- Cathode gas recycling and/or change in the gas flow configuration. A fuel return manifold, like the one employed in a 3 kW DIR stack by MELCO, can provide improved temperature distribution, conversion and current density.
- Modification of the method of catalyst loading onto the reformer plate. The idea is to suppress the conversion of the reforming reaction at the inlet of the plate by reducing the catalyst loading.

Compared to the DIR, the IIR stack presents greater difficulties with respect to the design for temperature uniformity (Okada et al., 1990). The IIR typically has an internal reformer plate for every five or six cells; this plate includes the catalyst. A specially designed manifold is used to feed fuel (with a high steam/carbon ratio) to the reformer plates and the hydrogen gas thus obtained is fed into the anodes of cells adjacent to the reformer plates. Since the endothermic effect of CH_4 conversion is locally large, it causes especially low temperatures in the anode inlet area. In the case of the DIR, this heat sink is present in every cell and can be corrected by fuel gas recycling or by a flow configuration as mentioned above. In the IIR, the heat sink leads to gradients in the stacking direction, which can only be controlled by three-dimensional stack design features. This has been demonstrated by MELCO for their 10kW and 30 kW IIR stacks.

2.2.3.3 Gas recycling

The need for thermal management coupled with the requirement to ensure smooth temperature distributions within the system has resulted in the recycling of gas streams in large scale MCFC stacks. A typical MCFC efficiency is 60% which implies that 40% of the chemical energy of the fuel is converted to heat. This heat must be efficiently dissipated for the smooth performance of the stack. In practice, anode or cathode gas recycling under pressurized conditions is the adopted cooling strategy. Also, recycling of the anode exhaust gas to the cathode inlet is necessary to close the CO_2 balance of the MCFC, at least to an acceptable extent. Izaki et al. (1992) systematically carried out a series of such pressurized recycling operations on a 18 cell 6 kW IHI stack with an active electrode area of 0.3120 m^2. In addition to the CO_2, both the anode as well as the cathode gases were recycled. They observed a logarithmic increase in the cell voltage with increase in gas pressure. Also, the methane formation rate was very slow and an increase in the H_2O partial pressure in the fuel gas decreased the methanation rate.

Anode gas recycling is one method to cool the stack. The recycling ratio is defined as the feedback flow rate to the inlet of the stack divided by the stack outlet flow rate. Apart from stack cooling, the anode gas recycle is often planned to prevent carbon deposition via the Boudouard reaction viz.

$$2CO \rightarrow C + CO_2$$

which is normally irreversible at 650°C. At constant fuel utilization, the anode outlet gas composition is nearly constant regardless of the recycling ratio, but the inlet hydrogen concentration decreases as the recycling ratio increases. Though recycling reduces the average voltage, the variation in individual cell voltages decreases. This is probably because the higher flow rate causes a more stable and uniform distribution of the flow. Also, it is possible to improve the fuel utilization by recycling under pressure. For instance, using reformed coal gas, Ogoshi et al. (1991) operated at 70% anode gas recirculation and 90% overall fuel utilization to obtain an average cell voltage of 0.738V at 150 mA/cm^2. This was equivalent to an efficiency of 53%.

When the stack is cooled by recycling the cathode gas, the recycling ratio must be changed with changing fuel utilization to keep the stack temperature constant. Experiments performec on a 6kW IHI stack indicate that as the fuel utilization increases, the cathode gas recycling ratio increases (Ogoshi et al., 1991). The average voltage, which was 0.81V when the cathoc gas was 70% air-30% CO_2 at a fuel utilization of 70%, decreased to 0.75V in the combined operation. If the oxygen utilization is kept constant, increased fuel utilization caused a slightly higher O_2 concentration in the cathode gas, but the cell voltage decreased because tl CO_2 concentration decreased.

Yet another option is CO_2 gas recirculation. This has been investigated by Ogoshi et al. (1991) by burning the H_2 and CO of the anode exhaust gas with excess air in a catalytic burner and supplying the combustion product to the cathode inlet as CO_2 source. This method is inexpensive but it dilutes the oxidant with nitrogen and hence lowers the cell performance. It is also possible to directly transfer CO_2 from anode exhaust to cathode inlet which leads to fuel utilizations close to 100% with corresponding gains in overall efficiency. In the mid-80's, several "active" devices were proposed which are essentially fuel cells operated in reverse to accomplish a transfer from one gas stream to another (Kang and Winnick, 1985). None of them, however, went beyond the conceptual stage. The search has now shifted to processes like pressure swing adsorption (PSA) and membrane separations for the selective recovery of CO_2. PSA, which has been evaluated both theoretically and experimentally in an IIR-MCFC test plant, displayed a higher overall system efficiency as compared to that for the combustion process (Sasaki et al., 1993). However, the requirement for compression in PSA makes this method energetically costly. Another possibility is to use temperature swing and thus make use of the fuel cell waste heat. For example, absorption cycles based on the use of carbonate formation from MgO, followed by thermal decomposition have been examined.

2.3 MCFC technology status

The MCFC, which as a concept is nearly 50 years old, has now reached the demonstration stage of precommercialization stacks. Several organizations around the world are active in the field of MCFC research and development. Table 2.2 summarizes some of the important large-scale installations in the recent past. This section presents the contributions as well as the research focus of the major players in this area.

2.3.1 U.S.A.

Though the United Technologies Corporation (UTC) and its subsidiary International Fuel Cells Corporation (IFC) were the pioneers in MCFC stack development in the U.S.A., the two leading players in this field at present are the Energy Research Corporation (ERC) and MC-Power Corporation. IFC has come up with stacks up to 1.932 m^2 with a concept termed "thin cell". A 25kW stack of this design is equivalent to 0.114 W/cm^2 at $150 mA/cm^2$. This research was part of IFC's programme, in collaboration with Toshiba, to develop an integrated stack unit which could be used as a self-contained power generator with a rating of 100kW to 1 MW.

TABLE 2.2 : MCFC Commercial Status (Hirschenhofer, 1993)

Organization	Installation	Year	Capa city (kW)	Remarks
ERC, U.S.A.	Pacific Gas & Electric, San Ramon CA		72	
ERC, U.S.A.	Santa Clara, CA	1996	2000	IR-MCFC; Versatile fuel (natural gas, biogas,coal gas or landfill gas)
ERC, U.S.A.	Destec Energy Systems, Plaquemine, LA	1993	20	Coal gas fuel
M-C Power, U.S.A.	Union Oil of California, Brea	1994	250	Partially integrated cogeneration unit
M-C Power, U.S.A.	Kaiser's Permanente Hospital, San Diego	1994	250	Integrated and packaged power plant
Hitachi, Japan	NEDO, Agaki Test Center		100	"Multiple Large Capacity" (ML(4 X 25 kW cell
Mitsubishi Electric Co., Japan	In-house		5	Direct internal reforming
Mitsubishi Electric Co., Japan	In-house	1992	100	Indirect internal reforming
Ansaldo, Italy	IBERDROLA	1995	100	
ECN, Netherlands		1994	250	Using slip stream from a coal gasifier IGCC project at Bugg
ECN, Netherlands		1995	250	Natural gas

Currently, the Department of Energy is playing an important role in the commercialization of MCFC technology, through its Fossil Energy program directed by the Morgantown Energy Technology Center (METC), Morgantown, West Virginia.

2.3.1.1 The Santa Clara Demonstration Project (SCDP)

The largest and perhaps the most quoted MCFC power plant is a 2MW system, called the Santa Clara Demonstration Project (SCDP). The City of Santa Clara is the host and the site for this demonstration project, which forms an important part of the commercialization programme of the Fuel Cell Commercialization Group (FCCG). The FCCG is a unique arrangement for the commercialization of MCFC technology, consisting of the Fuel Cell Engineering Corporation (FCE, which is a subsidiary of ERC, and the supplier of the power plant), and a large buyers' group consisting of several municipal and rural electric utilities in the USA and Canada.

2.3.1.2. Energy Research Corporation (ERC)

Energy Research Corporation, a Connecticut-based company, is by far the leading player in the MCFC area. ERC's MCFC programme is quite comprehensive, and has included technology development, field testing, and most importantly, forming a partnership with the users and the government for the commercialization of MCFC systems. ERC's MCFC stacks use the concept of internal reforming where natural gas is reformed in the cell stack itself over specially designed reforming catalysts. ERC calls this the direct fuel cell (DFC). Following the successful demonstration of the SCDP, ERC (through FCE) would be supplying 2–3 MW plants to the members of FCCG, for which purchase commitments have already been made. ERC has also set up the Fuel Cell Manufacturing Corporation (FCMC) for the purpose of eventual commercial manufacturing of MCFC power plants, as they are aiming for the market entry of a 2.8MW power plant by the turn of the century.

2.3.1.3. MC-Power Corporation

MC-Power, is commercializing MCFC technology developed by the Institute of Gas Technology (IGT). IGT has pioneered the internal manifolding concept (IMHEX stack design) and demonstrated its viability in terms of ease of assembly, gas sealing and electrolyte management. In 1992, a full-scale 0.929 m^2 19 cell stack was tested for long-term performance (12,000h). At present, two major demonstration projects are underway – a partially integrated cogeneration plant at the Union Oil of California (Unocal) Science and Technology Center in Brea, and an integrated and packaged power plant at Kaiser Permanente Hospital, in San Diego, both in California, and the size of these systems being 250-kW each.

2.3.2. Japan

In Japan, MCFC research is primarily sponsored by the New Energy Development Organization (NEDO) of the Ministry of International Trade and Industry (MITI). The focus of the R&D efforts is on both fuel cell stacks as well as on peripheral devices and system technology (balance of plant).

The Hitachi Corporation, which along with Mitsubishi Electric Company (MELCO) initiated MCFC development in Japan, is currently involved in the construction and testing of a large-scale 1 m^2 MCFC stack with the aim of demonstrating a 1 MW system in 1997. To facilitate the construction of a large cell without using meter-size tape-casting and sintering equipment, Hitachi evolved the "multiple large capacity" (MLC) cell. This type of a composite-separator stack consisting of four 0.36 m^2 subcells is easier to handle and assemble. Besides, it is characterized by low pressure drop and consequently, more uniform gas flow coupled with better temperature distribution. In the early 90's, two 25 kW stacks have been constructed and tested for over 4000h, both under atmospheric as well as pressurized conditions (6 atm.). In order to improve the long term performance of MCFC stacks, Hitachi is now laying emphasis on electrode structure and preparation procedures. The other pioneer in Japanese MCFC research i.e. MELCO, is currently focusing exclusively on the IR-MCFC, in collaboration with ERC. They constructed a 30kW, 5000cm^2 62 cell IIR-MCFC stack and performed a long-term endurance test in 1992-93. The IR-MCFC design has been adopted by Sanyo as well. In addition, MELCO has also pursued the concept of indirect internal reforming (IIR-MCFC) in cooperation with Kansai Electric Power Company (KEPCO). The goal of this project is the operation of a 192 cell 0.486 m^2 100 kW IIR stack for up to 5000h.

Another major company building and testing MCFC stacks is the Ishikawajima-Harima Heavy Industries Ltd. (IHI). They have opted for internally manifolded, pressurized stacks 100 kW prototype of 1 m^2 electrode area was demonstrated in 1993 with the aim of launch a 1 MW system in 1997. In addition, IHI has come up with a plate-type reformer for exter reforming in MCFC systems. IHIs' present efforts, after the successful demonstration of large-scale separator manufacture, is concentrated on tall stacking and thermal recycling. 50 cell stack of 0.3 m^2 area was operated for almost 2000 h generating 16.1 kW. The syst exhibited both uniform performance and high sealing efficiency and was subsequently sc up to a 50 cell 1.015 m^2 50 kW stack. An initial cell performance of 0.72 V at 150 mA/c was observed using simulated reformer gas at a fuel utilization of 0.70. More recently, Sa Electric company has built a 10kW MCFC stack (containing 40 cells of 0.24 m^2 area) utilizing petroleum light fraction as fuel. Similar 10kW externally reformed MCFC stack have also been tested by Toyo Engineering Corporation as well as Tonen Corporation.

In addition, the Technology Research Association for MCFC Power Generation System plans to conduct operational runs on a 1MW MCFC system to be completed in 1997.

2.3.3 Europe

Though MCFC's were invented in Europe, a sustained development programme has been underway only since the mid-80's. Apart from the Netherlands Energy Research Center (ECN), the others are still in the basic research and component development stage. ECN has been constructing and testing small-scale stacks of internally manifolded design since 1990. One of their major innovations is the FLEXSEP separator which has been successfully tested on a 10kW externally reformed stack in 1993. Two more 250 kW units were slated for construction and testing with industrial partners in 1995.

In Germany, Messerschmitt Boelkow Blohm GmbH (MBB) has tied up with ERC of the USA for a technology transfer program. The goal is to set up a MCFC production facility in the country by 1998. In Italy, Ansaldo, in collaboration with IFC, has already come up with a 300kW stack. In Denmark, the utility Elkraft has purchased a 7kW stack from ERC. Other countries to have initiated MCFC activities in the 90's include Spain and Sweden. A major impetus to MCFC activities in Europe has been provided by the Commission of the European Communities (CEC) which is funding some major MCFC development projects.

2.4 References

Anon., Molten Carbonate Fuel Cell System Verification and Scale-Up, Project 1273-1 final report, EPRI EM-4129, United Technologies Corp., CT 1985.

E.Antolini, J. Power Sources, 40 (3) (1992) 265.

E.Antolini, J. Eur. Ceramic Soc., 12 (2) (1993) 139.

A.J.Appleby, Ann. Rev. Energy, 267 (1988).

A.J.Appleby and F.R.Foulkes, Fuel Cell Handbook, Van Nostrand Reinhold, NY 1989.

B.Bergman, E.Fontes, C.Lagergren, G.Lindbergh, A.Lundblad, S.Schwartz, D.Simonsson and C.Sylwan, Proc. 1992 Fuel Cell Seminar, Tuscon AZ, USA, Nov. 29-Dec. 2, 1992, p73.

A.P.Brown, G.H.Kucera, M.F.Roche, D.D.Chu and E.Indachochea, Proc. 1992 Fuel Cell Seminar, Tuscon AZ, USA, Tuscon, AZ, USA, p125.

E.H.Camara and E.T.Ong, National Fuel Cell Seminar Abstracts, 1983, p46.

S.Cavallaro, S.Freni, R.Cannistraci, M.Aquino and N.Giordano, Intl. J. Hydrogen Energy, 17 (3) (1992) 181.

H.S.Chun, G.P.Park, J.H.Lim, K.Kim, J.K.Lee, K.H.Moon and J.H.Youn, J. Power Sources, 49 (1-3) (1994) 245.

D.Dharia, D.Kinnibrugh, P.Patel and A.Pigland, Electrode Materials, in Proc. DOE/EPRI Workshop on Molten Carbonate Fuel Cell, EPRI WS-78-135, EPRI, Palo Alto, CA 1979.

R.A.Donald, Manufacture of stabilized molten carbonate fuel cell porous anodes, U S Patent 4,752,500, Jan 21, 1988, Appl. 847,245 Apr. 2, 1986.

J.D.Doyon, T.Gilbert, G.Davies and L.Paetsch, J. Electrochem. Soc., 134 (1987) 3035.

M. Franke and J. Winnick, J. Appl. Electrochem., 19 (1989) 1.

S.Freni, S.Cavallaro, M.Aquino, D.Ravida and N.Giordano, Int. J. Hydrogen Energy, 19 (4 (1994) 337.

S.Freni, M.Aquino, N.Giodiano and S.Cavallaro, J. Power Sources, 39 (2) (1992) 203.

H.Fujimura, N.Kobayashi and K.Ohtsuka, JSME Intl. J., Series 2, 35 (1) (1992) 82.

S.Furukawa, S.Murakami, Y.Ito and M.Kimoto, Anodes for molten carbonate fuel cells, Jı Kokai Tokkyo Koho JP 63,138,658, June 10 1988, Appl. 86/285, 229 (1986).

T.J.George and M.J.Mayfield, Fuel Cells, Technology Status report, DOE/METC-90/026 1990.

K.K.Ghosh, Bull. Electrochem., 7 (11) (1991) 512.

L.Giorgi, M.Carewska, M.Patriarca, S.Scaccia, E.Simonetti and A.Di Bartolomeo, J. Pow Sources, 49 (1994) 227.

M.De Gurie, M.J.Shingler and E.Dincer, Doped cerium oxide for molten carbonate fuel c cathodes, EPRI Rep. ER-6983, Sep. 1990.

J.H.Hirschenhofer, IEEE AES Systems Magazine,8 (11) (1993) 21.

C.D.Iacovangelo, J. Electrochem. Soc., 133 (1986a) 1359.

C.D.Iacovangelo, J. Electrochem. Soc., 133 (1986b) 2410.

H.Ito, C.Nagai and S.Terada, Anodes for molten carbonate fuel cells, Jpn. Kokai Tokkyo Koho JP 63,66,855, Feb 25 1988, Appl. 86/216, 078 (1986).

Y.Izaki, T.Watanabe, Y.Mugikura, H.Kinoshita, E.Kouda, T.Abe, H.Matsuyama, T.Shimizu and S.Sato, in Proc. Int. Fuel Cell Conf., Makuhari, Japan, 1992, p 243.

T.Kakihara, C.Shindou, M.Koga and Y.Yamamasu, in Proc. 32nd Battery Symposium (Japan, 1991) p119.

M.P.Kang and J.Winnick, J. Appl. Electrochem., 15 (1985) 431.

A.Khandar, Ytrrium iron garnet as a molten carbonate fuel cell cathode, EPRI Rep. TR-101 069, Sep. 1992.

K.Kinoshita, Electrolyte structures for molten carbonate fuel cell technology, Proc. DOE/ EPRI Workshop on molten carbonate fuel cells, EPRI Report NO. WS-78-135, Electric Power Research Institute, Palo Alto, CA, Nov. 1979.

K.Kishida, Ber. Bunsenges. Phys. Chem., 94 (1990) 941.

N.Kobayashi, H.Fujimura and K.Ohtsuka, JSMA Intn. J. Ser. II, 32 (1989) 420.

H.Koch, B.Rohland and H.Wendt,Proc. 1992 Fuel Cell Seminar, Tuscon AZ, USA, Nov. 29-Dec.2, 1992, p277.

H.R.Kunz, J. Electrochem. Soc., 134 (1987) 105.

H.R.Kunz and L.J.Bregoli, Proc. 2nd Symposium Molten Carbonate Fuel Cell Technology, J.R.Selman, C.Maru, D.A.Shores and I.Uchida, Eds., PV90-16, The Electrochemical Society, Pennington NJ, 1990, 157.

H.R.Kunz and J.W.Pandolfo, J. Electrochemical Society, 139 (6) (1992) 1549.

S.Kuroe, M.Takeuchi, S.Nishimura and K.Ohtsuka, Proc. Int. Fuel Cell Conf., Makuhari, Japan, 1992, p 269.

G.L.Lee, J.R.Selman and L.Plomp, J. Electrochem. Soc., 140 (2) (1993) 390.

L.A.H.Machielse, R.J.Boersma, C.Croon, W.M.A.Klerks and G.Rietveld, in Proc. Int. Fuel Cell Conf., Makuhari, Japan, 1992, p 269.

L.G.Marianowski, E.T.Ong, R.J.Petri and R.J.Remick, Development of IMHEX® Molten Carbonate Fuel Cell Stacks, in 42nd Meeting Int. Soc. Electrochem., Montreux, Switzerland, 1991.

Y.Masao, T.Hiroshi, T.Fujiwara and W.Kaneko, Jpn Kokai Tokkyo Koho, JP 63,138 663 June 1988.

Y.Matsuno, A.Tsutsumi and Y.Oshida, Int. J. Hydrogen Energy, 20 (7) (1995) 601.

Y.Miyazaki, M.Yanagida, K.Tanomoto, S.Tanase, T.Kodama, H.Itoh, C.Nagai and K.Morimoto, in Abstracts 1988 Fuel Cells Seminar, p. 304.

T.Murahashi, in Proc. 2nd Symposium Molten Carbonate Fuel Cell Technology, J.R.Selman, C.Maru, D.A.Shores and I.Uchida, Eds., PV90-16, The Electrochemical Society, Pennington NJ, 1990, 100.

E.A.Ness, D.L.Johnson and R.R.Chandy, Proc. Fuel Cell Seminar, Tuscon, AZ, 1985.

M.Ogoshi, T.Shimizu, S.Sato, T.Matsuyama, H.Saito, T.Abe, T.Watanabe, Y.Izaki and Y.Mugikura, IHI Eng. Rev., 24 (1991) 1.

T.Okada, H.Ide, M.Miyazaki, T.Tanaka, S.Narita and J.Ohtsuki, in Proc. 25th Intersoc. Energy Conv. Eng. Conf., 1990, p207.

K.Ota, S.Mitsushima and N.Kamiya, Denki Kagaku, 56 (1988a) 435.

K.Ota, S.Mitsushima, S.Kato, M.Watanabe and N.Kamiya, Denki Kagaku, 56 (1988b) 647.

K.Ota, S.Mitsushima, K.Kato and N.Kamiya, Proc. 2nd Symposium Molten Carbonate Fuel Cell Technology, J.R.Selman, C.Maru, D.A.Shores and I.Uchida, Eds., PV90-16, The Electrochemical Society, Pennington NJ, 1990, 318.

K.Ota, S.Mitsushima, S.Kato, S.Asano, H.Yoshitake and N.Kamiya, J. Electrochemical Soc., 139 (3) (1992a) 667.

K.Ota, B.Kim, S.Asano, S.Yoshitake and N.Kamiya, Proc. Int. Fuel Cell Conf., Makuhari, Japan, 1992b, p 165.

R.D.Pierce, J.I.Smith and R.B.Poeppel, A review of cathode development of molten carbonate fuel cell, Meeting of the Electrochemical Society, Montreal, Quebec, Canada, Ma 9-14 (1982).

R.D.Pierce, J.L.Smith, G.H.Kucera, Investigation of alternative MCFC cathode materials at Argonne National Laboratory, Progress in Batteries and Solar Cells, Ed. A. Kozawa, J E S Press Inc. Ohio, USA, Vol 6 (1987).

A.Piguead, Electrolyte Structures for Molten Carbonate Fuel Cell Technology, AnnualRep for DOE Contract No. DE-AC03-76ET11304, Energy Research Corp., Danbury, CT, Feb.-Dec. 1990.

L.Plomp, J.B.J. Veldhuis, E.F.Sitters and S.B.van der Molen, J. Power Sources, 39 (1992) 369.

T.Saito, Y.Itoh, Y.Akiyama, K.Okudo, M.Nishioka, S.Murakami and N.Furukawa, J. Pow Sources, 36 (1991) 529.

A.Sasaki, S.Matsumoto, M.Fujitsuka, T.Shinoki and T.Tanaka, IEEE Transactions on Ene Conversion, 8 (1) (1993) 26.

S.Sato, in Proc. 2nd Symposium Molten Carbonate Fuel Cell Technology, J.R.Selman, H.C.Maru, D.A.Shores and I.Uchida, Eds., PV90-16, The Electrochemical Society, Pennington NJ, 1990, 137.

J.R.Selman, A.I.Ch.E. Symposium Ser. 204, 77 (1981) 138.

J.R.Selman, in Fuel Cell Systems, L.J.M.J.Blomen and M.N.Mugerwa, Eds., Plenum Pre 1993, pp 345-463.

D.A.Shores, J.R.Selman and E.T.Ong, Cathode Degradation, Final Report of University of Minnesota to the US Dept. Of Energy, Contract DE-AE21-86MC 23263, Dec. 1989.

S.Takashima, K.Ohtsuka, T.Kahara, M.Takeuchi, Y.Fukui and H.Fujimura, in Proc. Int. Fuel Cell Conf., Makuhari, Japan, 1992, p 265.

S.Takashima, K.Ohtsuka, N.Kobayashi and H.Fujimura, in Proc. 2nd Symposium Molten Carbonate Fuel Cell Technology, J.R.Selman, H.C.Maru, D.A.Shores and I.Uchida, Eds., PV90-16, The Electrochemical Society, Pennington NJ, 1990, 378.

T.Tanaka, M.Matsumura, Y.Gonjio, C.Hirai, T.Okada and M.Miyazaki, in Proc. 25th Intersoc.Energy Conv. Eng. Conf., 1990, p201.

K.Tanimoto, Y.Miyazaki, M.Yanagida, S.Tanase, T.Kojima, N.Ohtori, H.Okuyama and T.Kodama, Denki Kagaku, 59 (1991) 619.

K.Tanimoto, Y.Miyazaki, M.Yanagida, S.Tanase, T.Kojima, N.Ohtori, H.Okuyama and T.Kodama, J. Power Sources, 39 (1992) 285.

K.Tanimoto, Y.Miyazaki, M.Yanagida, S.Tanase, T.Kojima, N.Ohtori, H.Okuyama and T.Kodama, J. Hydrogen Energy, 17 (10) (1992) 821.

H.Urushibata and T.Murahashi, Proc. Int. Fuel Cell Conf., Makuhari, Japan, 1992, p 223.

J.B.J.Veldhuis, F.C.Eckes and L.Plomp, J. Electrochem. Soc., 139 (1) (1992) pL6.

E.J.Vesely, Corrosion of Materials in Molten Carbonate Fuel Cells, Final Report DE-AC21-86MC23265 (IIT Research Institute, Chicago, 1990).

T.Watanabe, Y.Mugikura, Y.Izaki, E.Koda, H.Kinoshita and T.Abe, Proc. 27th Intersociety Energy Conversion Engg. Conf., San Diego, CA, U.S.A., 1992.

G.Xie, Y.Sakamura, K.Ema and Y.Ito, J. Power Sources, 32 (1990a) 125.

G.Xie, Y.Sakamura, K.Ema and Y.Ito, J. Power Sources, 32 (1990b) 135.

G.Xie, K.Ema and Y.Ito, J. Power Sources, 35 (1991) 123.

H.Yabe, Y.Ito, K.Ema and J.Oishi, J. Power Sources, 24-3 (1988) 207.

C.Y.Yuh and A.Piguead, Determination of optimum electrolyte composition for molten carbonate fuel cells, Final Report (ERC Danbury, CT, 1989), DOE/MC/23264-2756.

C.Y.Yuh and J.R.Selman, J. Electrochem. Soc., 139 (5) (1992) 1373.

CHAPTER 3

COAL GASIFICATION

Coal is a complex mixture of organic and mineral matter with carbon as the primary constituent. The composition can typically be represented by $CH_{0.8}$. Apart from the hydrocarbon portion, it contains non-combustible inorganic impurities which constitute the residual ash as well as some sulphur. The gasification process conventionally involves the reaction of coal with a gasifying agent like steam. The latter completely converts the organic content to gas leaving behind the ash.

3.1 Process Chemistry

The modern process of coal gasification involves the endothermic reaction of carbon atoms contained in coal with water vapor, according to equation 3.1 at high temperatures to yield carbon monoxide (CO) and hydrogen (H_2). The CO, in turn, can further react with either the steam or the H_2. While the primary reaction of the solid coal with steam is highly endothermic, the two secondary reactions are exothermic. The entire process can be described by the following equations:

	ΔH (kJ/mol)
$C + H_2O \rightleftharpoons H_2 + CO$	+118.5
$CO + H_2O \rightleftharpoons H_2 + CO_2$	-42.3
$CO + 3H_2 \rightleftharpoons CH_4 + H_2O$	-206

The gasification process is favored by high temperature and hence it is normally carried out above 700°C. For the reaction 3.1 to proceed from left to right it is necessary that heat be transferred at high temperatures.

Most coal gasification processes are based on the concept of direct combustion of a portion of coal feedstock with oxygen or air introduced in the same vessel where the gasification takes place:

$$C + O_2 \rightarrow CO_2$$

Combustion and gasification occur at the same time, the first reaction providing heat for the second to occur. At any steady-state condition the energy balance of the system is thus zero (balanced reaction), and the combination of the reactions listed above theoretically gives no net flow of energy.

Apart from thermodynamic considerations, the kinetics of gasification is also a primary concern since it dictates the rate of carbon conversion and the reactor size for a given

throughput. When considering the kinetics of coal gasification, it has to be realized that both coal and lignite undergo a series of chemical and physical reactions (pyrolysis) when they are brought to the temperature necessary for gasification. During this process, coke is formed and gases as well as liquids such as tar, oil and water are released. At higher temperatures where pyrolysis and gasification occur simultaneously, the liquids may be converted to gases by the gasifying agent. Finally, the coke itself becomes gasified.

The kinetics of gasification is governed by a series of physical and chemical processes viz.

- Transport of steam through the gas film surrounding the coal particle (film diffusion)
- Transport of steam into the particle pores (pore diffusion)
- Chemical reaction on the pore surface and
- Transport of the products (CO and H_2) back into the bulk gas phase.

Coke itself is a porous solid and the gasification reaction takes place on the inner surface. Therefore, the steam has to first permeate through a film formed of product gases before diffusing into pores and reacting at the walls with the carbon. In steam gasification, depending upon the temperature, any of these three successively occurring steps could be rate limiting. Under atmospheric pressure and temperatures below 1000°C, the chemical reaction is the slowest. Above 1000°C, the pore diffusion is rate determining so the reaction can be improved by accelerating this step, for instance, by increasing the operating pressure. At still higher temperatures, i.e. beyond 1300°C, film diffusion becomes limiting and thus the process kinetics can be enhanced by using strategies such as turbulent mixing.

3.2 Engineering aspects

The coal gasification process can be carried out in various reactor configurations viz. a fixed bed, a fluidized bed or an entrained bed. The manner in which the coal and the gasification medium are brought into contact determines not only the design of the gasifier, but also the method of reaction, the quality of the gasification products and the required composition of the gasification medium. Furthermore, the processes have to be adjusted to allow for the properties of the coal feedstock such as particle size, caking capability and amount as well as composition of mineral matter. Yet another variable involved in the design is the mode of addition of heat to the primarily endothermic gasification reaction. There are two possibilities of heat transfer to the gasifier viz.

- Autothermic coal gasification in which the reaction heat is generated within the gasifier itself. A mixture of oxygen and steam is used as the gasifying agent whereby a portion of the coal is burnt and the remainder reacts with steam.
- Allothermic gasification where the heat is generated outside the gasifier by burning

either coal or its products in a separate combustion chamber with air. This heat can then be transferred to the gasifier either by superheated steam, steam/gas mixtures or by solid heat carriers.

Eventually, the choice of the gasifier is decided by the gasification by-products as well as by the scale of operation. For the production of fuel gas to be used on a small scale (2-10×10^3 m^3/h), a fixed-bed air blown producer or fluidized bed process may be considered; for large scale work (> 30×10^3 m^3/h), a Lurgi fixed-bed of Winkler fluidized-bed process using air and steam may be more suitable. For ammonia or methanol synthesis, the Koppers-Totzek process appears to be preferable since it yields a clean gas with the desired composition for subsequent processing.

The peculiar characteristics of coal, such as the ash content and composition, tendency to agglomerate, sulphur content, reactivity, and so on, make coal gasification a complex process with many alternative routes. The following sections present a brief description of each of the three basic gasifier configurations commonly employed in industry. A comparison of the processes based on these reactors is given in Table 3.1.

3.2.1 Fixed bed gasifier

In a fixed-bed gasifier, a bed of coal particles moves downwards in a countercurrent flow of oxygen and steam. Before arriving at the gasification zone, the coal bed passes through a devolatilization zone where it is heated by the hot gas coming up from the gasification zone. This step strips the coal of its volatile contents such as tar, higher hydrocarbons, phenols etc. which are passed into the produced gas. The reactions producing CO, H_2, CO_2 and CH_4 occur in the gasification zone and the product composition is influenced by the operating pressure. It is observed that increasing amounts of methane is formed at higher pressures. In order to attain reasonable gasification rates, the gas velocity must be high and the pressure drop low. This implies limitations on the feedstock coal in terms of particle size and caking capability. A permeable coal charge which will allow through-flow of the gasification medium is an essential prerequisite for gasification in a fixed bed. In practice, this can be achieved only when lumpy coal of a certain size (5 to 30 mm) is used. Also, proper operation requires a uniform downward movement of the coal over the entire cross-section and a uniform upward counter-flow of the gasification medium. This is possible only when the coal does not agglomerate or disintegrate in the gasifier, and also, when the ash does not agglomerate. It is also imperative to maintain an optimum temperature in the gasification zone so as to prevent the melting and clumping of the ash. This can be accomplished using large amounts of steam in the gasification medium, even though a substantial part of it travels through the

TABLE 3.1 Comparison of Lurgi, Winkler and Koppers-Totzek processes

	Lurgi	Winkler	Koppers-Totzek
Operation mode	Fixed bed	Fluidized bed	Entrained bed
Coal type	Non-coking only	Any type; non-coking require pretreatment	Any type
Fuel size	Sized coal only; fines must be briquetted	Any size - fines to sized coal	Finely pulverized coal dust
Oxygen consumption	Low	Intermediate	High
Intermediate compression of gases	Not required	Required	Required
Byproducts	E.g. tars, phenols and light oils	No byproducts	No byproducts
Particulate content of raw gas	Low	High	Low
Product gas composition (vol. %) $CO : H_2 : CH_4$	30.6 : 52.8 : 15.2	40.3 : 55 : 3.9	63.6 : 35 : -

gasification zone without being consumed.

The product gas leaving the gas generator at the top contains pyrolysis products which are formed in the upper layer of the fixed bed. Most processes use a dry ash removal; thus, the reaction temperatures must be below the sintering point of the ash. The best known process o this type is the Lurgi gasifier which operates at pressures up to 35 bar (35×10^5 N/m^2) and is used on a commercial scale.

Moving-bed reactors have been utilized for almost a century to generate hydrogen-rich gas, from coal or lignite, by injecting steam and air, from the bottom of a vessel filled with coal. Continuous rather than batch operation has been achieved by use of a rotating grid on the bottom which removes the ash. Improvements in metallurgy, process control, and flow distribution made it possible to develop oxygen-blown pressurized gasifiers based on moving-bed technology, as those utilized nowadays.

3.2.2 Fluidized bed gasifier

The need to utilize caking coals (which tend to agglomerate in the upper portion of moving-bed gasifiers) and the complications presented by tar and oils condensing during cooling, have resulted in alternative processes where gas is formed at much higher temperatures and coal is either suspended in a fluid bed or injected through special burners.

The mechanisms and reaction conditions in a fluidized bed gasifier are essentially similar to those in a fixed bed. However, the material and heat exchange in a fluidized bed are not so clearly defined as in the case of a fixed bed. Thus, the degasification and gasification zones are not separate from each other which results in an increased pyrolytic cracking of the degasification products.

In a fluidized bed gas generator, the velocity of the gasifying agents, i.e. oxygen and steam, should be just high enough to suspend the coal particles. Coal can be continuously fed while ash is withdrawn. To avoid agglomeration effects, the operating temperature of the conventional fluidized bed gasifiers must be below the ash sintering point i.e. $\sim$ 1000°C. This again involves the use of excess steam in the gasification medium. Fluidized bed technology is used in the Winkler process and is especially suited for lignite and highly reactive hard coal which release relatively smaller amounts of ungasified fly-ash.

It is important to note that not just the temperature, but also the average residence time of gas-vapor molecules have an effect on produced gas composition. Coal is an agglomerate of carbon, heavy hydrocarbon compounds, ash, and other elements. When exposed to heat, the portion called volatile matter will evaporate and join the gas phase: if these vapors are not given enough time to react with steam, or if the temperature is not sufficiently high (say above 900°C), the vapors remain unreacted and will eventually condense when gas is cooled, forming tar and oils. This is a major process complication to deal with, since this not only results in a reduction in gas yield but also a main process complication to deal with, as the tars tend to plug heat exchangers, pipes, and compressor blades and pollute condensed waters

from coal gasification facilities.

3.2.3 Entrained bed gasifier

The entrained-bed gasifier employs fine coal dust which is partially oxidized in a flame. The coal dust and the gasification medium are homogeneously mixed and passed through an empty reaction chamber with a special burner. The gasification medium is a combination of oxygen and steam, consisting of less than 0.5 mole steam/mole oxygen. High linear velocities of oxygen and steam are essential for this process. Immediately after entering the chamber, the reaction occurs spontaneously with the formation of a flame with the temperature shooting up to 2000°C or more in the core of the flame. Because of the high flame temperature, the coal particles undergo instantaneous gasification, with reaction periods of 1s or less. Thus, agglomeration is avoided even with strongly caking coals. At the end of the flame zone, the carbon is completely consumed and the gas composition is essentially determined by the water gas equilibrium, i.e.

$$CO + H_2O \rightleftharpoons H_2 + CO_2$$

The product gas leaves the reaction chamber at a temperature of about 1500°C. An advantage of the high reaction temperature is that all the gasification products as well as the higher hydrocarbons are almost completely converted to the components of the homogeneous water gas. The only exception is CH_4 which forms less than 0.1% by volume of the exiting gas. Moreover, the product gas does not contain any tar. Thus, in this gasifier, the byproducts' yield is almost nil except for the ash or slag which is discharged in a liquid form and is withdrawn at the bottom of the reactor. Yet another major attraction of this process is that it can use virtually all types of coals. The best known entrained bed reactor is the Koppers-Totzek gasifier, which is used especially to make synthesis gas for production of ammonia and fertilizers.

3.2.4 Other Processes

Apart from the three basic gasifier designs described above, improved versions of these processes are under various stages of development. Table 3.2 summarizes the salient features of these gasifiers, a majority of which are operational on the demonstration/commercial scale.

Table 3.2 **Modified coal gasification processes**

Process	Features
Texaco	Pressurized process using coal in water slurry; Wide choice of feedstock; No organic by-product problems; High temperature and oxygen required
Shell-Koppers	Operation similar to Texaco except no water in the feed; Better efficiency
High temperature Winkler	Pressurized Winkler with limestone addition; High throughput; Fuel requirement same as Winkler process
British Gas/Lurgi Slagger	Thermal output 2-3 times that of conventional Lurgi process at comparable O_2 consumption; Low net liquor production; Methanation possible in a single reactor
Ruhr 100	Uses high pressure and two separate gas offtakes at different shaft levels; High throughput with a wide range of coals; High methane content in product gas combined with a low tar yield
Saarberg Otto	Slag bath pressurized process; Can tolerate a wide range of coal
Hygas	Two stage fluidized bed high pressure process; High methane concentration; Can be used for all coals
Fixed-bed BHEL	Fixed bed gasification process for non-caking coals
PEDU BHEL	Single stage fluidized bed gasification of Indian coals
Cogas	Multistage fluidized bed pyrolysis unit and char gasification reactor; Co-production of SNG and synthetic oils; No O_2 used

3.3 Gas clean up

The variety of elements present in coal results in complex side reactions of these components between themselves and with the combustion and gasification products. For instance, sulphur contained in coal reacts with oxygen, carbon monoxide, hydrogen, and water vapor to form gaseous compounds such as H_2S, COS, SO_2 and mercaptan. Similar reactions may occur between nitrogen and chlorinated compounds.

The presence of by-products such as H_2S, COS, HCl and NH_3 in the synthesis gas poses serious problems not just for its utilization (such as in fuel cells) but also in the gasification and cooling equipment due to high temperature, high partial pressure of hydrogen, and mechanical stress. The effect of such contaminants on every component of the coal gasification plant has to be carefully evaluated.

The specific characteristics of each coal, its ash composition, grindability, etc. all influence the resultant gas composition and may dictate a specific process selection. This aspect has a significant effect on potential utilization of coal gasification coupled with modular fuel cell system. Every plant will require a special design in order to accommodate for specific coal characteristics. This may pose a limitation in the early development of small-size modularized coal-based fuel cell power plants.

A coal-based fuel cell power plant is conceptually similar to a plant based on natural gas or liquid hydrocarbon feedstock. The fuel processor consists of a coal gasifier, followed by cooling and purification stages and an optional CO conversion equipment. However, due to the peculiar composition of synthesis gas from a coal gasifier, which is rich in contaminants and may contain tars, oils and ash, the type of treatment the gas needs to be subject to is much more complex. Shift conversion (for further production of H_2 from CO and H_2O) can substantially occur, in reactors similar to those of steam-reforming plants. Ash, fines and other particulate, plus tar and oils must be removed, each at its own optimal temperature, in order to avoid plugging ducts, reactors, or exchangers. Furthermore, air separation, water treatment, ash handling, and coal storage have to be included in coal gasification facilities. Such auxiliary equipment may represent over 25% of the investment cost for a coal gasification plant designed for, say, a 150-MW fuel cell stack system.

TABLE 3.3 MCFC tolerance limits to major contaminants

Contaminant	Remarks	Tolerance limit
Particulates	Incl. ZnO from H_2S cleanup	<0.1 g/l
Ammonia		< 1 ppm
H_2S		< 1 ppm
HCl	Incl. other halides	< 10 ppm
Trace metals	From H_2S cleanup	< 1 ppm
Zn	Formed during desulphurization	< 20 ppm
Tar		< 2000 ppm

Based on experimental studies, it is widely accepted that the gas purity levels required for an MCFC system are far more stringent than those for the integrated gasifier-combined cycle (IGCC) systems. The tolerance levels of MCFC for some of the commonly found contaminants are shown in table 3.3. The following sections describe some of the gas-cleanup strategies employed in an IGMCFC system.

3.3.1 High temperature gas cleaning techniques developed in the Netherlands†

3.3.1.1 Sulphur

For the removal of the sulphurous components H_2S and COS from coal gas at high temperature, only those processes qualify which have a solid mass as their sorbents. Physical adsorption is not applicable because of the unwanted co-adsorption of CO_2, but adsorbents whose action is based on chemical adsorption (e.g. metal oxides) are applicable. There is a lot of difference in the sulphidation rate of such adsorbents. Besides, the way in which regeneration can be effected and the extent to which COS can be removed are also essential considerations. Also, improvements in the chemical and mechanical properties of the adsorbent can be achieved by applying metal oxides to a carrier. However, until now, the study of high temperature desulphurization by metal oxides has paid little attention to the development of reactor types in combination with a sorbent or to the regeneration route.

Based on the above mentioned selection criteria, the following desulphurization processes for three different temperature levels have been identified :

- 250°C: active carbon with COS-conversion in series (working temperature 175-200°C) and ferric oxide on silica (working temperature approximately 350°C)
- 350°C: iron oxide on silica and
- 600°C: zinc titanate $(ZnO)_{0.8}$. TiO_2 in moving bed configuration.

3.3.1.2 Dust

Although quite a lot of attention was and has been paid to dust removal at high temperature, experience with these techniques in reducing environments such as in coal gas is still limited. In addition to the unfamiliarity with the behavior of HT gas cleaning systems in reducing environments, the stickiness of the ash particles at high temperatures is a particular problem. Therefore cyclones are considered as less suitable for use at temperature above 400°C.

For higher temperatures sliding granular bed filters appear to be the best option. For the necessary final cleaning of the coal gas, ceramic candle filters can be used. On the basis of the available data the following clean-up techniques were selected for the three temperature levels:

† From a study done by ECN, KEMA, Stork Boilers and TNO as part of the Netherlands Clean Coal Programme, supported by Novem (Netherlands agency for energy and the environment).

- 250°C: cyclones and cloth filters with polymeric filter materials or candle filters; a conventional (wet) scrubbing of the gas in a gas scrubber is also feasible at this temperature level
- 350°C: cyclones and candle filters and
- 600°C: sliding granular bed filters and candle filters.

3.3.1.3 Halogens

Relatively little is known about the removal of halogens at high temperatures. On the basis of thermodynamic considerations it can be stated that Na and Ca based absorbents are most suitable. There are no developments taking place as regards regenerative processes. All the suitable processes work with natural minerals or bulk chemicals. The differences are confined to temperature and reactor type. With respect to the latter a distinction can be made between pneumatic injection of powdered sorbents or systems with fixed beds with coarse grain sorbents and related systems. The choice of sorbents depends on the temperature, the water vapor content, the desired degree of removal and the sequence of collection processes of the various impurities in the gas. Especially qualified are commercial materials based on $Ca(OH)_2$ or $NaHCO_3$ (if necessary Na_2CO_3). For the systems with a dry dedusting the option of pneumatic injection of powdered sorbent has been selected. At the 250°C temperature level the halogens can be removed by scrubbing the coal gas instead of a dry dedusting.

3.3.1.4 Alkali metals

If and to what extent the removal of alkali metals and other trace elements will be necessary, cannot be clearly said with the present available knowledge about the volatilization of trace elements in slagging gasifiers and their behavior in the passage after the gasifier. Gas turbine requirements can lead to limits to the remaining part of gaseous concentrations of alkali metals and trace elements such as lead and zinc in coal gas. Further study is desirable, including further thermodynamical analyses linked to operational measurements on cold gas clean-up facilities.

3.3.1.5 Nitrogenous compounds

With a dry gas cleaning system consisting of a dust/halogen removal stage and a desulphurization stage, the nitrogenous components (NH_3, HCN) are not removed. When the coal gas is burned in the gas turbine, this will result in the formation of a certain amount of chemical NO_x. The techniques by means of which NH_3 and HCN are removed from the coal gas are still in an early stage and until now no experience has been acquired with proven techniques in gas turbines such as staged combustion where coal gas is concerned. So we still have to rely on techniques by which the NO_x formed is eliminated. In that case only selective catalytic reduction (SCR) of NO_x is qualified. The catalyst which is used for this has a life of

ten years and commercially available. However, application of SCR involves a considerable investment. Where scrubbing of the coal gas is applied as part of high temperature gas cleaning, NH_3 and HCN are largely removed in the scrubber and techniques which prevent the formation of thermal NO_x, such as the injection of steam or nitrogen, will be sufficient.

3.3.1.6 Evaluation of gas-cleaning systems

Within the framework of this system study, the following high temperature gas cleaning systems have been selected for a closer thermodynamic analysis:

- 250°C: dedusting, dehalogenation and a partial denitrification by scrubbing in a venturi scrubber; desulphurization by active carbon preceded by a COS convertor; further denitrification by injection of nitrogen and, if necessary, steam in the coal gas.
- 350°C: dedusting by means of cyclone and candle filters, desulphurization by means of iron oxide on silica; dehalogenation by means of pneumatic injection of soda; the formed halide salts are trapped in the above mentioned candle filters; denitrification by selected catalytic reduction (SCR) in the waste hear boiler.
- 600°C: dedusting by sliding granular bed filters followed by candle filters; desulphurization by zinc titanate $(ZnO)_{0.8}.TiO_2$ in moving bed configuration; dehalogenation and denitrification as in the 350°C variant.

In systems with a wet gas cleaning, increasing the temperature which included desulphurization results in an increase in the net efficiency. In variant S250 (Shell), the rise of the efficiency is caused by the increase of the steam turbine power and the decline of the internal plant load, especially that of the sulphur extraction system. It has to be noted, however, that this consumption of electricity has been estimated on the basis of a broad design for the sulphur extraction system and that its accuracy is therefore limited. The power of the gas turbine remains as good as constant because the composition of the coal gas stays almost the same. In the T250 (Texaco) variant, the expander and the gas turbine generate more power because the water vapor in the coal gas does not condense, which is the case of TBAS. This implies that quite a lot of heat is needed for the heating up of the coal gas after desulphurization; this becomes evident in a decline in the power of the steam turbine. For both the variants, the mentioned gain in efficiency at a desulphurization temperature of about 200°C is well within 1% point as compared to the basic variant.

Transition to dry gas cleaning techniques enhances the process efficiency. For variant S350, the efficiency is almost 2.8% point higher than that of the basic variant. A rise in both the gas turbine power as well as the steam turbine power are responsible for this improvement. On the other hand, there is a rise in the internal plant load of the oxygen plant. This has not been integrated in the cases of S350 and S600, so these need more electrical power for the

compression of air. A further increases of the gas cleaning temperature hardly results in an increase in the efficiency; the increase in the gas turbine power is almost completely nullified by a decline of the steam turbine power.

For variant T350 the profit with regard to the basic variant amounts to 2.4% point. This profit is caused by the larger power generation of the expander, gas and steam turbine. The increase in the power of expander is caused by a greater pressure drop, a higher gas temperature and a relatively greater mass flow because of the high water vapor content. A further increase in the gas cleaning temperature to 600°C is accompanied by another small increase in efficiency. Figure 4.1 shows that this must be attributed to the presence of the expander.

In general, it can be concluded that a gain in efficiency of 2.3% points can be realized, if one switched to dry gas cleaning techniques with the gas cleaning taking place at about 350°C. In this case the convection cooler almost exclusively consists of an evaporation section. A further increase of the cleaning temperature to 500 or 600°C only results in a slight improvement of efficiency.

3.3.2 Work done at IGT

The Institute of Gas Technology (IGT) has been conducting experimental and process economic studies on two conceptual high temperature approaches to removing certain chemical contaminants from coal-derived fuel gases that are deleterious to molten carbonate fuel cell performance. One process under investigation at IGT is a regenerable high temperature fuel gas desulphurization process known as the mixed metal oxide process. In this process, a select mixture of metal oxide-containing sorbents is used to remove sulphur-containing compounds from hot (>540°C) fuel gases by reaction. The spent sorbents are then regenerated with an oxygen-containing gas such as air and recycled product gas from the sorbent regeneration. With the proper selection of sorbents it is expected that this process will not only be able to reduce the sulphur content of the coal-derived fuel gas to less than 50 ppm(v) but will also be able to recover this sulphur as elemental sulphur without the need for a reductant such as fuel gas or coke. The reason for the expected ability to recover the sulphur as elemental sulphur is that one of the sorbents in the mixture is selected based on its ability to be regenerated with SO_2 and produce elemental sulphur. Therefore, even if some SO_2 is produced, it can be recycled back to the bed for conversion to elemental sulphur.

The other high temperature contaminant removal concept under investigation at IGT relates to the removal of HCl from coal-derived fuel gases. For many years, IFT has been involved in the development of both molten carbonate fuel cells and high temperature thermal energy

storage using low melting point mixtures of alkali carbonates within an inert ceramic matrix. Theoretical work at Physical Sciences, Inc. indicated that the alkali carbonates were excellent candidate materials for removing HC1 from high temperature fuel gases. Since IGT had already acquired significant expertise with ceramic-supported molten alkali carbonate materials and had developed a promising, cost-effective mass production technique for these materials, extension of this knowledge to the development of a sorbent for high temperature HC1 removal was considered possible.

3.3.2.1 Bench-scale testing of the mixed metal oxide process

The subject of the bench-scale studies on the mixed metal oxide process has been the use of a 90% by weight cobalt titanate/10% by weight zinc oxide mixture. The cobalt titanate was chosen for its elemental sulphur producing capability and zinc oxide was chosen for its excellent affinity for sulphur. The bench-scale unit consists of a 4-in. ID x 10-in. OD x 7-ft long fixed-bed reactor housed within a 5 ft, 4-zone 22,000 watt electrically heated furnace. The reactor currently being used was prepared from a nominal 10-in. Schedule 80 carbon steel pipe that was lined with 1-7/8 in. of Harrison Walker HW 3c-80 aluminosilicate castable refractory. The unit also contains a 120 SCFH air compressor for regeneration of the sorbent and a 168 SCFH recycle compressor for recirculating either dry fuel gas or tail gas from the regeneration. A dry, sulphur-free fuel gas is supplied from pressurized cylinders. Steam is supplied to the recirculated fuel gas by a 54 SCFH steam generator and sulphur-containing gases are added to the fuel gas from a pressurized cylinder using a mass flow controller (0-9 SCFH).

Two gas preheaters are used to preheat the fuel gas and the regeneration gas before introduction into the fixed-bed reactor. The unit also contains primary and secondary sulphur collection vessels at the bottom of the fixed-bed reactor to recover elemental sulphur from the regeneration product gases. Two gas chromatographs are used to monitor the feed and product gases during sorbent sulphidation and regeneration.

The initial sorbent charge to the bench-scale reactor consisted of a random mixture of 6060 grams of cobalt titanate sorbent and 600 grams of zinc oxide sorbent. The cobalt titanate sorbent was in the form of 3/16-in. pellets. These pellets were prepared for IGT by United Catalysts, Inc. The pellets were nominally 100% $CoTiO_3$. The zinc oxide sorbent that was used in the mixture was a commercial preparation from Harshaw (Zn-0103T). Harshaw Zn-0103T contains 75% ZnO with the balance being a mixture of alumina, magnesia, calcia, and chromia. This zinc oxide media was tested by IGT under a previous DOE contract (DE-AC21-78ET11330) and was found to be regenerable and have a sulphur removal capacity of about 14 lb sulphur/100 lb sorbent.

In the bench-scale tests, the 6.66 kg mixture of cobalt titanate and zinc oxide sorbents were sulphided and regenerated a total of eleven (11) times. Sulphidation of the mixture was conducted at temperatures between 1200° and 1500°F and near-atmospheric pressure. A simulated coal-derived fuel gas containing approximately 40% N_2, 17% H_2, 13% CO, 13% CO_2, and 17% H_2O was used during most of the sulphidations but because the non-condensibles (i.e. N_2, H_2, CO, and CO_2) were recycled, the fuel gas composition often changed during the testing because of extraneous reactions such as the water gas shift reaction. The H_2S level in the feed gas ranged from 5,000 to 50,000 ppm(v). The higher H_2S levels were used primarily to speed up the sulphidations. Regeneration of the sulphided sorbents was conducted at initial bed temperatures of 1200° to 1650°F, atmospheric pressure, and with a variety of gases including air, $N_2/O_2/SO_2$ mixtures, and N_2/SO_2 mixtures.

The results of the bench-scale tests were not as good as expected from the previous laboratory-scale tests. Although the sorbents survived the testing, it was determined that these particular sorbents require a space velocity during sulphidation of less than 300 h^{-1} in order to remove more than 90% of the sulphur from the fuel gas. However, the sulphur removal capacity of the sorbent mixture under these conditions was quite good. During the later cycles of testing, the sorbent was loaded with sulphur to between 10 and 15 lb/100 lb without a significant decrease in sulphur removal efficiency.

Elemental sulphur production during regeneration of the sorbent mixture was also less than expected. It was anticipated from the laboratory-scale studies that the sulphur in the product gas from the regenerating bed would be about 25% elemental sulphur and 75% SO_2. In the bench-scale regeneration tests, elemental sulphur represented 14.3% or less of the total sulphur in the product gas. Analysis of the regeneration data revealed that the probable cause for the lower than expected elemental sulphur yields was a severe kinetic limitation. Elemental sulphur yields per unit time per unit mass of sorbent ranged from 2.2×10^{-6} to 1.34×10^{-5} g sulphur/min/g sorbent regardless of the space velocity or temperature of the regeneration. The only factor that appeared to have an effect on the sulphur yield per unit time was the initial sorbent sulphur loadings. Those regenerations where the sulphur loadings were high produced sulphur at the highest rates. Typically, the sulphur yields in the bench-scale tests were about a factor of 6 less than those measured in the laboratory-scale studies with the cobalt titanate sorbent under similar conditions. The only difference between the laboratory-scale studies and the bench-scale studies was that the sorbent size was increased from 1/8-in. to 3/16 in.

An extrapolation of the bench-scale results, assuming a sulphur production of 1×10^{-5} g sulphur/min/g sorbent, indicates that a space velocity on the order of 100 h^{-1} would be

required to produce a product gas with elemental sulphur representing 25% of the total sulphur in the gas stream. More important, at these sulphur production rates, it would take nearly a week to regenerate the sorbent if 100% elemental sulphur was desired. This need for low space velocities for both fuel gas sulphur removal and reasonable elemental sulphur concentrations in the product gas from the regeneration indicates the need for improved sorbent reactivity. One possibility is to optimize the cobalt titanate sorbent used in these studies. The cobalt titanate sorbent used was a nominal 100% $CoTiO_3$, and the crystallite sizes in the sorbent were probably quite large. Future plans include investigation of alternative formulations of the cobalt titanate sorbent in the IGT laboratory-scale test facility before proceeding with further bench-scale tests.

3.3.2.2 Preliminary process economic studies

The preliminary process economic studies on the mixed metal oxide process and the HC1 removal sorbent were conducted concurrently with the bench-scale tests. Consequently, the assumptions made regarding the mixed metal oxide process reflect the results of the laboratory-scale studies rather than the bench-scale studies. However, assuming that further improvements can be made in the reactivity of these sorbents, these economic studies may be reasonable accurate.

The preliminary process economic studies on the mixed metal oxide process considered six different configurations for the process. The reason for considering this many configurations was that several options existed for handling the product gas from the regeneration. Regeneration of the sorbent produces a gas containing N_2, SO_2, and elemental sulphur. After the elemental sulphur is removed from the gas by condensation, a mixture of N_2 and SO_2 remains.

The first configuration includes a Wellman-Lord SO_2 removal process to handle the product gas (fig. 3.1). In this configuration, SO_2 in the product gas is recovered by the Wellman-Lord process and recycled back to the bed undergoing regeneration to produce additional elemental sulphur.

In the second configuration, a lime flue gas desulphurisation process is incorporated in the design (fig. 3.2). After elemental sulphur removal and partial product gas recycle, the SO_2 in the remaining product gas is simply scrubbed by the lime flue gas desulphurisation process. The sulphur in this stream is then discharged as a calcium sulphite sludge.

In the third configuration the Foster-Wheeler RESOX process is used to handle the N_2/SO_2 stream after elemental sulphur recovery and partial product gas recycle (fig. 3.3). In this

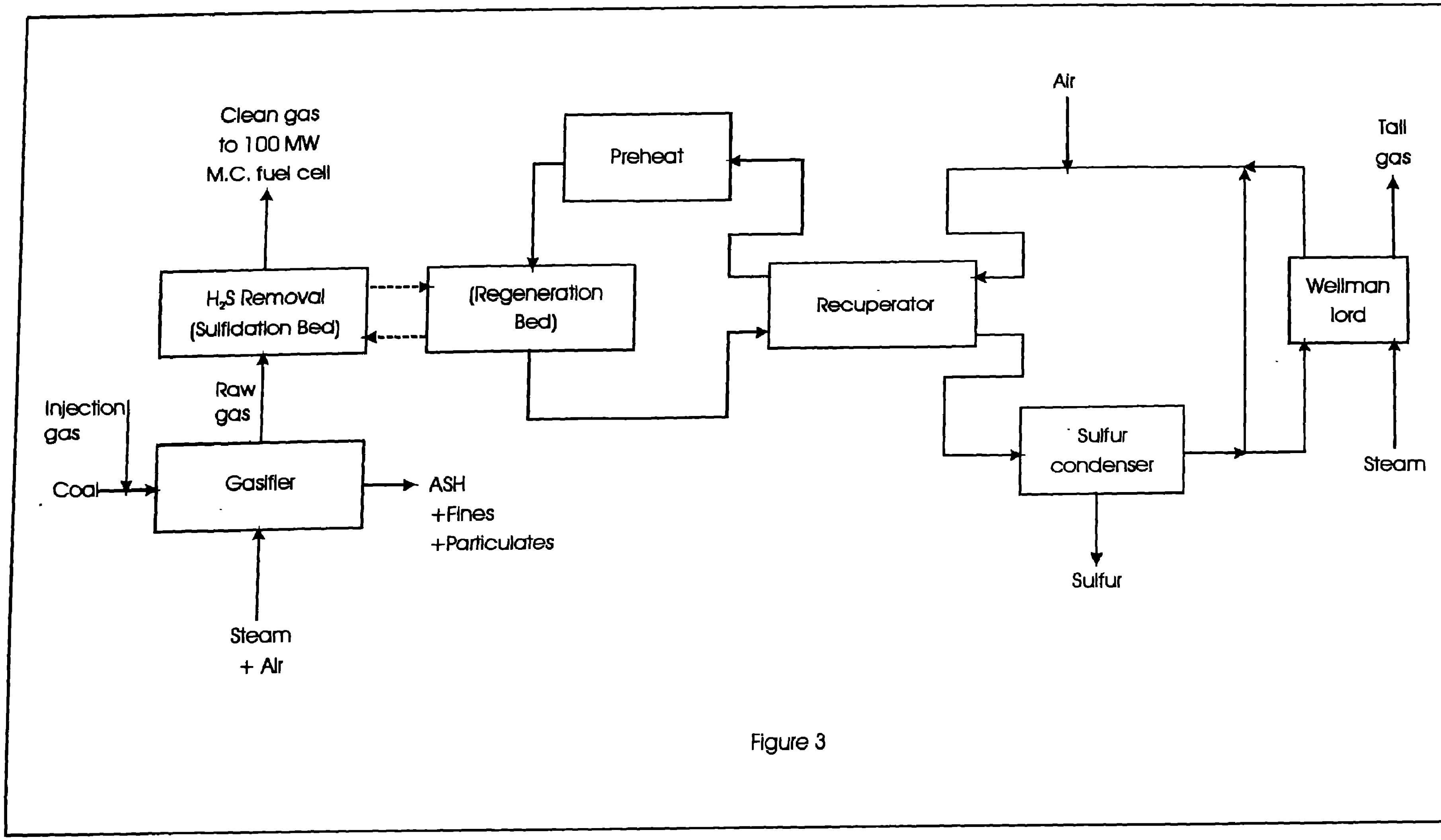


Figure 3.1. SO_2 recycle with Wellman-Lord unit

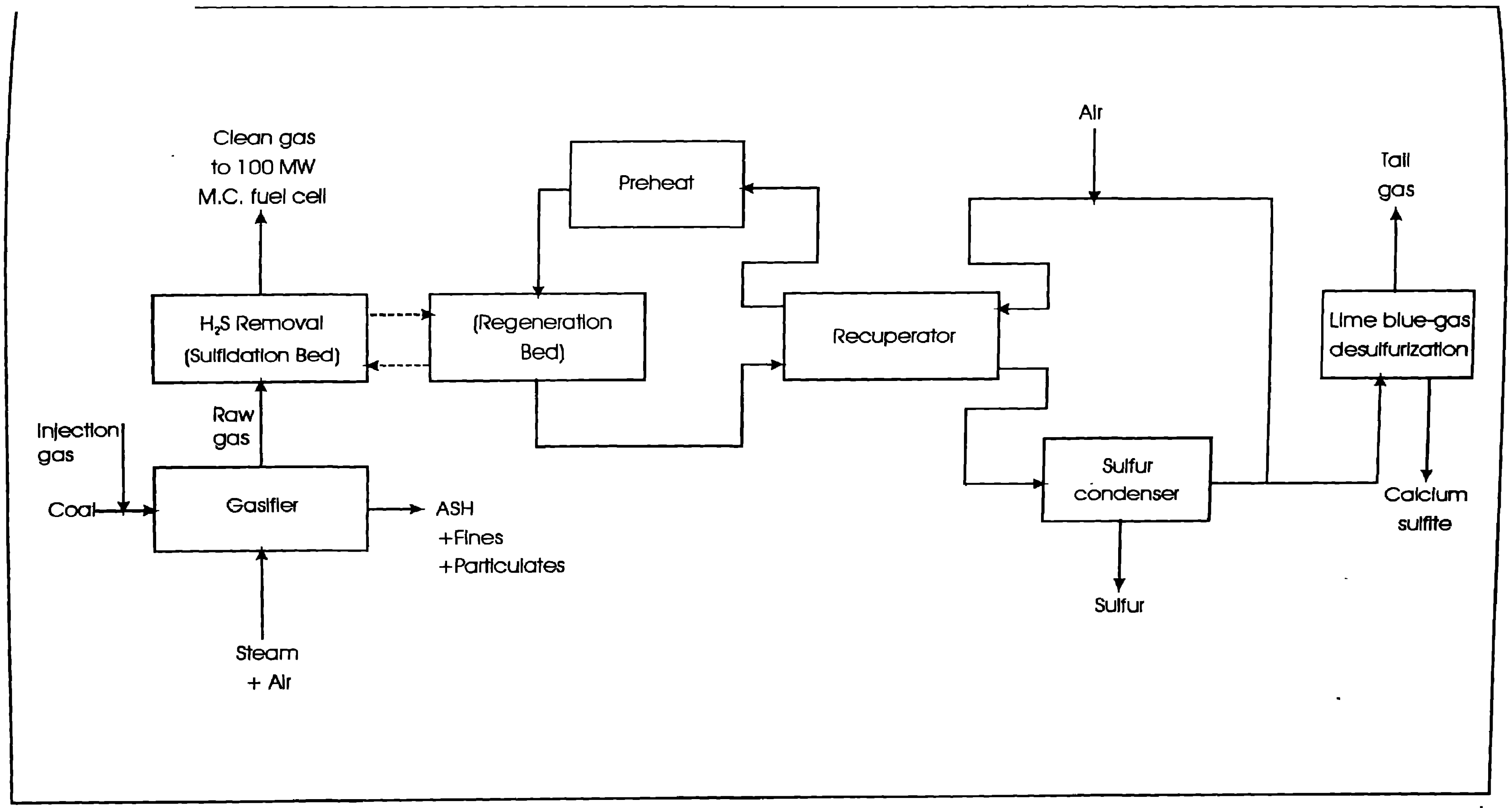


Figure 3.2. Tail gas treatment by lime scrubbing

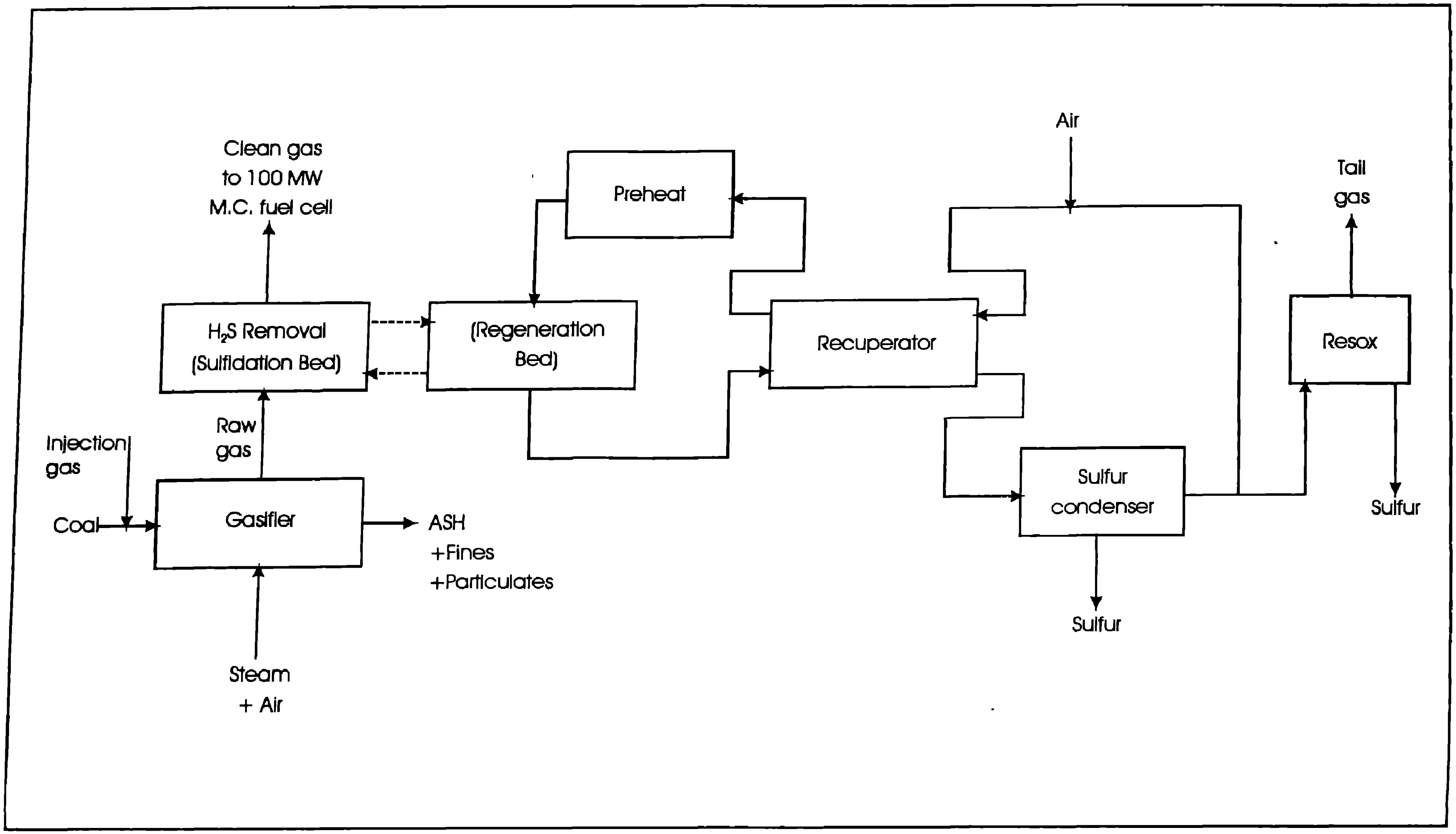


Figure 3.3. Tail gas treatment by RESOX unit

process, the SO_2 in the gas is converted to elemental sulphur in a fluidized bed of coke.

In the fourth and fifth configurations, the possibility of recycling the product gas back to the gasifier after elemental sulphur recovery is considered(fig. 3.4). In the gasifier, the SO_2 is reconverted back to H_2S and the N_2 is discharged with the coal-derived fuel gas.

In the fourth configuration, it is assumed that much of the product gas is recycled to the bed undergoing regeneration. Only a fixed portion of the product gas needed to control the buildup of N_2 in the system is recycled to the gasifier. In the fifth configuration, it is assumed that all of the product gas is recycled to the gasifier making the regeneration a simple once-through system.

The major effect of the above two configurations is that the raw coal-derived fuel gas will have significantly more sulphur; the sulphur from the coal and the sulphur being recycled. For a fixed cycle time for the sorbent bed, this has the effect of increasing the bed sizes needed for fuel gas desulphurization.

In the sixth configuration, a new concept for regeneration is considered (fig. 3.5). Air is replaced by separate N_2 and O_2 supplies. Regeneration is accomplished in this configuration by adding pure oxygen to a recirculating N_2/SO_2 stream, thereby eliminating the need for tail-gas treatment. The primary trade-off in this configuration is the cost of pure oxygen relative to the cost of treating or recovering the SO_2 in the product gas by a separate process.

Some of the assumptions made in the preliminary process economic studies of the mixed metal oxide process include (1) a plant size of 100 MW (2) a plant availability of 65% (3) a sulphur by-product credit of $70/long ton (4) a sorbent cost of $8.50/lb which assumes a salvage value of 40% for the cobalt titanate sorbent (5) a sorbent life of 3 years (6) a sorbent bed cycle time of 16 hours (8 hours for sulphidation and 8 hours for regeneration) and (7) a product gas in which 25% of the sulphur in the stream is elemental and 75% is SO_2. All of the estimated costs in the economic studies are in January 1984 dollars.

The preliminary economic studies on the six configurations are evaluated. Of the six configurations, the one in which oxygen rather than air was used to regenerate the sulfided sorbents was found to be the most economic. For a 100 MW plant, the capital cost of this configuration is about $110/kW and the impact on the cost of electricity (COE) from the plant is about 6 mills/kWh. The most costly configuration is the one in which all of the tail gas from the regeneration process is recycled to the gasifier (i.e. a single pass regeneration). The estimated capital cost for this configuration is $322/kW and the impact on the COE is 20

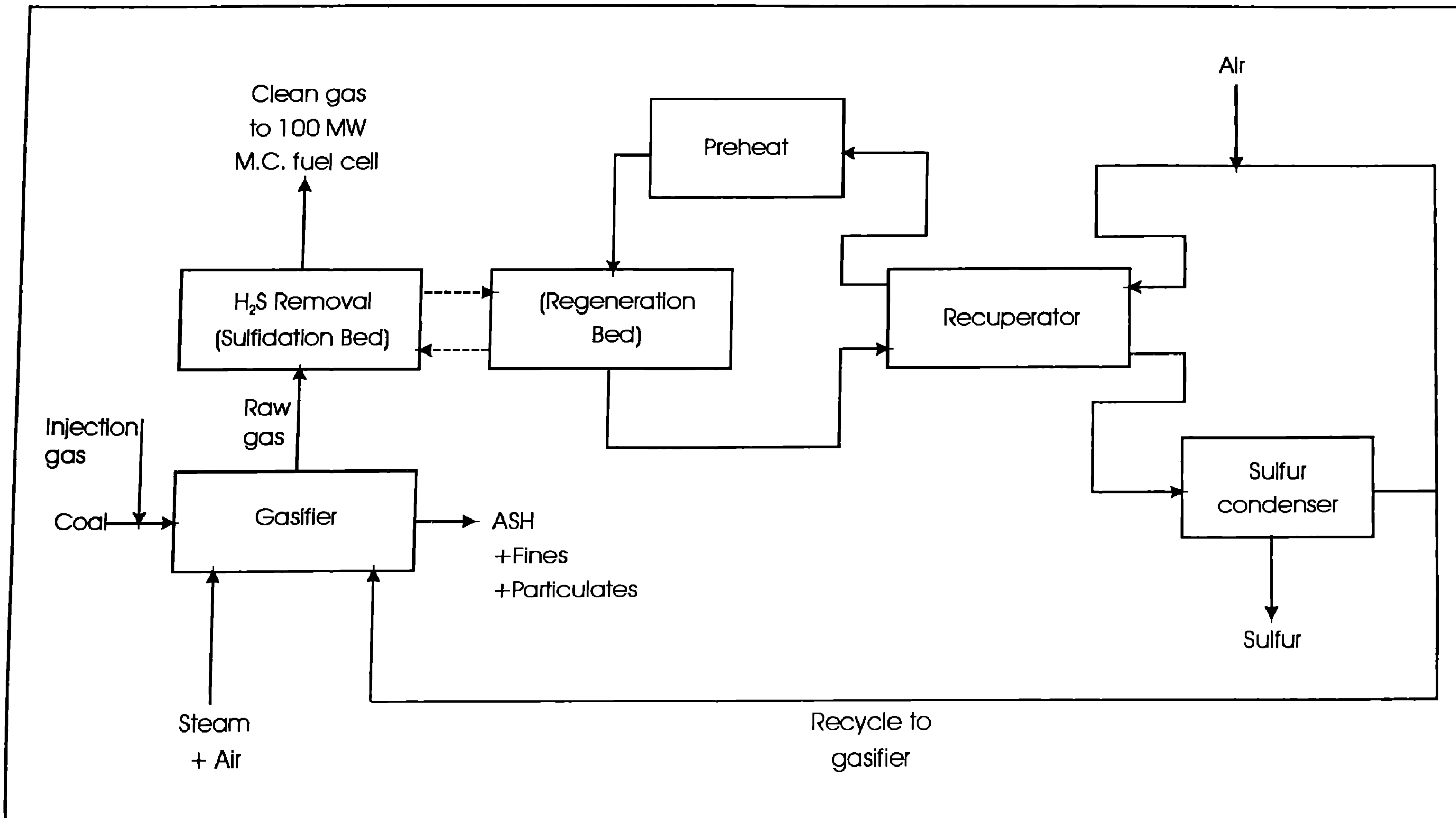


Figure 3.4. Tail gas recycling to gasifier

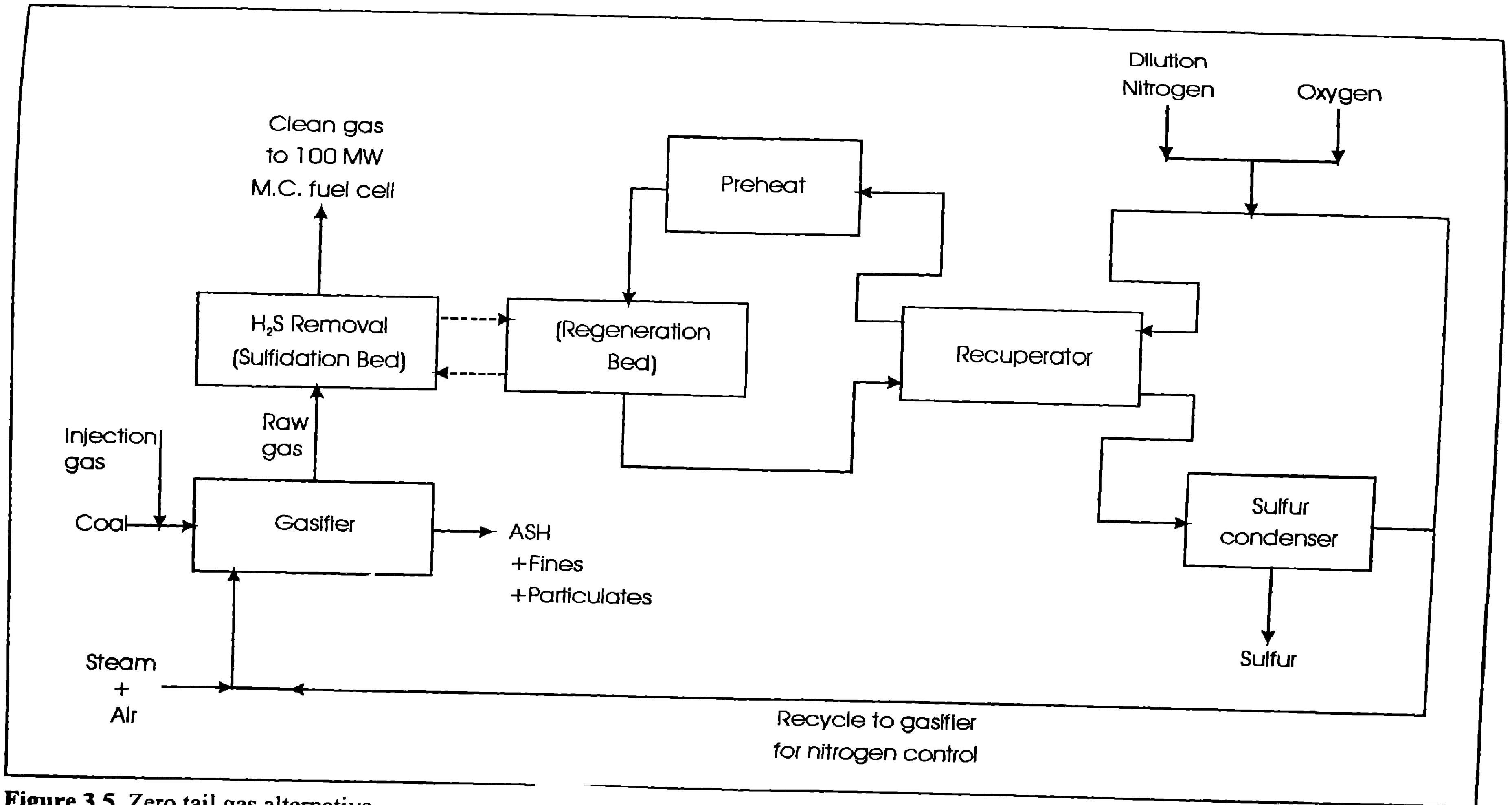


Figure 3.5. Zero tail gas alternative

mills/kWh. The reason for the high cost of this particular approach is the fact that the size of the sorption vessels and the quantity of sorbent required is about four times greater than in the other cases.

All of the remaining configurations evaluated are nearly equivalent in capital cost and impact on the COE. The capital cost of these configurations is about \$150/kW and the impact on the COE is about 8 mills/kWh.

The process economic studies on the IGT molten alkali carbonate sorbent for high temperature HC1 removal assume that the sorbent would be disposed of after use. It is also assumed that the sorbent capacity is 16 lb HC1/100 lb sorbent and that the fuel gas to be treated contains 300 ppm (v) of HC1. With these assumptions, the cost of the sorbent is the overriding cost of this approach.

The cost of the IGT molten alkali carbonate containing sorbent is estimated at \$0.74/lb. This represents \$0.49/lb for the chemicals (magnesium oxide, lithium carbonate, and sodium carbonate) and \$0.25/lb for fabrication of the sorbent. At this cost for the sorbent and assuming a disposal cost of \$40/ton, using this sorbent would cost approximately \$4.75/lb HC1 removed. For a fuel gas containing 300 ppm(v) HC1, the impact on the COE from a coal gasification/molten carbonate fuel cell power plant would be about 5 mills/kWh.

3.3.2.3 Future Work

Based on the findings from this particular project, IGT planned to continue development of both the mixed metal oxide process and the molten alkali carbonate sorbent. In particular, the idea was to conduct optimization studies on the cobalt titanate sorbent and cost reduction studies, including testing, on the molten alkali carbonate sorbent. In these studies, alternative formulations of the cobalt titanate sorbent would be prepared and tested for improved reactivity. The possibility of substituting barium carbonate for some of the expensive lithium carbonate in the molten alkali carbonate sorbent would also be explored. At the conclusion of these studies IGT plans to conduct further bench-scale studies on both the mixed metal oxide process and the molten alkali carbonate sorbent using actual coal-derived fuel gases.

3.4 The Indian Experience

Coal is the largest occurring source of commercial energy in India with the total gross reserves estimated around 83 million tons. Because of the huge reserves of low grade coal (approx. 62 million tons), effective coal utilization via gasification has generated considerable

TABLE 3.4 Commercial coal gasification plants in India

Location	Process	Feedstock	Start year	End Use	Remarks
The Fertilizer Corp. of India, Ramagundam	Koppers-Totzek	Bituminous coal dust	1969	Ammonia synthesis	3 gasifiers; capacity ($CO + H_2$) 2×10^6 m^3/d
The Fertilizer Corp. of India, Talcher	Koppers-Totzek	Bituminous	1970	Ammonia synthesis	3 gasifiers; capacity ($CO + H_2$) 2×10^6 m^3/d
The Fertilizer Corp. of India, Korba	Koppers-Totzek	Bituminous coal dust	1972	Ammonia synthesis	3 gasifiers; capacity ($CO + H_2$) 2×10^6 m^3/d
Neyveli Lignite Corp., Neyveli	Winkler	Lignite	1963	Ammonia synthesis	3 gasifiers; capacity 2×10^4 m^3/h

interest. The initiative was taken by institutions such as Central Fuel Research Institute (CFRI), Dhanbad, which is located in the coal belt. Other organizations like BHEL and IICT joined in later. Besides, several universities and research institutions across the country are also involved in fundamental and exploratory research on coal gasification and related areas. This section presents a brief account of the major developments on pilot scale gasifiers for local coals. A list of important commercial installations is presented in Table 3.4.

One of the earliest gasifiers in the country was a down draft suspension gasification plant developed in 1952 by CFRI, Dhanbad. It employed a 150mm dia. gasifier with a capacity of 30 kg/h of pulverized coal (80% through 200 mesh). Non-caking coal (caking index < 3) of the Raniganj coalfield along with oxygen enriched air were employed in this unit which was used for the production of fuel gas and synthesis gas. A major constraint faced with this system was the continuous need for oxygen enriched air, complete with elaborate safety controls. In addition, periodic cleaning was required to remove the deposits which built up during the course of operation. Once tests with non-caking coals were completed, the plant was dismantled.

CFRI has also evaluated other gasifier designs for their suitability to Indian coals. In order to

utilize the abundantly available low grade, undersized coals for the production of synthesis gas, a pilot plant based on Koppers-Totzek type gasifier was put up in 1958. It was a one-burner type installation with a throughput of 110kg/h of coal and was self- sufficient in all aspects, starting from the preparation of coal up to the final cooling and cleaning of synthesis gas. Several pilot plant tests were carried out with caking bituminous coals from the coalfields of Jambad Bowlah, Lower Kenda, Talcher, Singrauli, Umerer and Argada as well as on the lignite from Neyveli and Kutch coalfields. This installation still exists and is operated intermittently to test coal/lignite at the user's request.

To study the gasification characteristics of non-caking coal along with the possibility of pressure gasification technique, a Lurgi pressure gasifier was developed in 1962. The plant could gasify 0.8 tons of coal per hour using steam-oxygen mixture as the gasifying agent. It was well equipped with a gas cleaning system, tar recovery system and safety devices wherever applicable. This setup was used for the detailed investigation of several non-caking coals viz. bottom seam of Talcher coalfields in Orissa, king seam coal of Singareni (Kothagudem) field in Andhra Pradesh, Dobrana seam coal of Raniganj field in West Bengal and Burhar seam coal of Shahagpur in Madhya Pradesh. The studies established the amenability of Indian coals to pressure gasification without any operational difficulties. The plant operates intermittently as it is used as a test facility whenever a particular type of coal i to be tested.

The Fertilizer Corporation of India, Sindri demonstrated a slagging type gas generator pilot plant using coke with limestone in the early 60's. The gas output varied from 3000-4000 m^3/h and the thermal efficiency of the gasifier was in the 80-90% range. However, this plant was tested only for a short period and has not been operational since the mid-sixties.

Indian Institute of Chemical Technology (IICT), Hyderabad erected a Lurgi pilot plant which has been operational since the mid-80's. The system was designed for 30 bar operation with a capacity of 1 ton coal/h. This installation mainly investigated:

- The oxygen-steam gasification of non-caking Singareni coals for the manufacture of synthesis gas which could be converted to SNG by further catalytic methanation and
- The use of air-steam gasification for the production of fuel gas for combined cycle power generation.

IICT also prepared a techno-economic feasibility report on the basis of pilot-scale tests conducted in 1989-90 on the moving bed dry ash gasification process to evaluate high ash coal from North Karanpura, Bihar. The major parameters investigated were the pressure of operation and the ratio of steam to oxidant in the gasifying medium. It was observed that hig pressure operation results in higher carbon conversion and improves the performance with

reference to composition, specific throughput and heating value of the gas. Higher steam to oxidant ratio, on the contrary, has an adverse effect upon the thermal efficiency of the process. In addition, oxygen-blown gasification is technically superior to air-blown gasification since the calorific value of the output gas is higher because of the absence of inerts. Besides, operating with air requires more number of gasifiers with larger vessel volumes. This study estimated that about 449 t/h of coal would be required to generate a net power of 585.7 MW using 13 air blown gasifiers.

A fixed bed high-pressure gasifier capable of gasifying 6 tons/h of coal to produce 0.4 million m^3/d of clean low-CV gas has been designed by Bharat Heavy Electricals Limited (BHEL). In addition to the gas, by-products such as tar, oil and liquor etc. are also obtained. It was installed and tested as a part of the Combined Cycle Development Plant (CCDP) facilities adjoining their boiler works at Tiruchirapalli. In this process, the gases are burned to drive a gas turbine; this is combined with a steam raising operation driving a steam turbine which improves the efficiency of power generation. The gasifier uses lumpy coal of graded size and 4/is capable of operating at 11 bar in conjunction with the combined cycle plant and at 20-25 bar in an independent mode. The CCDP was commissioned in 1983 and has an electric output of 5 MW. In addition, BHEL has also come up with a Process and Equipment Development Unit (PEDU) for fluidized bed gasification of low grade, less reactive coals for the production of low-CV gas.

3.4.1 Work done by BHEL

Unlike foreign coals, the Indian coals have very high ash content of up to 50%. Bharat Heavy Electricals Limited (BHEL) is committed to utilize this low grade fuel for generation of electrical power. Pressurized Fluidised Bed Gasification (PFBG) has been identified as the best route for that. BHEL developed a 18 TPD PFBG at Coal Research Facilities, Hyderabad. Based on the experience of 18 TPD PFBG, BHEL embarked upon designing and retrofitting a 150 TPD PFBG to CCDP at Trichy. Neither 18 TPD nor 150 TPD Gasifier was incorporated with any kind of system which can improve upon the gasification efficiency by recovering the substantial energy being lost through unburnt carbon. In this regard two processes such as slagging as well as agglomeration are being tried elsewhere. But unlike Indian coals, foreign coals have high sulphur, low ash content and low ash fusion temperature. As a result of low ash content, the fraction of unreacted carbon in bed ash will be more in comparison to that of Indian coals which have very high ash content. Moreover the ash fusion temperature in case of Indian coals is higher than that of foreign coals. Therefore, the developmental effort to enhance the carbon conversion efficiency may be suitable by the slagging and ash agglomeration processes for foreign coals. In case of Indian coal, slagging and agglomeration require higher heat input as well as high temperature combustion, making the option

unsuitable. Therefore, there was a need to develop an indigenous method to minimise the unburnt carbon loss from the PFBG, developed by BHEL. To serve this purpose, the 150 TPD gasifier was designed with a cyclone ash recycling system which conveys the cyclone fines using clean cold fuel gas. However, as the conveying gas will absorb heat in the gasifier it may affect adversely the overall performance of the gasifier.

With this in view, BHEL has developed a fluidised bed gasifier integrated with a carbon burn up system at the bottom of the gasifier to arrest the carbon loss through the bottom ash removal and a recycle of cyclone fines system to arrest the elutriated carbon loss from the gasifier. The plant consists of gasifier, carbon burn up system, cyclones, coal feeding system, ash extraction system, exhaust system and steam generator. The gasifier is a 200 mm I.D. internally refractory lined vessel. The diameter of refractory lined free board varies from 200 mm at the bottom to 250 mm at the top. The distributor is of perforated conical type. Air steam mixture is introduced into the air plenum and passes through the distributor. Coal is fed pneumatically into the gasifier above the distributor. To recover the energy loss from the unburnt carbon with bed ash the carbon burn up system, a fluidised bed combustor, is coupled with the gasifier right below the air plenum-distributor assemble. The ash withdrawal system is connected at the bottom of the combustor. The cyclone fines collected in the first cyclone is recycled back into the gasifier simply by gravity without the assistance of any external agency.

Finally, the gas, escaping from the first cyclone, passes through the second cyclone and pressure let down valve and reaches the chimney to get flared up. The hydrodynamics and control of twin fluidised bed along with gravity flow recycling of cyclone fines were studied in a cold model test rig. Separately, a number of tests were conducted using high ash Indian coal. The gasifier bed was operated at around 950°C with superficial velocity around 1.1 m/sec. The combustor bed temperature was varied between 750°C to 800°C. It was found that the unburnt carbon in the discharged bed ash was reduced to nearly 0.2%. The process schematic of BHEL's coal gasification plantis shown in fig 3.6.

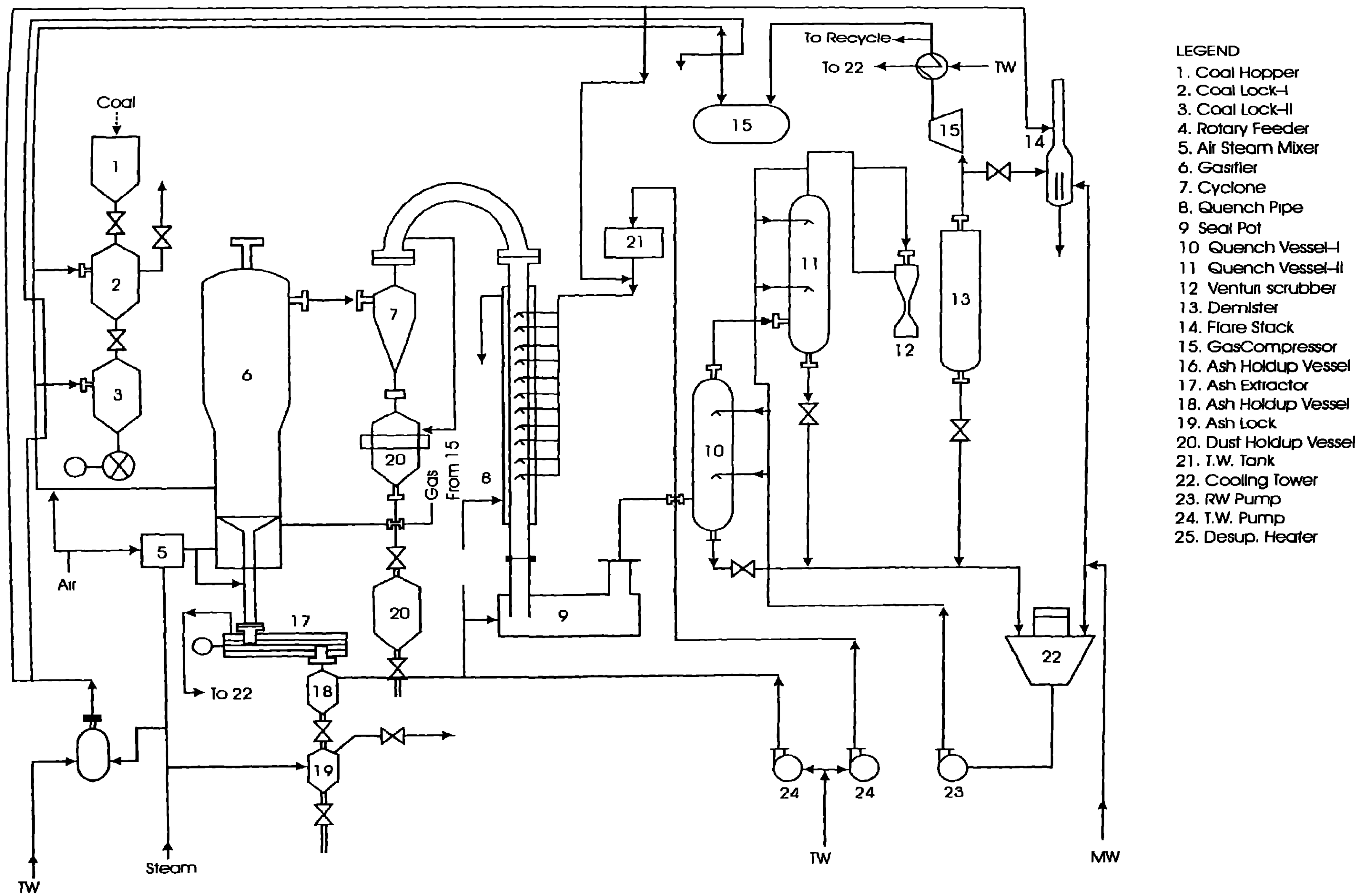


Figure 3.6. BHEL's pressurized fluidized bed coal gasification (PFBG) schematic

CHAPTER 4

MCFC DEVELOPMENT AT TERI

TERI's earlier work on fuel cells was in the area of phosphoric acid fuel cells (PAFC) as it was felt that small PAFC systems could be set up as decentralized power plants in rural areas. In fact, the technical feasibility of power generation from PAFC using reformed biogas was demonstrated using an imported 2.5 kW PAFC stack and a biogas fuel processer built by TERI. The complete system was located at the Okhla municipal sewage treatment plant at Delhi. Subsequently, as the potential of the high temperature fuel cell to use coal gas as a fuel was realized, the focus of TERI's activities has been to further understand and introduce this technology to India so that coal based power generation in the country would become more efficient and environmental friendly. However, since Indian coals are characterized by high ash content, it was felt, based upon previous experience, that imported coal gasification technologies designed for superior coals may not be readily adaptable to Indian coals.

A separate study was therefore, considered necessary in order to assess the performance of a molten carbonate fuel cell using Indian coal gas. The original plan was to assemble the single cells using electrodes and electrolyte matrix procured from research or commercial groups abroad for carrying out tests with pure H_2 and simulated coal gas. However, it turned out that this idea was not feasible; therefore, this group had to develop the MCFC components from scratch. Though the information contained in the published literature served as a starting point, the actual methodology was seldom described in detail. Thus, this group had to rely almost entirely upon a "trial-and-error" approach in arriving at suitable procedures for the fabrication of the single cell components viz. the electrodes and the electrolyte matrix. Several methods which were tried are summarized in Tables 4.1 and 4.2. The following sections describe the typical experimental methodology and the corresponding results.

Table 4.1 Methods tested for electrode fabrication at TERI during this project

Method	Remarks
Cold pressing & *in-situ* sintering	• Very low porosity (10-20%) • Breaks while removing from die • Difficult to fabricate large size thin elecrodes
Hot pressing & *in-situ* sintering	• Breaks due to rapid evaporation of solvents during heating • Time-consuming process • Difficult to fabricate large size thin elecrodes
Doctor blade method	• Getting appropriate slip rheology, porosity and strength involves a large number of trials • Improvements possible either by changing the ingredients and/or the mixing ratio of the ingredients*
Rolling and sintering	• Electrode bends during sintering • Carbon deposits on the surface creates a barrier to gas diffusion • Sintering has to be done externally prior to cell assembly
Rolling with reinforcement	• Potential for making larger electrodes and in large quantities, as needed for a stack, appears uncertain • Bending of electrode reduced drastically • Also acts as a current collector with high collection efficiency
Powder sintering	• Reproducibility of the electrode quality is difficult as controlling porosity requires very sophisticated vacuum facilities • Conceptually, perhaps the simplest method • Could be considered sometime in the future

*** This method appears to be most promising at present. It would be followed in subsequent studies, as it can give repeatable quality. It can also be adopted for continuous production in a tape casting method.**

Table 4.2 **Methods tested at TERI for electrolyte matrix preparation**

Methods	**Remarks**
Cold pressing & heating at 1000°C	• Matrix breaks while removing from the die • Matrix crumbles to a powder after heat treatment • Method discontinued at present
Cold pressing using different binders	• Matrix breaks while removing from the die • Matrix crumbles to a powder after heat treatment • Method discontinued at present
Cold pressing of electrolyte (with binders and solvent) with the ceramic support	• Matrix edges break while removing from the die • Carbonate melts upon heating (but regains shape and strength at room temperature) • Difficult to fabricate large matrices
Heating of separate tapes of carbonate mixture and ceramic support	• Carbonate tapes are highly hygroscopic and need to be stored with care • Matrix loses its shape once the binders are burnt out • This method would be tested further with a better ceramic matrix and in a more controlled manner
Heating a single tape of ceramic & electrolyte powder at 525 °C	• Matrix becomes a semisolid support to the electrolyte at cell operating temperatures • Also acts as a gas sealant*
Sintering a tape of ceramic matrix, followed by electrolyte impregnation	• Preliminary results appear inconclusive • Further evaluation required regarding strength of the sintered matrix under compression

*It appears that there is some inhomogeneity due to phase separation.

4.1 Experimental methodology

This section deals with the experimental methods adopted during the course of this project for the preparation, characterization and evaluation of various components and sub-components of both the electrolyte retainer matrix as well as the electrodes.

4.1.1 Component development

4.1.12.1 Anode Fabrication

The pure nickel powder for the anode (negative, fuel supplying electrode) was purchased from Aldrich Chemicals and had the following specifications :

Particle size	: 3 micron
Purity	: 99.7%
Specific gravity	: 8.9.

Method 1: The nickel powder, organic binder, organic solvent and surfactant were mixed together to form a thick paste which was then rolled to form a green tape of uniform thickness. This tape was pasted onto a SS-310 wire mesh which acts as the current collector. We decided to employ a current collector since it was observed to increase the current collection efficiency during the monocell tests. A further improvement in current collection was observed by replacing the SS wire mesh with a 1mm thick perforated nickel plate. As mentioned previously in Table 4.1, several other techniques of electrode fabrication were also tested. In most of the cases, no reinforcement was used and the anodes were sintered *in-situ*. The *in-situ* sintering has the problem of carbon deposition from the binder but this limitation was overcome by sintering in a controlled environment.

The characteristics of a typical nickel anode fabricated in our laboratory (fig. 4.1) was as follows :

Thickness	: 0.6 ± 0.02 mm
Reinforcement	: SS304 (60 mesh)
Current collection	: Perforated Nickel plate
Size :	: 70 mm (dia.)

Method 2: The nickel powder was mixed with the binders viz. polyethylene glycol and polyvinyl alcohol and cast in a die to form a green electrode of required size and uniform thickness. The porosity of the electrode was controlled by adjusting the quantity of the binder in the mixture. The green anode was sintered at 1273 °K for 3 h in a nitrogen atmosphere. The ratio of the substrate to the binder in our studies was in the range of 60:40 by weight in order to obtain a porosity of 60%.

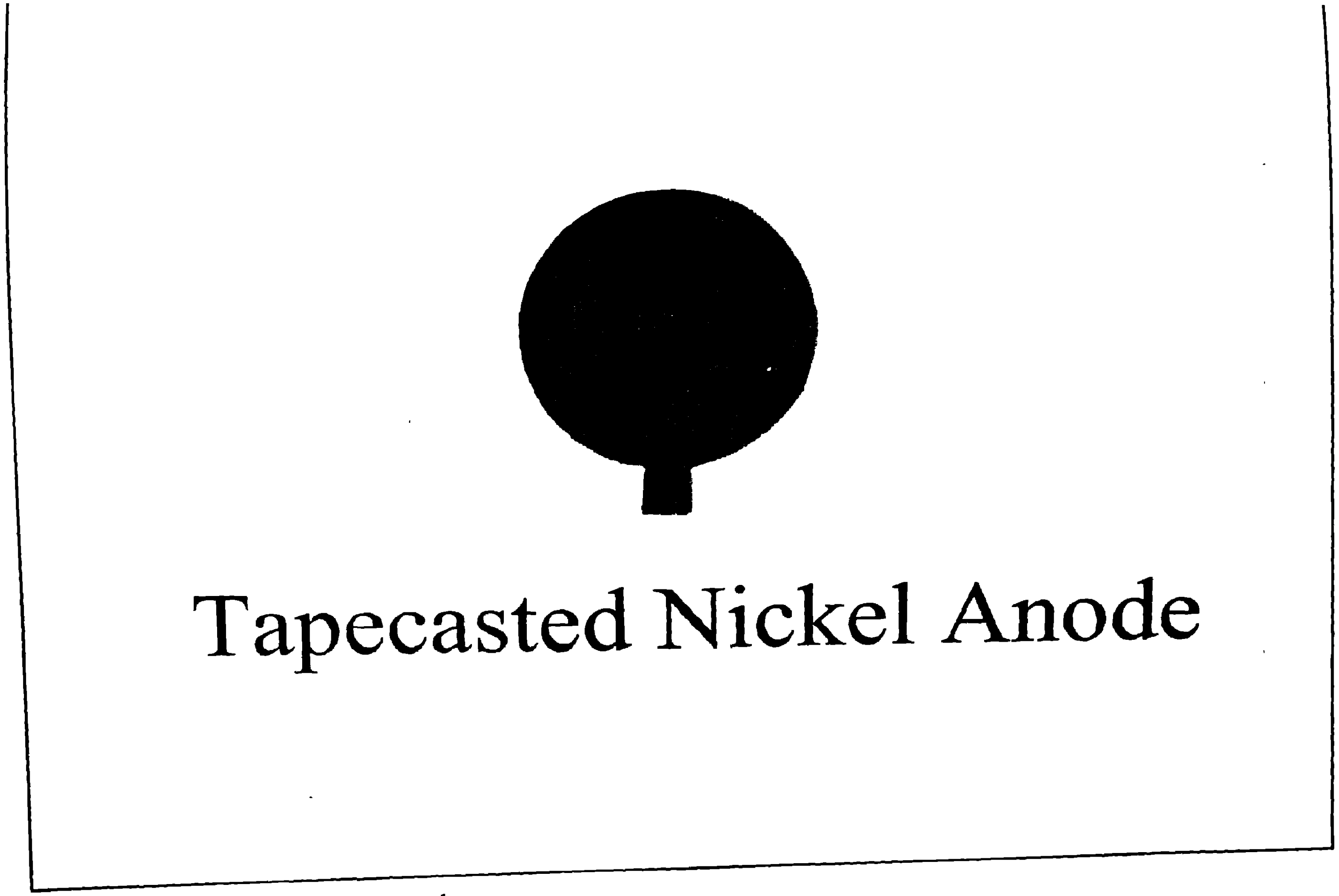


Figure 4.1. MCFC single cell – anode

4.1.1.2 Cathode Fabrication

Method 1 : The cathode (positive, oxidant supplying electrode) was prepared from pure nickel powder having a thin coating of NiO on its surface. The preparation methodology was broadly similar to that for the anode. The nickel powder, organic binder, organic solvent and surfactant were mixed together to form a thick paste which was then rolled to form a green tape of uniform thickness. The tape thus formed was then pasted on a SS-310 wire mesh which acts as electron supplier. Prior to this method, other methods without electrode reinforcement were used and the cathodes were sintered *in-situ*. However, *in-situ* sintering has the problem of electrode cracking. This problem is yet to be solved. No nickel oxide was employed directly in the cathode preparation. The *in-situ* oxidation of the electrode in the cell housing in the presence of air and oxygen brought about the oxidation of the surface layer to give a thin coating of nickel oxide. This oxidation of the nickel contact surface was aided by the molten salt atmosphere near the tile-electrode interface.

The characteristics of the cathode developed by this group (fig.4.2) were as follows :

Material	: Nickel with a NiO surface
Thickness	: 0.5 ± 0.02 mm
Reinforcement	: SS304 (60 mesh)
Size	: 70 mm (dia.)

Method 2: A slurry of powdered nickel, polyvinyl alcohol and polyethylene glycol was cast in a die (dia. 25mm), dried and sintered at 973 °K in an inert (nitrogen) atmosphere for 1 hour to obtain a porous Ni plate. The Ni plate was dipped in 1M $AgNO_3$ solution for 30 minutes before calcination at 1323 °K for 10 minutes to get the cathode composite containing sintered NiO on the the surface. The porosity of the electrode was controlled by varying the ratio of Ni powder to the binder content. The composition used was 5-10 g polyvinyl alcohol and 5-10 g polyethylene glycol for every 100g of Ni to get a porosity of 55% (Appendix-III).

4.1.2.2 Matrix

The electrolyte matrix in an MCFC acts as the electrolyte retainer without taking part in the electrochemical reaction. Its major function is to hold the electrolyte in its capillary pores and thus prevent

i) mixing of fuel and oxidant gases (gas cross-over leading to direct chemical reaction or combustion).

ii) free flow of the molten electrolyte and

iii) rapid evaporation loss of the electrolyte.

In addition, the carbonate ions have to be efficiently transported from the cathode to the anode, in order to sustain the fuel cell current output. However, the matrix also causes ohmic polarization which ultimately reduces the cell performance.

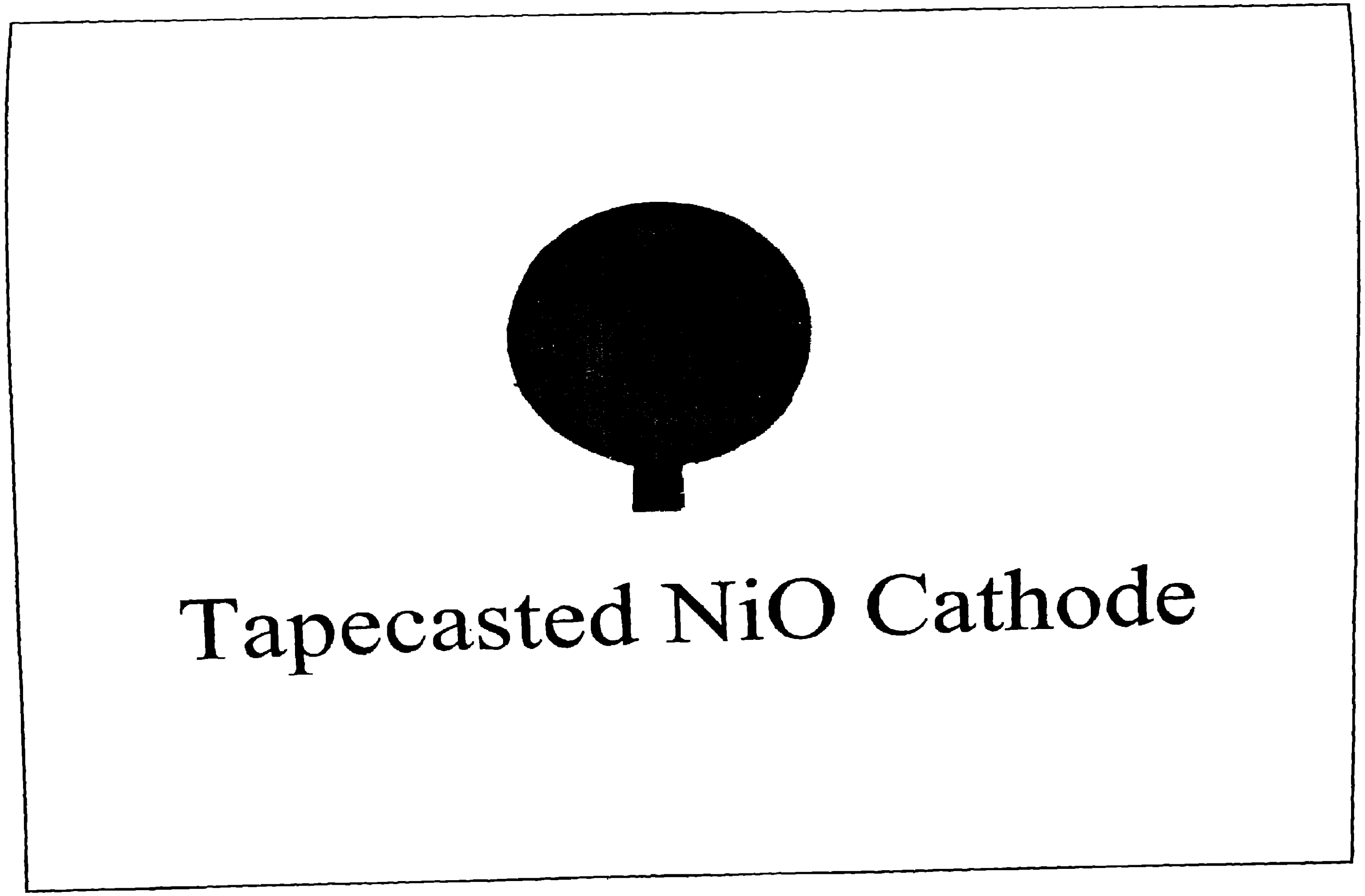


Figure 4.2. MCFC single cell – cathode

The following sub-sections describe the matrix composition as well as the fabrication methods which were tried at TERI.

Selection and Preparation of Ceramic Powder: The basic material for the matrix is the ceramic powder which plays a vital role in holding the molten electrolyte in place in the MCFC. The electrolyte is a solid binary or ternary eutectic of alkali carbonates at room temperature which becomes a liquid at the cell operating temperature of 650°C. $LiAlO_2$ was identified as the ceramic material for the fabrication of matrix tiles since it possesses better electrical resistivity, thermal stability and mechanical strength as compared to other ceramics like magnesia (MgO) and alumina (Al_2O_3). More specifically, the gamma (γ) form of $LiAlO_2$ was chosen since this is the only form which is stable at the high operating temperature of the MCFC. The preparation involved heating an equimolar mixture of Li_2CO_3 and alumina to form α $LiAlO_2$ which was sintered at 1273°K for 24 hours to obtain γ $LiAlO_2$. In the earlier stages of the project, the γ $LiAlO_2$ had to be prepared in-house but presently, the group is working with γ $LiAlO_2$ procured from a commercial supplier in the U.S.A.

Electrolyte Composition: The eutectic binary mixture contains 62 mol% Li_2CO_3 and 38 mol% K_2CO_3. The ratio of the binder to the rest of the components (carbonate mixture and ceramic powder) was around 1:8 by weight. The ratio of carbonate mixture to the ceramic powder can be adjusted as per the requirement. The composition in our experiments was approximately ceramic powder 42 wt%, carbonate mixture 47% and organic binder 11 wt% which resulted in a porosity of 60%. At 923°K, which is the operating temperature of the MCFC, the percentage filling would be about 90%.

Fabrication - Two-tape method: In this method two separate tapes were made - one from the ceramic support (lithium-aluminate) and the other from the carbonate salt mixture (lithium and potassium carbonate).

The γ-$LiAlO_2$ was suspended in methanol with poly-vinylalcohol as a binder and polyethylene glycol as the plasticizer. The mixture was ground in a ceramic ball mill for 24 h and then concentrated in a rotary evaporator in order to control the viscosity of the mixture slurry. The matrix tape was prepared by tapecasting the slurry with a doctor blade (fig. 4.3) assembly fabricated in our laboratory. A salt tape was also fabricated in a similar fashion. The porosity of the matrix, after burning out organic compound, was 65% at room temperature (as indicated by mercury intrusion porosimetery). The tapes were then heated at 520°C to melt the carbonate mixture. The salt volume was calculated from the salt weight and its density at room temperature *(ref: P.L. Spedding, J. Electrochem. Soc. 117(2) 177(1970))*. The electrolyte loading ratio was defined as follows :

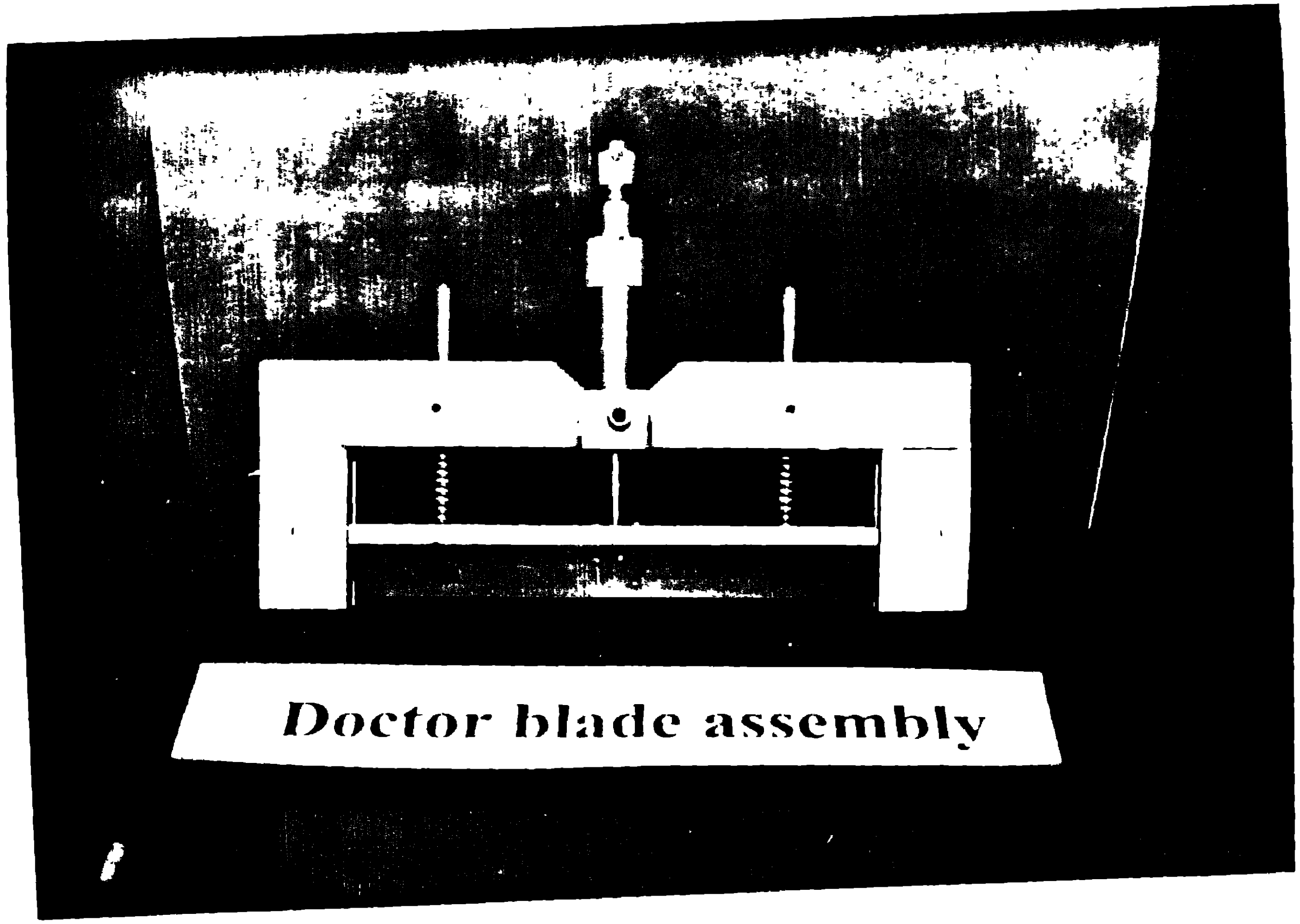


Figure 4.3. Doctor blade assembly used for the fabrication of electrolyte matrix, as well as elctrodes

$$\text{ELR} = V_{salt} / V_{matrix\ pore}$$

where V_{salt} = salt volume at room temperature

$V_{matrix\ pore}$ = matrix pore volume at room temperature.

However, since the potassium-carbonate is highly hygroscopic, this technique was found unsuitable. A variation of this method is now being tested.

Fabrication - Single-tape method: This method involves the preparation of one single tape containing both the ceramic support and electrolyte mixture. The ceramic powder was subjected to dry grinding in a ball mill with agate jars using 5mm diameter agate balls in order to remove coarse particles. The powder was then mixed with poly vinyl alcohol(binder) and poly ethylene glycol(plasticizer). This slurry was ground in a ball mill for a fixed time till thorough mixing occurred. Thereafter, the electrolyte eutectic mixture was added and the grinding continued until a paste with the required slip characteristics was obtained. The paste was then caste into 1mm thick sheets using a doctor blade assembly. The tape formed was dried at a lower temperature followed by heating at a temperature just above the melting point of the electrolyte. The resulting tape was used in the monocell testing (a typical matrix tape is shown in fig. 4.4). This method displayed excellent reproducibility. An observation of the matrix indicates that the ceramic support does not form a solid structure but is retained inbetween the electrodes as a semi-solid fluid. The edges of this matrix act as gas sealant and hence no external sealant is required in the monocell.

4.1.2 Non- Electrochemical Characterization

Non-electrochemical characterization of the base materials used for electrode and matrix fabrication encompasses

i) Surface characterization, which consists of both physio-sorption and chemisorption measurements and

ii) Structural characterization, which involves estimation of pore size and pore volume distribution as well as the crystalline structure of the ceramic material.

4.1.2 Surface Characterization

BET Surface area determination

The BET surface area was determined using the multipoint method on a Quantasorb Jr. (Quantachrome, USA – fig.4.5) surface area analyzer which operates on the Nelson Eggertsen Dynamic Flow Method.

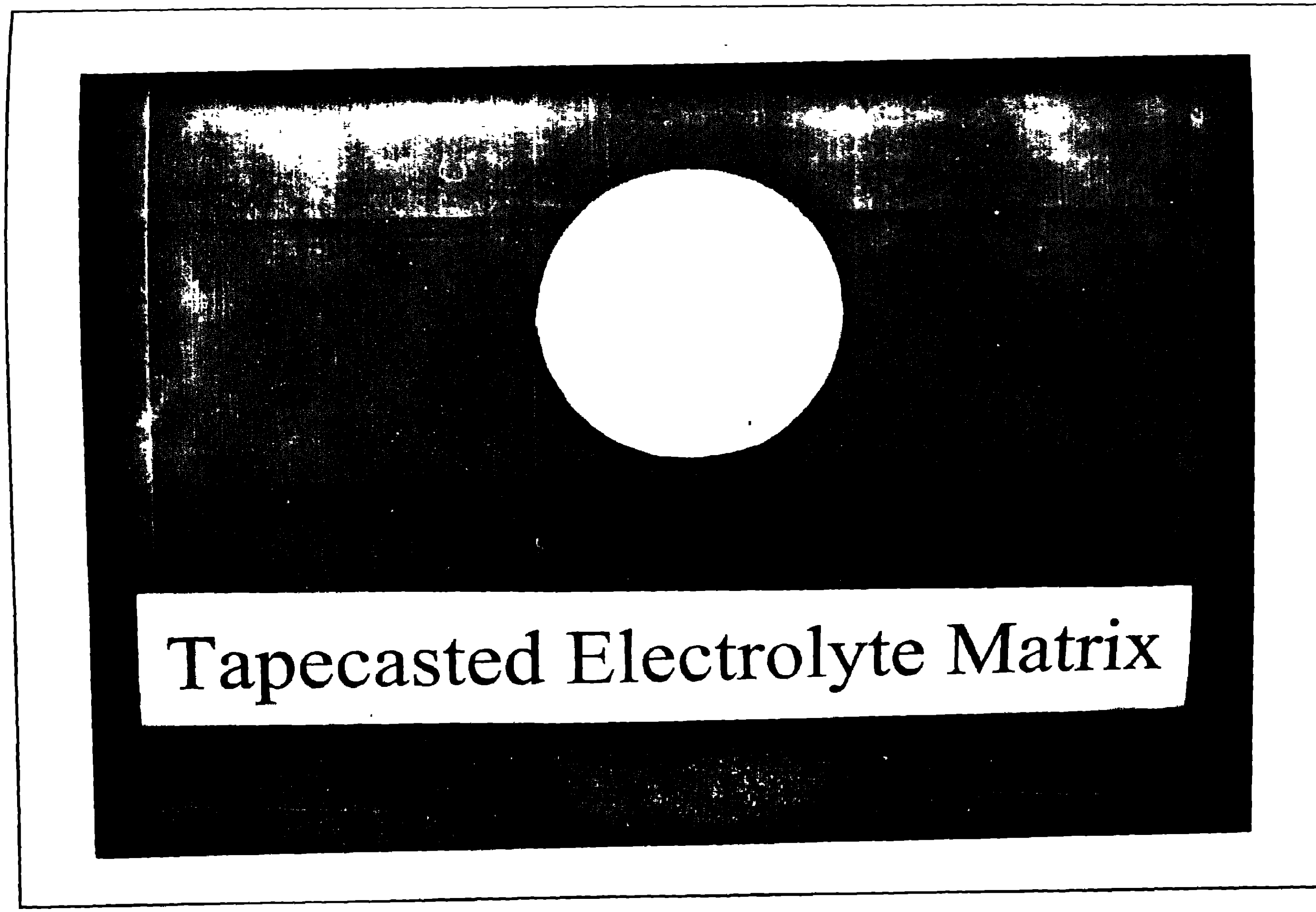


Figure 4.4. Electrolyte matrix prepared using doctor blade assembly

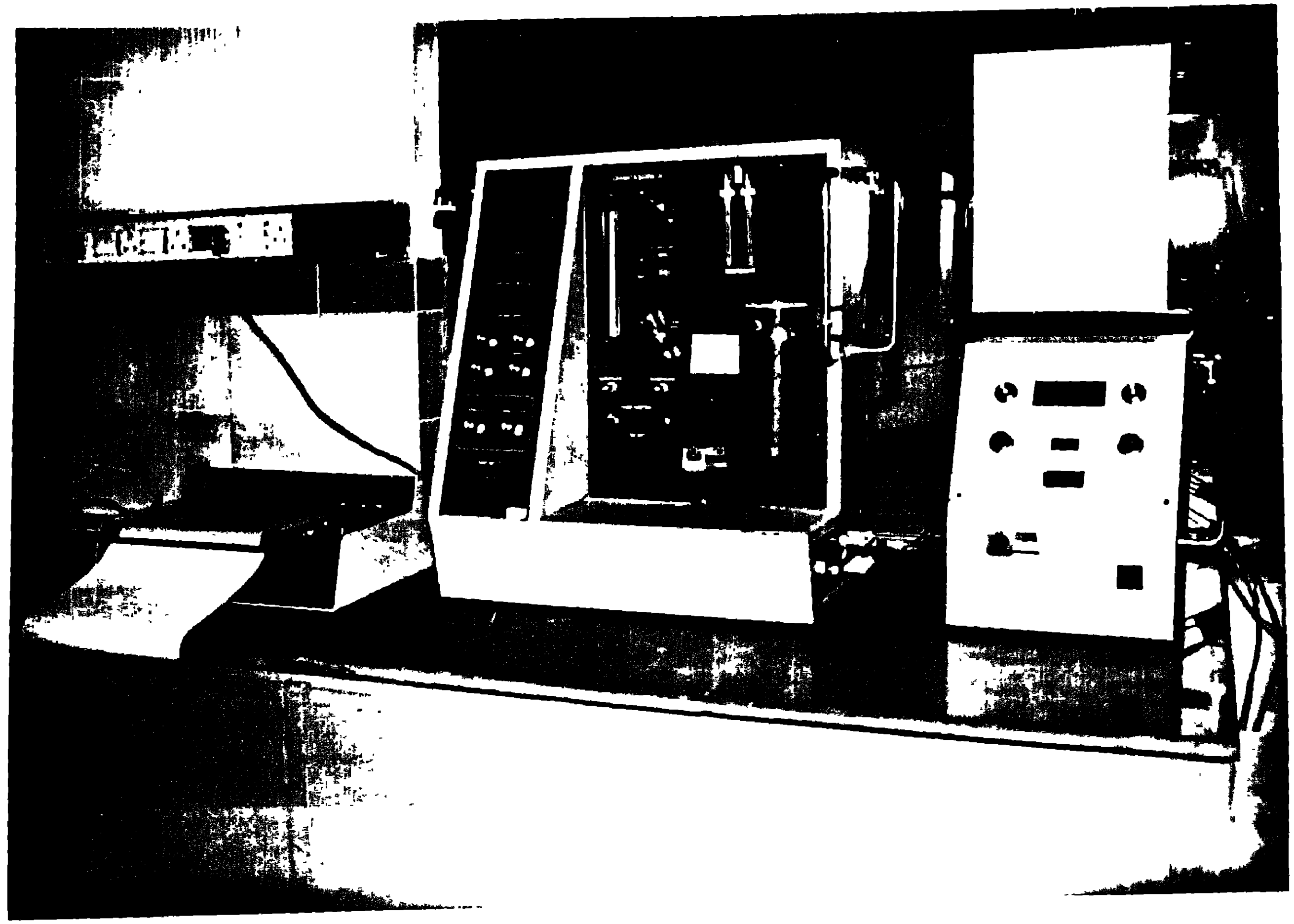


Figure 4.5. BET surface area analyzer (shown with the linear mass flow controller on right)

The technique involves immersing the sample in liquid nitrogen kept in a Dewar flask and then adsorbing a known amount of the adsorbate gas (N_2). The ratio of the adsorbate with respect to the carrier gas (He) is kept fixed. The process of adsorption and desorption was monitored by a thermal conductivity detector on the basis of changes in thermal conductivity as a result of adsorption of the N_2 from its mixture with He. The adsorption and desorption peaks were automatically integrated by a built-in integrator; in addition, a printout of these peaks was obtained on a strip chart recorder (Curken, USA). The adsorption and desorption peaks were calibrated for each gas composition vis-a-vis a known quantity of N_2 injected in the 'IN' septum port. There are three critical parameters in the BET surface area determination viz. the weight of the sample, relative pressure of the adsorbate gas to the carrier and the weight of the adsorbate adsorbed on the sample surface at several relative pressures in the range $0.05 < P/P_0 < 0.35$. The weight of the sample was measured by an electronic balance, once the degassing was complete. The relative gas flow rates were adjusted using a linear mass flow controller accessory. The weight of the adsorbate adsorbed on the sample surface at any given pressure was calculated from the ideal gas equation. The integration counts due to desorption (desorption peaks were preferred because of their truer gaussian nature as compared to adsorption peaks) are compared with those from the calibration of the standard. The total surface area (S_t) was calculated from the following equation :

$$S_t = \frac{X_m N A_{cs}}{M_a}$$

where

X_m=

M_a = Adorbate molecular weight

N = Avogadro's number

A_{cs} = Cross-sectional area of adsorbate molecule.

The specific surface area is given by :

$$Specific\ surface\ area = \frac{S_t}{weight\ of\ the\ sample}$$

Consistency of this result can be confirmed via single point BET calculation for $P/P_0 = 0.30$ using the following expression :

$$S_t = \frac{A}{A_{cal}} V_{cal} A_{cs} \frac{P_a N}{RT} (1 - \frac{P}{P_o})$$

Chemisorption Methods

The experiments were conducted once again on a Quantasorb Jr. sorption instrument by the pulse chemisorption method described by Kovalinka and Scolsen. The methodology involves gassing out the sample in helium at 723°K for one hour followed by cooling the sample to room temperature with the helium flushing continued for another ten minutes. The gas was then changed to hydrogen with a simultaneous stepping up of the temperature at the rate of 10 K/min to 723°K. The sample was then reduced at this temperature for two hours. Thereafter, the gas flow was changed to helium and the heating mantle was removed to allow the sample to cool down to room temperature. Once the sample attained ambient temperature, the gas was changed to nitrogen. At the same time, hydrogen gas was allowed to fill the injection loop (loop volume $1 cm^3$). The sample was then subjected to repeated cycles of hydrogen injections with the integrated peak areas being noted after each injection. The process was continued till the integrated peak areas were within 1%. The volume of gas adsorbed was estimated by :

$$V_{ads}^{stp} = \Sigma \left[\frac{A_c - A_i}{A_c}\right] V_c \left[\frac{273}{273 + T_{amb}}\right] \frac{P_a}{760}$$

where

A_c = Area of unadsorbed injection signals

A_i = Area of partially adsorbed signals

V_c = Volume of hydrogen injected.

Here

$$V_{ads}^{stp} = V_{hydrogen} \; [ml \; H_2 \; (STP)/gram]$$

4.1.2.2 Structural Characterization

The structural characterization mainly involves determining the pore volume and pore size distribution. We have employed two methods namely physiosorption and mercury porosimetery for this purpose.

Physio-sorption method

While evaluation of the specific surface area involves the lower part of the adsorption isotherm i.e $0.05 < P/P_o < 0.35$, the estimation of pore size and cumulative pore volume

distribution involves the entire desorption isotherms. The calculations are usually based on the desorption isotherm data because it represents the lower equilibrium branch of the isotherm which is closer to the ideal thermodynamically stable conditions. Normally, while using the dynamic flow method, nitrogen is the preferred adsorbate since it is extensively characterized. The dynamic flow desorption technique employed by us evaluates not only the pore size and cumulative pore volumes, but also the equilibrium vapour pressure of a covered surface (such as a liquid in a capillary or pore) to the equilibrium pressure of the same liquid on a plane surface by the following relationship :

$$\ln\left[\frac{P}{P_o}\right] = -\frac{2}{r_k}\gamma\frac{V_{mol}}{R\,T}\cos\theta$$

where

r_k	=	Kelvin radius of the capillary pore
γ	=	surface tension of the liquid (8.85 erg/cm^2 at 77.4°K which is the b.p. of N_2)
V	=	molar volume of the liquid (34.7 cm^3 for N_2)
θ	=	contact angle (0° for N_2)
R	=	universal gas constant (8.13 x 10^7 ergs deg^{-1} mol^{-1})

Mercury porosimetry method

Mercury porosimetry is based on the capillary law governing liquid penetration into small pores. In the case of a non-wetting liquid like mercury filled in cylinderical pores, the situation is described by the Washburn equation :

$$D = -\left[\frac{1}{P}\right] 4\ \gamma\ \cos\phi$$

where

D = pore diameter

P = applied force

γ = surface tension

ϕ = angle of contact

The volume of mercury V penetrating the pores is measured directly as a function of applied pressure by the Poresizer 9320 (Micromeretics, U.S.A. fig. 4.6)). The Poresizer 9320 is a 30,000(207 MPa) mercury porosimeter covering the diameter range from approximately 360 to 0.006μm. The unit has two built-in low pressure ports and one high pressure chamber.

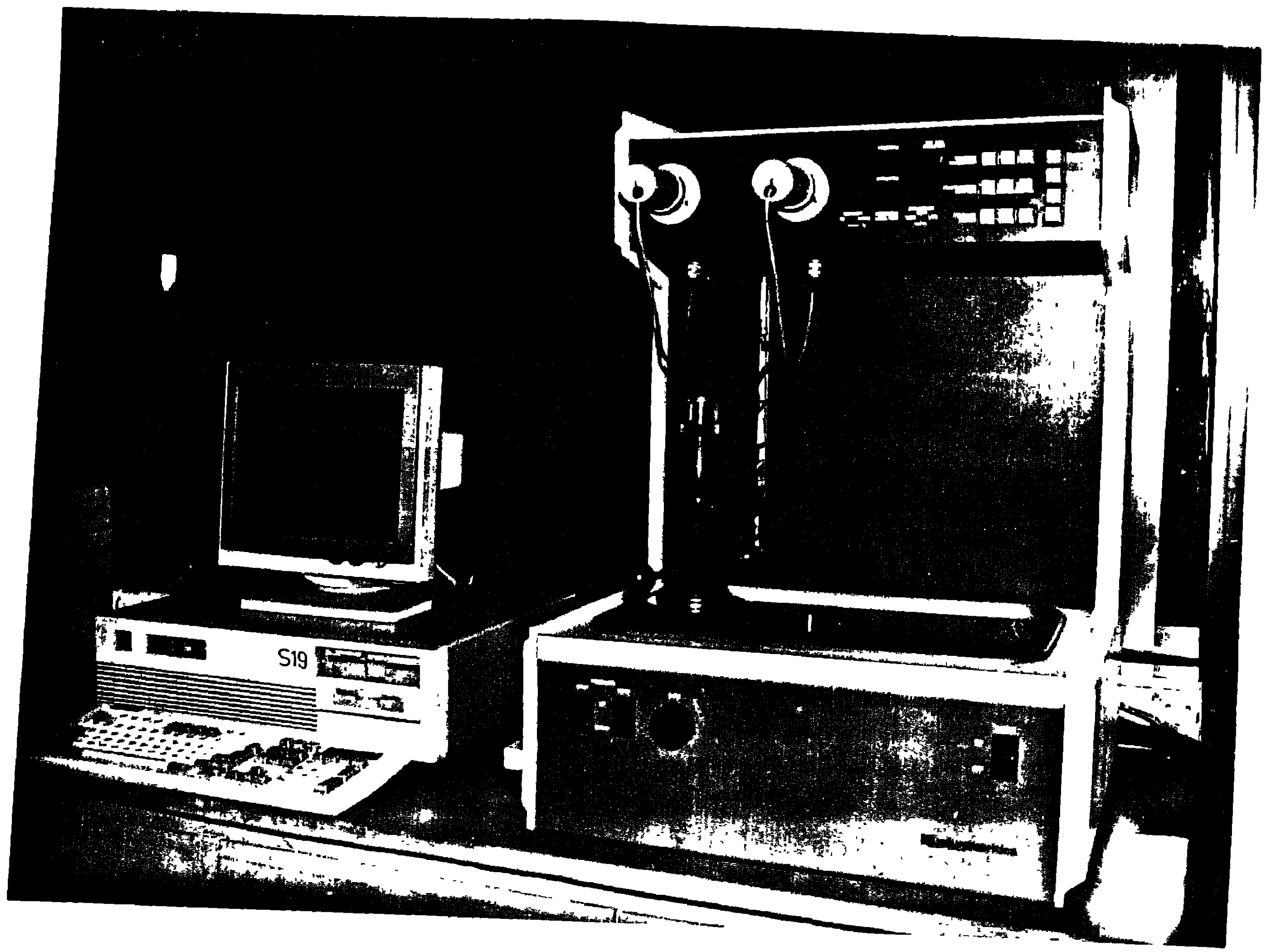


Figure 4.6. Mercury porosimeter

Data collection, data reduction and data display are processed by a dedicated personal computer. The poresizer measures the volume distribution of pores in materials by mercury intrusion or extrusion. Mercury has a high surface tension and is non-wetting to all materials with the exception of a few noble metals. These properties cause a moving surface in contact with a solid to assume the minimum surface area and the largest radius of curvature at a given pressure. An increase in pressure on mercury shifts the balance between the surface tensions and the surface area causing the radius of curvature of the mercury contacting the solid to become smaller; when the radius is equal to that of a pore entrance, mercury fills the volume within the pores.

4.2 Results

4.2.1 *Optimization of α $LiAlO_2$ preparation*

The α-$LiAlO_2$ was prepared by heating Li_2CO_3 and Al_2O_3 at different temperatures to evaluate the optimum conditions for its preparation. The results of a preliminary mass balance analysis are summarized in Table 4.3.

Table 4.3 Effect of temperature on α-$LiAlO_2$ preparation

sample no.	sample weight (g)	temperature (°K)	Heating duration (h)	stirring	final weight (g) observed	final weight (g) expected	% deviation
A	B	C	D	E	F	G	$\frac{F-G}{B-G}$
1	17.6	873	10.00	no	17.1	13.2	88.64
2	15.6	923	3.50	no	14.9	13.2	70.83
3	12.8	973	3.25	yes	11.9	11.7	18.18
4	9.2	973	4.00	yes	7.6	7.6	12.50
5	17.6	973	10.00	no	13.2	13.2	55.00
6	17.6	973	10.00	yes	13.2	13.2	2.50

From these results, it was observed that after heating at 973 °K for 3.25 h, the percentage deviation was 18.18, while after 4 hours it was reduced to 6.67. It shows that the rate of reaction is very high between these times. Hence, during the remaining course of 6h (assuming the reaction to be completed in 10 h), the deviation should reduce and finally approach zero at the end of 10h. Keeping this in mind, sample nos. 5 and 6 were treated at 973 °K for 10 h. During this period, sample 6 was stirred intermittently to have a well mixed blend of the unreacted components. A comparison of the percentage deviation of the stirred and un-stirred showed the value for the unstirred one to be 55% while that of the stirred one was only 2.5%. This is possibly because of the formation of $LiAlO_2$ at the top surface which effectively acts as a gas barrier and thus prevents removal of the CO_2 formed during the reaction.. This results in a chemical equilibrium in an isolated environment and no further conversion takes place. During the process, the temperature of the mixture was not raised above 973 °K in order to avoid the chemical decomposition of Li_2CO_3 (melting point 891 °K). Since this reaction takes place when Li_2CO_3 is in the liquid state, it is essentailly a solid-liquid reaction.

The conversion of lithium aluminate from its α-form to γ-form was performed as per the procedure mentioned in the published literature viz. heating α-$LiAlO_2$ at 1273 °K for 24 h. The final product was sent for X-ray diffraction (XRD) analysis to Indian Institute of Technology, Bombay. The results of the XRD analysis confirmed that the powder prepared was γ-$LiAlO_2$. Table 4.4 presents a comparison of the XRD data obtained for the samples prepared at TERI with that of standard γ-$LiAlO_2$.

Table 4.4 **Comparison of γ-lithium aluminate XRD data : TERI sample vs. standard**

Observed			Standard			
2θ (°)	d (A°)	I/I°	2θ (°)	d (A°)	I/I°	hKl
22.8	3.896	100	22.296	3.984	100	101
24.87	3.576	14	24.369	3.650	40	100
28.80	3.096	26	28.267	3.155	50	111
33.83	2.646	80	33.395	2.681	90	102
35.20	2.547	92	34.687	2.584	90	200
42.10	2.144	12	41.599	2.169	30	211
48.00	1.893	13	48.867	1.862	50	212
50.70	1.798	9	50.228	1.815	30	113
56.68	1.622	15	56.252	1.634	30	310
58.80	1.569	9	58.364	1.580	30	311
61.87	1.498	46	61.420	1.508	80	302
65.00	1.433	5	66.943	1.397	10	321
70.55	1.333	16	70.147	1.340	50	204
72.82	1.297	22	72.428	1.304	70	322
78.82	1.282	10	78.455	1.218	70	214

4.2.2 Electrode Structure Analysis & Porosity

Porosity is defined as the ratio of the voids to the solid volume and is usually expressed in percentage. It is the major non-electrochemical parameter that affects the cell performance. The pore size distribution of porous electrodes is yet another fundamental parameter determining the extent to which the available surface of the electrocatalyst participates in the electrochemical reaction. A large porosity indicates that a larger surface area is available for the electrocatalyst to react. With the same porosity, the distribution of the pore size also changes the cell performance. Molten electrolyte can penetrate deeply into the smaller size pores and hence small size pores act as electrolytic network. Electrolytes have less tendency to penetrate into the larger pores but the gases penetrate into these pores easily as the pressure gradient is small. So the large reticulate pores act as reactant gas supplier. At the medium agglomerate size pores the mixing of the reactant gas and electrolyte takes place and so does the chemical reaction. Electrodes were fabricated using calculated amount of material to achieve the desired porosity. The porosity of the fabricated electrodes was measured by the mercury porosimeter method.The electrodes were analysed after sintering in a porosimeter to determine the porosity and get an idea about the pore size distribution and total pore volume.

The observed porosity by mercury intrusion was higher than the expected porosity in each case. This is possibly because of the calculation assumption all the pore spaces of the electrode are filled with binder. But in reality there are micro-pores which remain unfilled even during the compaction of the mixture upto the desired thickness. Thus the binder only fills the comparatively larger pores.

The bending strength of the fabricated electrodes as observed from the simple hand tests is quite high. The strength of the electrodes can be further increased by allowing the crystals to have a stronger bonding among themselves. This can be achieved by sintering the electrodes for a longer duration.

4.2.3 Half-Cell Test

This test enables an independent evaluation of anodic and cathodic activities (depending upon whether hydrogen or oxygen(air) is passed through the working electrode holder) vis-a-vis a reference electrode. For molten carbonate fuel cell this test was done by Joseph M. King, Jr.(1977) of UTC Connecticut, USA. As the kinetic reaction rates of MCFC are very high, the half-cell test, besides being very complex is also less significant. On the other hand, the mono-cell test provides a good indication of the MCFC endurance and thus is more reliable

from the viewpoint of evaluating material suitability. The procedure for the half-cell test of MCFC is also not fully developed and hence was not carried out in our laboratory.

4.2.4 *MCFC Mono-Cell*

The monocell unit used in the first phase of MCFC work consists of two SS310 identical blocks of 90 mm x 90mm x 30mm size having a central circular groove (7mm diameter) to hold the electrodes. These are the porous gas diffusion electrodes developed according to the methodologies discussed in Sec. 4.1. They are placed with one side facing the grooved ends of the housing and the other facing the electrolyte matrix. The electrolyte matrix is applied separately in between the two electrodes. A 1cm cavity at the back of grooved side acts as the housing for the electrical heaters, which are used for direct heating of the cell housing to the MCFC operating temperature. The electrodes rest upon centrally sawtooth groove tips (pitch 3 mm and depth 3mm), which provide the uniform gas (fuel or oxidant depending upon whether it is the anode or the cathode) distribution on one side of the electrode. Non-porous sawtooth grooves on blocks for gas distribution are integrated in the mono-cell housing block. The grooves have a 3mm pitch with 3mm depth with an angle of 60° at the edge. So when the anode and cathode plates are placed on the grooves the stress produced is evenly distributed and gradually stress density decreases. The housing material is chosen to be stainless steel 310 since it has a high resistance to CO_2 at 650°C. A very fine thin perforated sheet is placed inbetween the electrodes and the sawtooth to reduce the effect of local stress concentration on the electrode. The plate simultaneously acts as a current collector. The blocks act as output teminals. To prevent the short circuit between the terminal a thin mica sheet is placed between the blocks. The blocks are kept together using tie rods, nuts and bolts. To prevent the short circuit due to tie rods and nuts, asbestos sheets are used in between the tie rods and blocks. The effective electrode area is only 3.14 x 3.5 cm x 3.5 cm ie 38.465 sq. cm. To prevent the gas cross-over, the sealing was done by using ceramic powder ($LiAlO_2$). This material is not only impervious to the gases, it is also corrosion resistant and possesses good compressiblity. At the high operating temperature of the MCFC, the edge seals are provided by the molten carbonate itself.

4.2.5 *Gas distribution and safety system*

Gases were fed from cylinders through the inlets provided in the anode and cathode block.The pure gases were purchased locally and were of IOLAR grade purity. The gas flow rates into the mono-cell were controlled through ball rotameters (Instrumentation Engineers, Hyderabad). Separate rotameters were used for each of the anode as well as cathode gas components. Details of the composition of the simulated coal gas, along with the flow rates employed, is listed in Table 4.5. Since the simulated coal gas contains toxic and explosive gases like carbonmonoxide and hydrogen, a safety system was incorporated in the mono-cell

set up. The entire test rig was kept in a room with exhaust fan and a five channel gas monitor (Subtronics, Bombay) with a provision for different gas detector attachments to check any leakage or accumulation of the dangerous gases in the vicinity of the test facility.

4.2.6 Gas Analysis

A sampling port was incorporated in the inlets of the cathode as well as the anode for withdrawing gas samples for chromatographic analysis. Samples were regularly taken from these collection ports and analysed on a Nucon 5700 gas chromatograph (GC) to estimate the gas compositions. Pure argon with a flow rate of 20-30ml/min was used as the carrier gas. All runs were performed using a carbosphere 80-100 mesh column and a thermal conductivity detector (TCD). Separate calibration runs were carried out for each of the gases using standard samples. This was followed by a calibration gas mixtures which would help in estimating the % composition of the various components in the feed gases.

4.2.7 MCFC monocell testing

The fuel cell stack consists of a number of single cells connected either in series or in a series and parallel combination to produce the desired potential and current. Hence the performance of the single cell directly affects the performance of the stack/module. The mono-cell was assembled using the anode, cathode and matrix developed at TERI. The cell output was measured using high accuracy voltmeters and ammeters and the data was continuously recorded using an 8 channel datalogger (Polycorder Model 704, Omnidata, USA). Single cell tests (commonly known as mono-cell tests) were initially carried out using the ideal gases hydrogen, oxygen and carbon-dioxide. The anode gas (hydrogen) was later replaced by simulated coal gas and the mono-cell performance was compared in the two cases.

Figures 4.7 & 4.8 shows the overall layout of the single cell test rig.

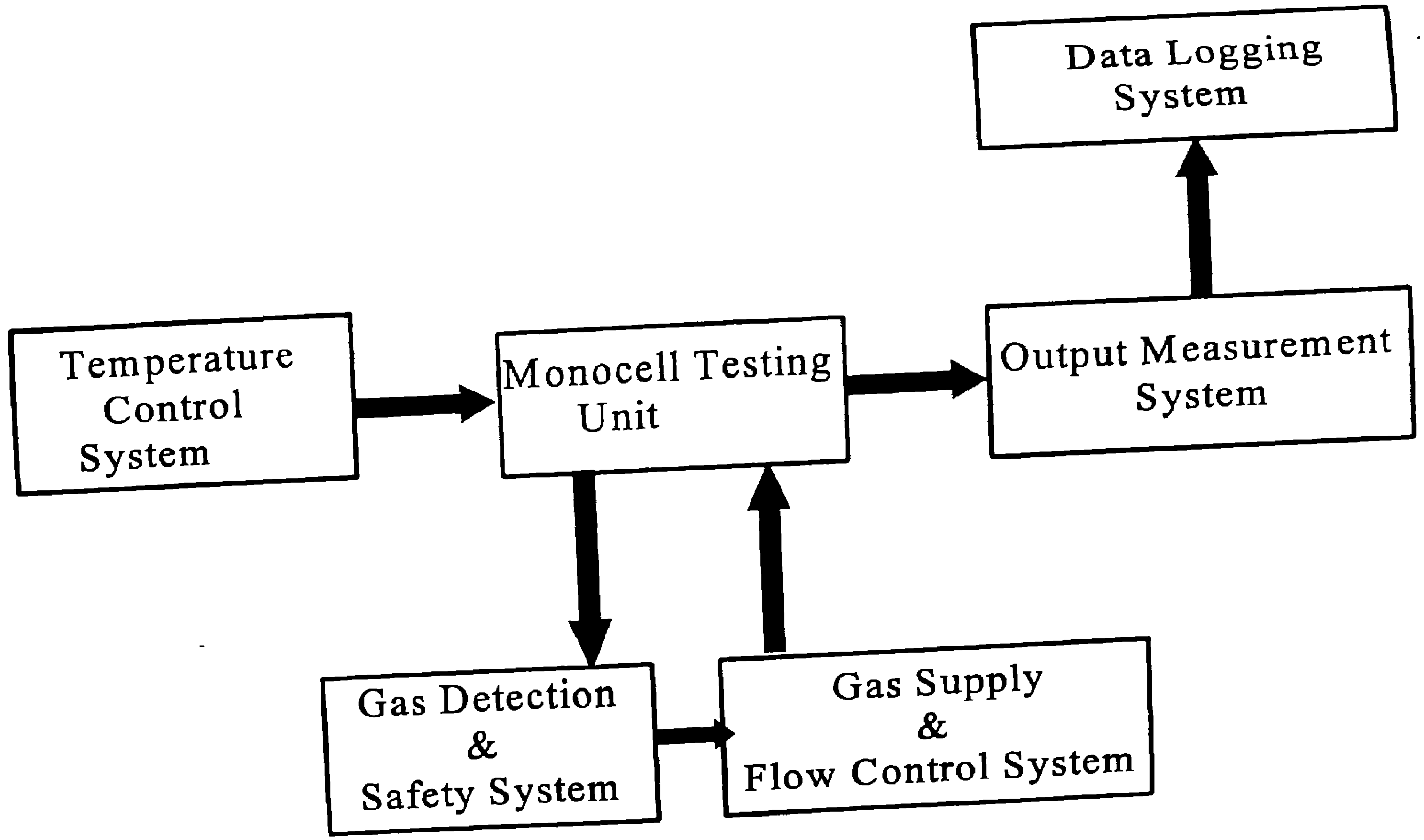


Figure 4.7. Block diagram of monocell testing facility

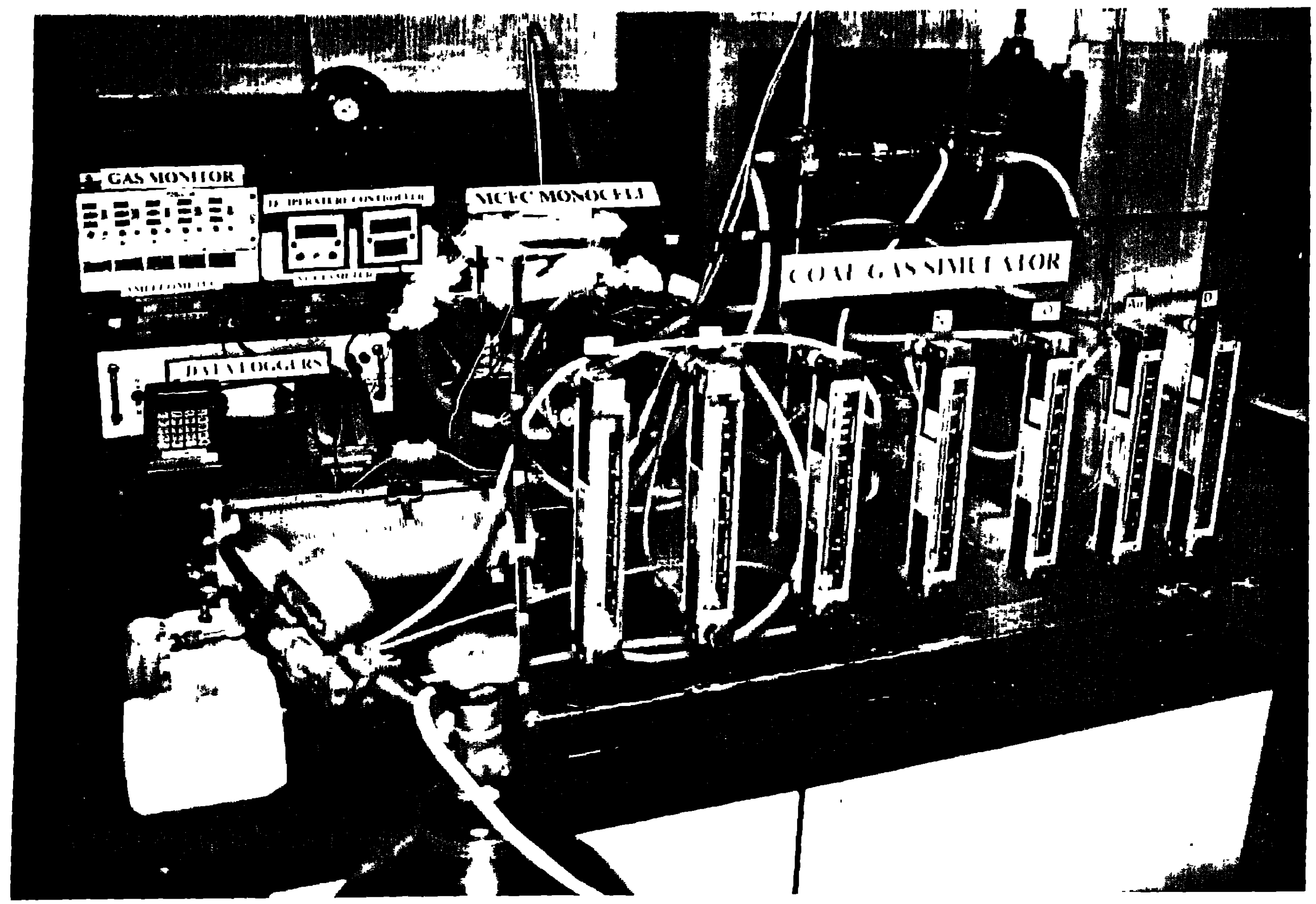


Figure 4.8. View of monocell test set up using simulated coal gas

The overall set up also shows the gas distribution system which enables the measurement of the gas flow rates to the anode and the cathode. The anode input gas is hydrogen and carbon dioxide and the cathode input gas is a mixture of air and carbon dioxide. The CO_2 is supplied externally as it should not be diluted at the anode and oxgen interface. The whole set up is heated using electrical heaters in the cell block cavities. Electrical output is tapped from the two blocks through nickel current collector (anode side) and SS mesh (cathode side). The voltage and current are measured at different loading using two Kiethley model 197 digital multimeters. The electrical control systems enable the setting of fixed current inputs (galvanostatic) to the mono-cell for measuring the corresponding output in terms of voltage via digital multimeter.

Monocell testing procedure

The monocell assembly is brought to the operating temperature of 650°C gradually, by controlled heating. During this stage, the anode and the cathode are supplied with essentially inert gases. When the temperature reaches 625°C, gradual introduction of hydrogen to the anode is started. Recording of the cell temperature, gas flow rates, cell voltage and current is also started at this point, using the datalogger. The open circuit voltage begins to build up at this stage. When the voltage reaches a stable value, electrical load is applied, again gradually. This is done until the voltage drops to a low level, where sustaining a current through the external resistance becomes difficult. When simulated coal gas is used, the same procedure is followed initially, i.e. up to the introduction of hydrogen. After this stage, the other constituents of the coal gas, viz. carbon monoxide and nitrogen are introduced. The gas mixture samples are periodically analysed and the flowmeters (rotameters) adjusted from time to time to compensate for pressure variations in the various gases.

Sample experimental results are summarized in Tables 4.5 and 4.6.

TERI REPORT NO. 93CE61(1996)

Table 4.5 Coal gas compositions & experimental gas flow rates for mono-cell testing at TERI

Anode Feed	**Coal Type**							
	Singareni		Singareni/NK		N.K		N.K	
Gas	Vol % (Dry Basis)	Flow Rate (cc/min)	Vol % (Dry Basis)	Flow Rate (cc/min)	Vol % (Dry Basis)	Flow Rate (cc/min)	Vol % (Dry Basis)	Flow Rate (cc/min)
CO_2	13.4	39.5	14.00	45.29	12.4	33.9	13.5	36.8
CO	11.2	33	10.2	33	12.05	33	12.1	33
H_2	12.8	37.76	12.8	41.6	13.11	35.9	12.58	34.3
N_2	61.5	181.57	62.06	200.7	61.41	168.17	60.77	165.73
O_2	0.2	---	---	---	---	---	---	---

Table 4.6 **Monocell performance : pure hydrogen vs. simulated coal gas**

Parameter	**Pure hydrogen**	**Simulated coal gas**
Open Circuit Voltage	0.844 V	0.723V
Maximum Power Drawn	156 mW	100 mW
Minimum Voltage	0.528V	0.398V
Maximum Current	0.297 A	0.229 A
Maximum current density at which power drawn	35 mA/cm^2	30 mA/cm

Modifications / improvements

We are still continuing the monocell testing, with regular improvements /modifications in the cell components (anode, cathode and matrix). Some of the improvements currently underway are:

- Fabrication of a new monocell block with an electrode area of 150 cm^2 with improved gas distribution channels (fig. 4.9). Work is also under way to develop electrodes and electrolyte matrix of that size.
- Improvements in the procedures for making of electrodes and electrolyte matrix
- Minimizing the contact resistances in the fuel cell output measurement circuit
- Use of mass flow controllers for controlling the gas flow rates, and to better monitor the effect of change in gas compositions on the cell output
- Procurement of a tapecasting machine, where the existing doctor blade assembly can be used – this would allow controlled, slightly faster and repeatable 'runs' while making the electrodes and matrix.

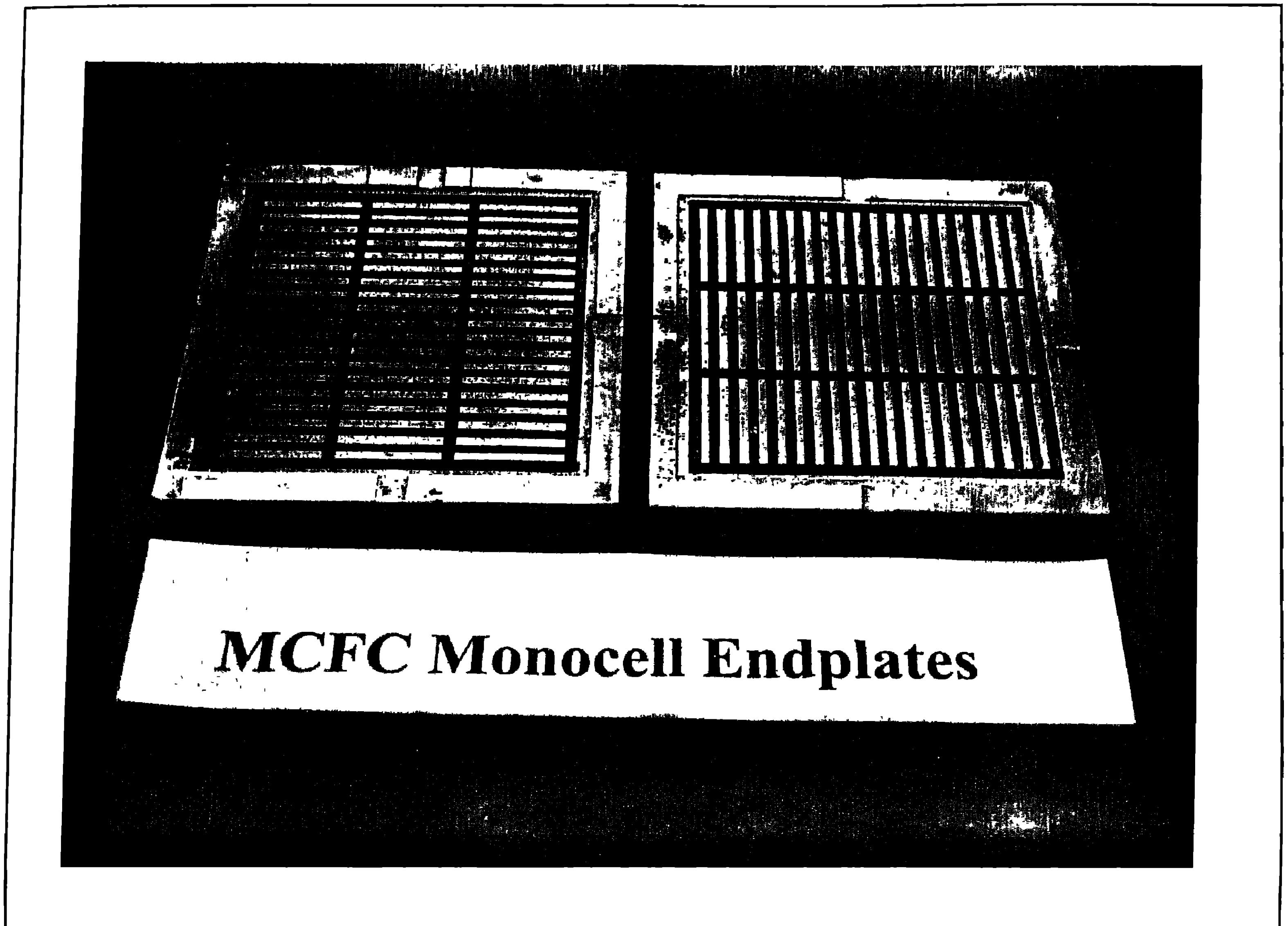


Figure 4.9. Monocell endplates

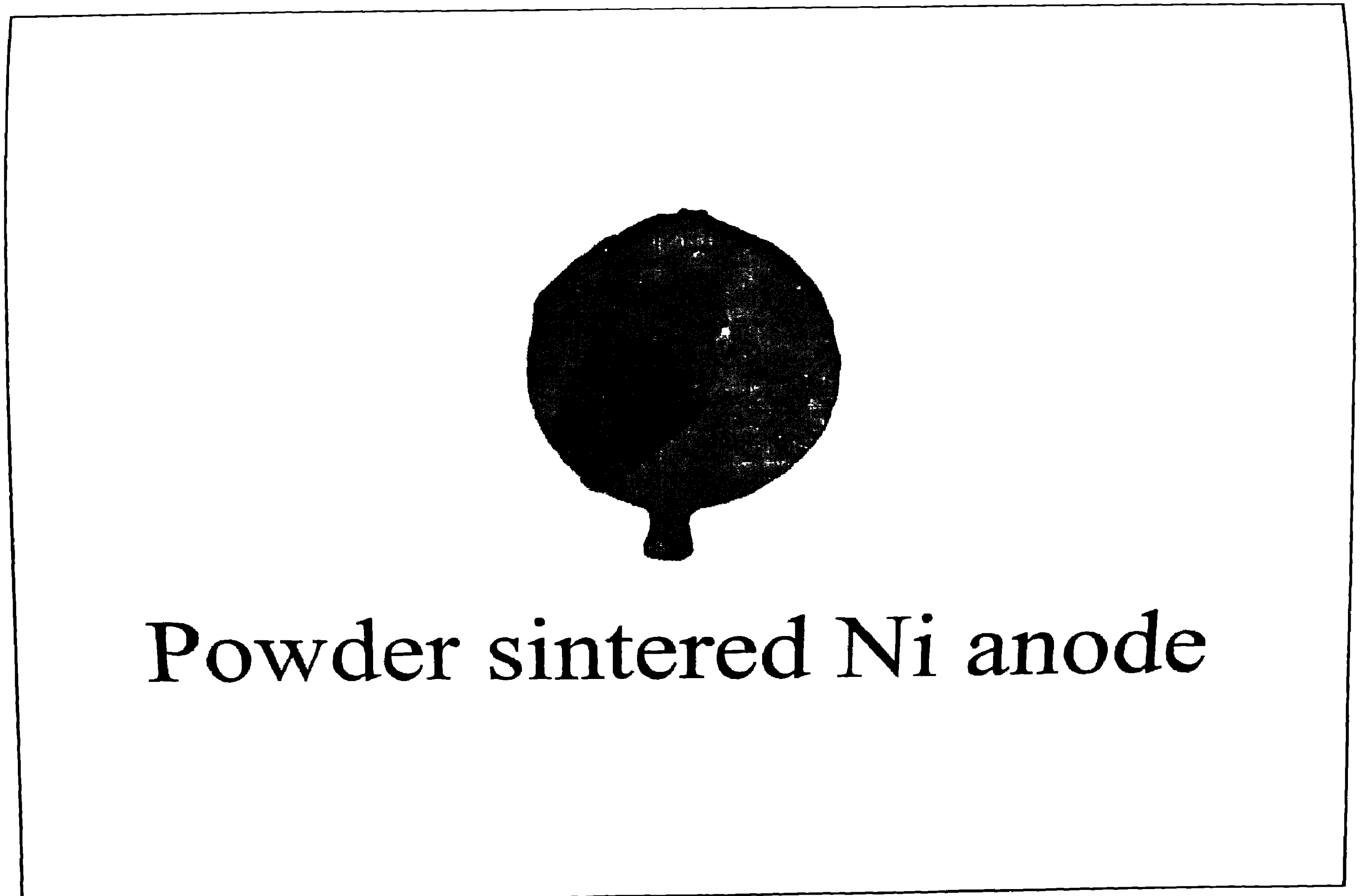


Figure 4.10. Powder-sintered Ni anode

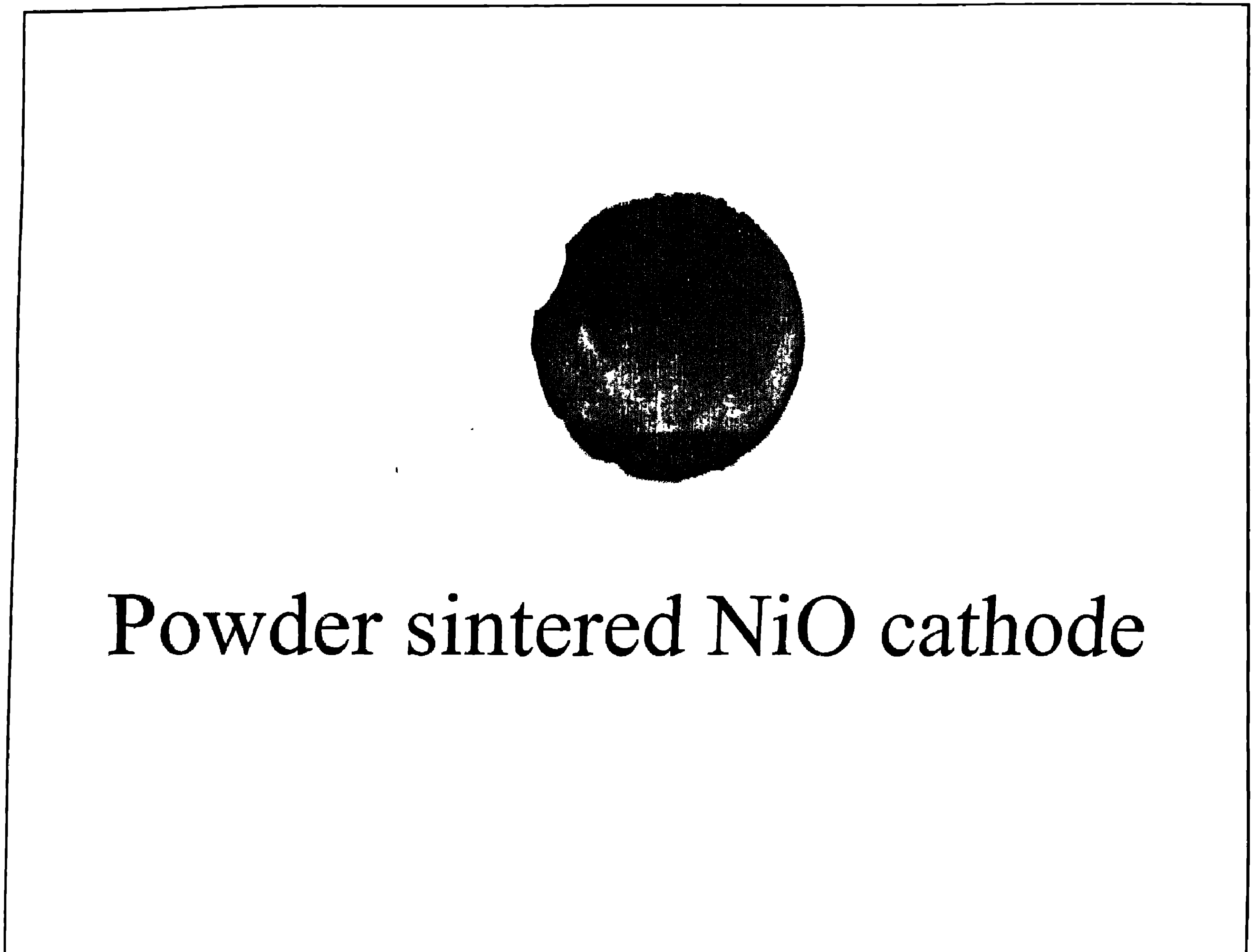


Figure 4.11. Powder-sintered NiO cathode

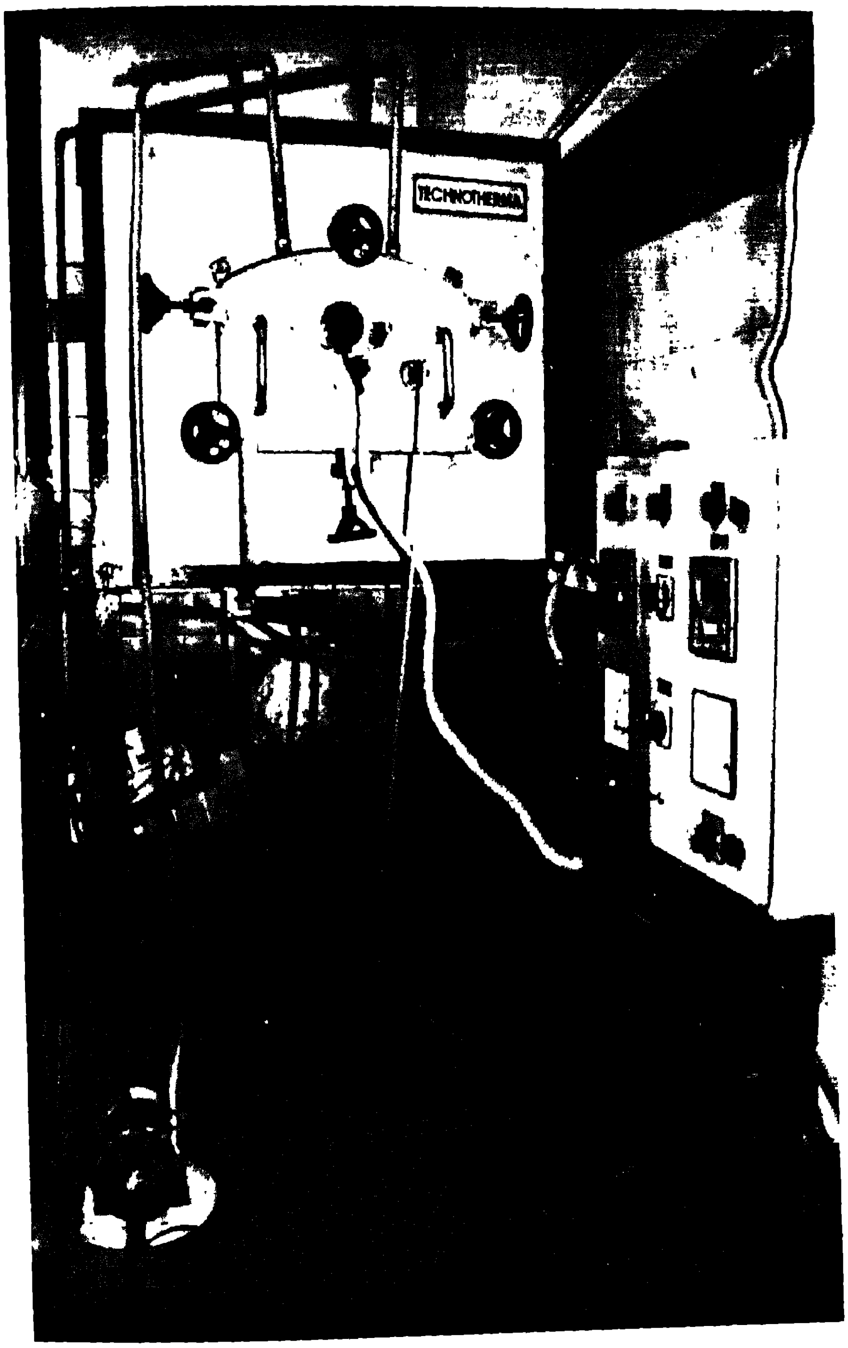


Figure 4.12. High temperature controlled atmosphere furnace used for sintering electrodes

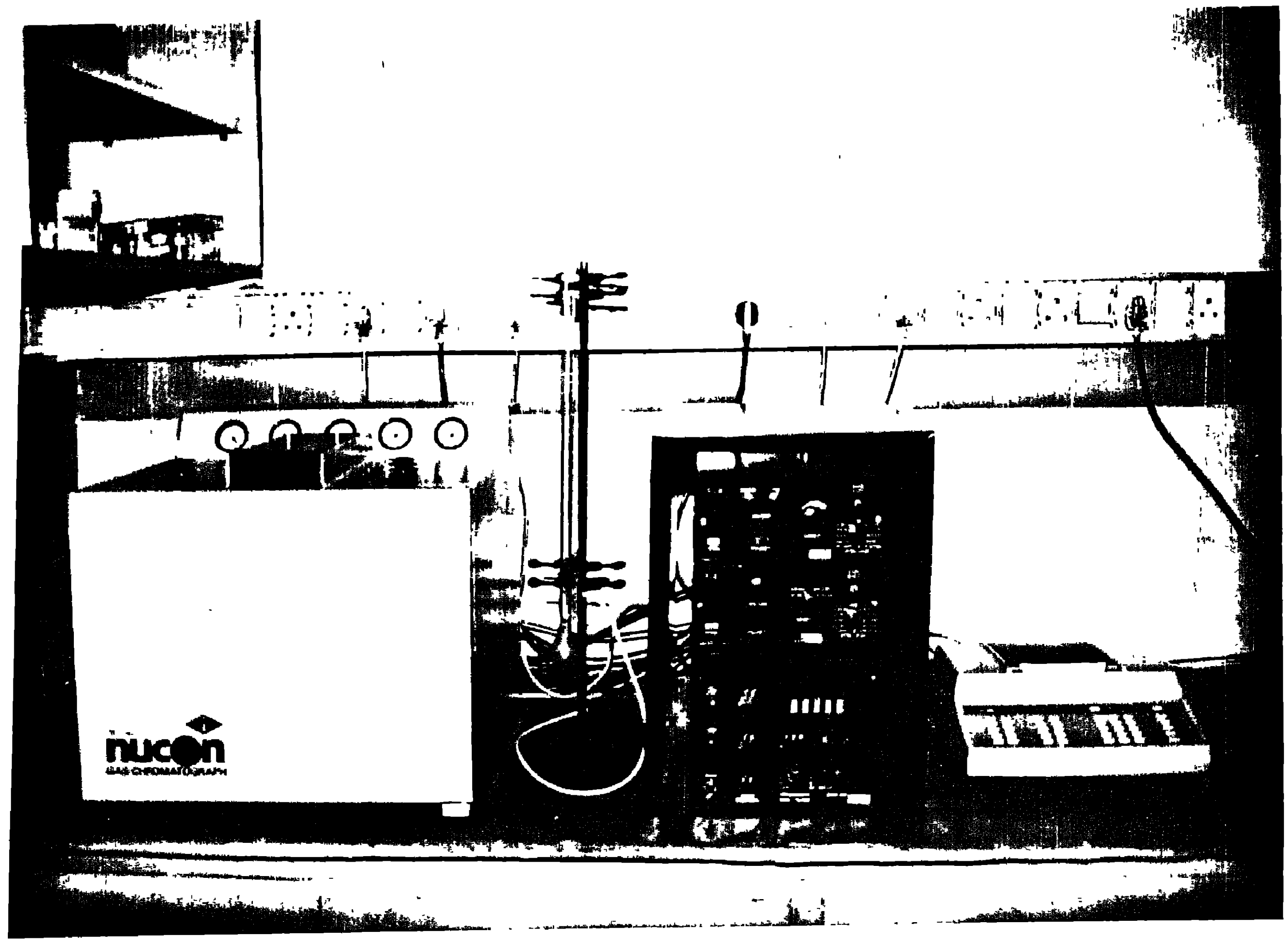


Figure 4.13. Gas chromatograph used for coal gas analysis

CHAPTER 5

Integrated coal gasification - MCFC (IGMCFC) system

As discussed elsewhere in this report, high temperature fuel cells, namely molten carbonate fuel cells (MCFC), and solid oxide fuel cells (SOFC) are well suited for integration with a coal gasifier for power generation for the following reasons :

1) Coal gas contains a significant portion of carbon monoxide. MCFC and SOFC can not only tolerate CO – which acts as a poison for the electrocatalyst in low temperature fuel cells such as the phosphoric acid fuel cell (PAFC), alkaline fuel cell (AFC) and proton exchange membrane fuel cell (PEMFC, also called 'solid polymer fuel cell'), they can use CO as a fuel in the electrochemical reaction for power generation, mainly via the water gas shift reaction, which converts CO into hydrogen..

2) The waste heat available from even MCFC is at a high enough temperature (550 °C) to raise steam for further power generation in a bottoming cycle, so that the overall efficiency of the process is increased to around 60–65%.

These have given rise to a concept which is receiving great attention worldwide, viz., the integrated (coal) gasification-molten carbonate fuel cell (IGMCFC) system. The simplest way of visualizing an IGMCFC system is by replacing the gas turbine in an integrated (coal) gasifier-combined cycle (IGCC) plant with an MCFC system. Coal gas after the cleaning stage is fed to the MCFC stack to generate electricity, and the waste heat from the MCFC stack is used to raise steam to drive a steam turbine. Where there is a need for high grade process heat (steam) the IGMCFC system can be used in the cogeneration mode straightaway.

5.1 Plant Configurations

It can be seen that a complete IGMCFC system includes three major technologies – coal gasification along with gas clean up, the MCFC subsystem and the waste heat recovery steam generator with the steam turbine bottoming cycle. As the technologies are still evolving (except, perhaps, for the last stage), different process configurations are possible. It must also be mentioned that, to date, no actual system exists incorporating all the three stages.

As discussed in Chapter 3, there are three major classes of coal gasifiers, namely fixed bed, fluidized bed and entrained bed gasifiers, which can further be operated at higher pressures or close to the atmospheric pressure. The gas from the coal gasifier can again be cleaned using a low temperature gas cleaning route or a high temperature gas cleaning system.

From the foregoing two paragraphs, it can be seen that the following process configurations are possible :
1) an IGMCFC system with a low temperature gas clean up (or the so-called wet gas cleaning) system (fig. 5.1), and
2) an IGMCFC system with a high temperature gas clean up (also called hot gas cleaning) system (fig. 5.2).

The temperature of the coal gas from the gasifier would be around 1000°C or much higher depending on the type of gasifier used, and that from the wet gas clean up stage would be less than 100°C. As the operating temperature of the MCFC stack is around 650°C, the cleaned gas has to be reheated to around 500°C in order to avoid a thermal shock or severe temperature non-uniformity between the fuel gas inlet and the outlet in the MCFC stack. Though this reheating after the wet gas clean up could be done through heat exchange with any of the high temperature gas streams, this necessitates an additional stage in the process, and an accompanying loss in the overall efficiency.

It is felt that the overall efficiency of the process can be improved by adopting a hot gas clean up route. In such a design, the temperature drop in the coal gas would be progressively lowered from the gasifier through the high temperature clean up and into the MCFC stack, as opposed to the previous route in which the coal gas from the gasifier is passed through a quench vessel and scrubbers, and again reheated before feeding into the stack. It should be noted that this is true even of gas turbine systems, where use of hot gas cleaning improves the combustion efficiency, and thereby the overall efficiency.

However, hot gas cleaning techniques are still under development. Based on our discussions with coal gasification experts in this country, it appears that the rather stringent purity levels of the fuel gas required for the MCFC would be very difficult to obtain using high temperature cleaning. Therefore, till such time that such cleaning systems are developed and are available at costs comparable to those of wet gas cleaning systems, the latter option would have to be followed in early demonstration projects in the country.

If the gasifier is operated at high pressures and the MCFC stacks at lower pressures, then the pressure of the coal gas from the high temperature gas cleaning section has to be lowered. This can be done in an expander (turbine), generating additional power.

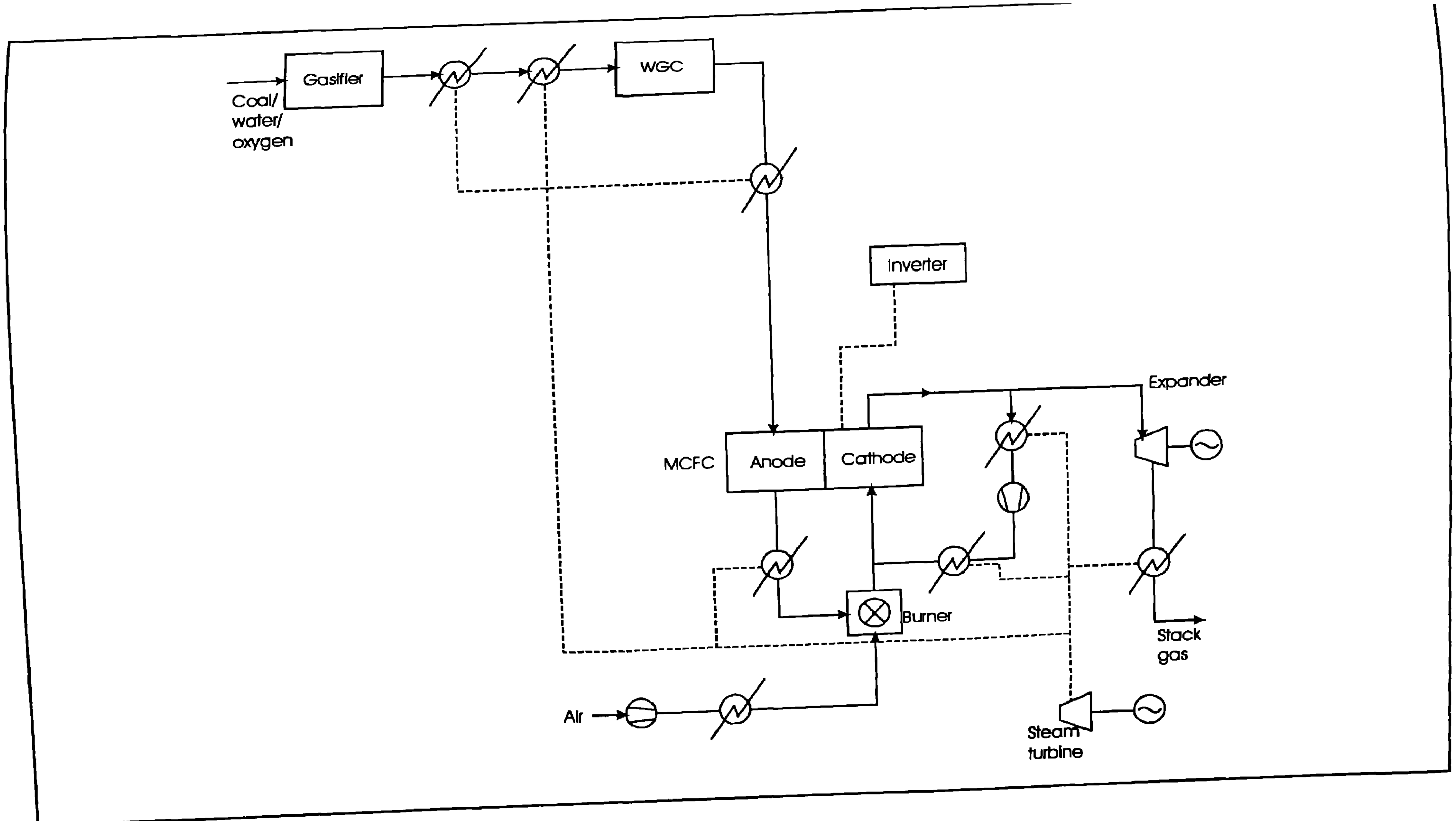


Figure 5.1. IGMCFC with wet gas cleanup

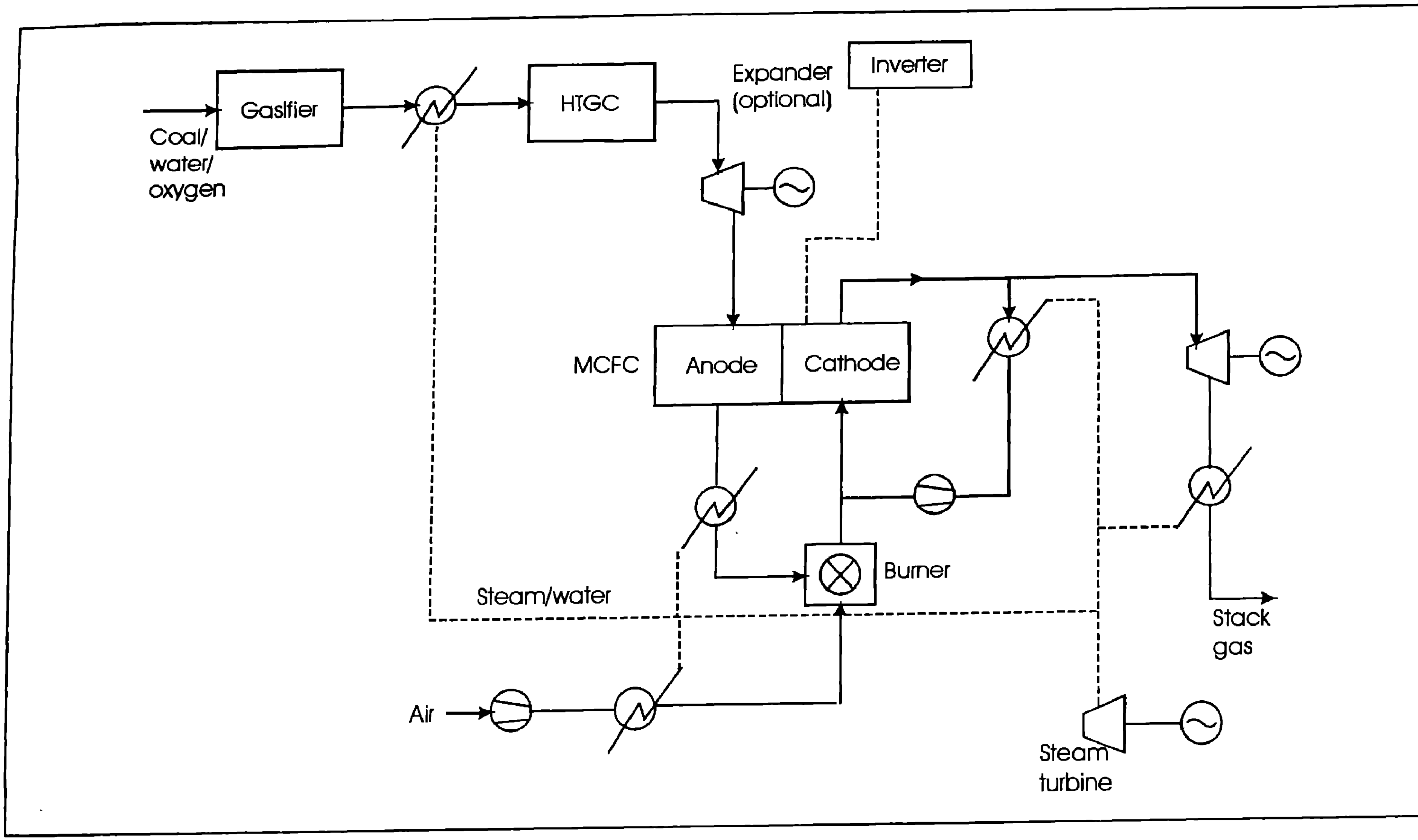


Figure 5.2. IGMCFC with hot gas cleanup

5.2 Modeling of an MCFC System

In order to understand the performance of an MCFC system with coal gas derived from Indian coals, a mathematical model was developed. The major subsystems of this model are (1) a coal gasifier (including the gas clean up system, lumped together), (2) an MCFC stack, and (3) a waste heat recovery system.

The major reactions involved in coal gasification and the corresponding heat required (+) or evolved (-) are:

							ΔH (kJ/mol)	
C	+	H_2O	⇌	H_2	+	CO	+118.5	(1)
CO	+	H_2O	⇌	H_2	+	CO_2	-42.3	(2)
CO	+	$3H_2$	⇌	CH_4	+	H_2O	-206	(3)

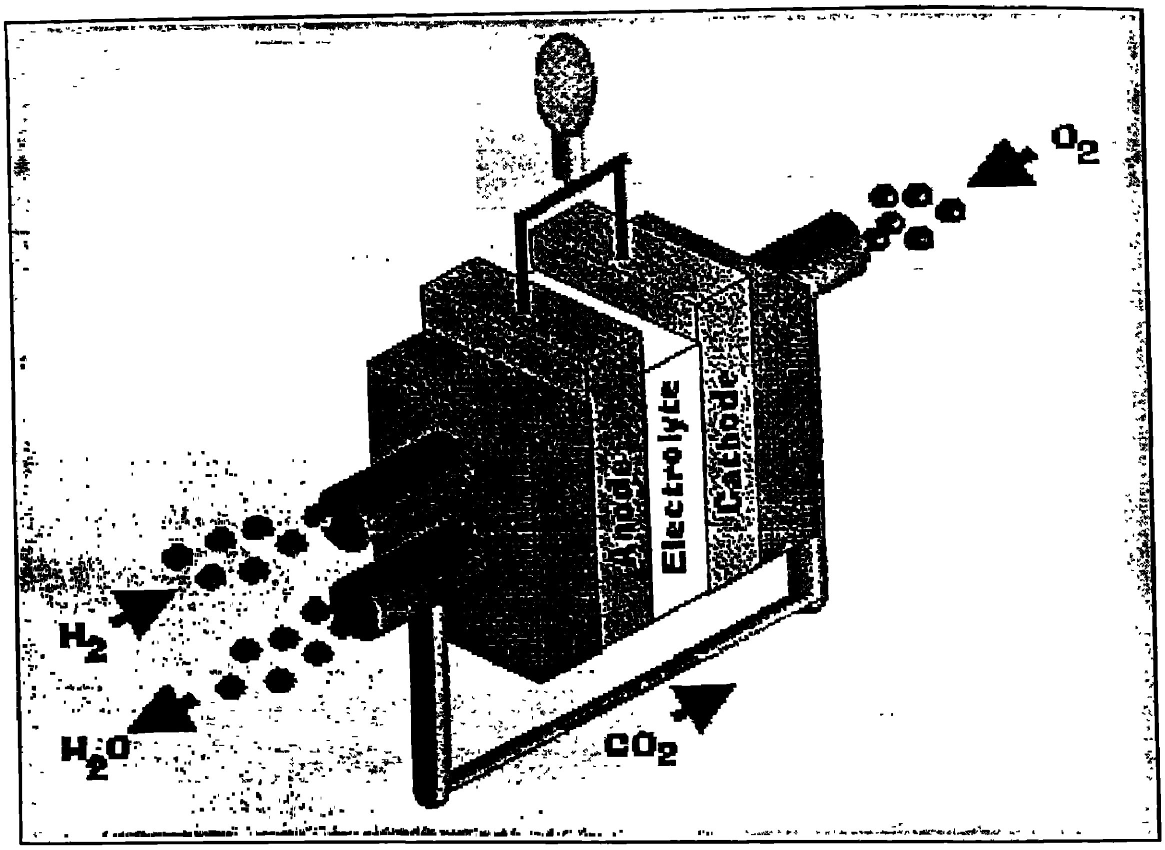
For the sake of simplicity, and since the exact reaction mechanism is extremely difficult to model without extensive test data, only reactions (1) and (2) are retained as representative of the coal gasification stage. Performance data regarding the gas composition and coal consumption from BHEL's process equipment design unit (PEDU) unit at Hyderabad were used, in order to model the gas output from a gasifier using Indian coal.

The fuel cell system is modeled with the following elements : the anode reaction, the cathode reaction (fig. 5.3) and the waste heat output stage. The anode reaction, in turn, consists of the electrode reaction, where hydrogen is consumed producing water and carbon dioxide (eqn. 4), and the water gas shift reaction (same as eqn. 2), through which carbon monoxide is converted to hydrogen, which, in turn, is consumed in the anode reaction.

$$H_2 + CO_3^{2-} \rightarrow H_2O + CO_2 + 2e^- \qquad (4)$$

The water gas shift reaction is limited by equilibrium which fixes the concentration levels of the individual gas species, more importantly the ratios of the partial pressures of the gases at any given temperature. At the MCFC operating temperature of around 650°C, the equilibrium relation is as shown in equation 5.

$$K_{shift} = \frac{p_{H_2}\, p_{CO_2}}{p_{H_2O}\, p_{CO}} \qquad (5)$$



MCFC reactions

Anode: $H_2 + CO_3^{2-} \rightarrow H_2O + CO_2 + 2e^-$

Cathode: $CO_2 + ½ O_2 + 2e^- \rightarrow CO_3^{2-}$

Figure 5.3. MCFC Reactions

The equilibrium constant K_{shift} can be obtained from an equation of the form

$$\ln(K_{shift}) = a + \frac{b}{T} + \frac{c}{T^2} + \frac{d}{T^3} \qquad (6)$$

At the MCFC operating temperature of 650°C, K_{shift} is around 2 .

The carbon dioxide needed for the cathode reaction, in a practical MCFC system, has to be supplied by separating and recycling CO_2 from the anode exhaust stream. This model assumes such a recycling loop, and since this does not affect the overall material balance,

does not represent the CO_2 loop explicitly.

At this stage, it becomes necessary to define two parameters which directly affect the fuel cell performance, viz., *utilization* and *current density*. At the anode, normally, all the fuel gas (hydrogen + carbon monoxide) is not consumed in the anode reaction. Similarly, at the cathode, all the oxidant gas (carbon dioxide + oxygen) is not utilized. In fact, the flow rates of the anode and cathode gas streams in practical fuel cell systems are so maintained that considerable portions of fuel and oxidant gases exit unconverted.

Utilization of the fuel gas, or *fuel utilization* (u_f), is defined as the fraction of the fuel gas (or of the main reactant in the fuel gas) that reacts electrochemically in the fuel gas. If hydrogen is the only reactant present in the fuel gas,

$$u_f = \frac{N_{H_2,inlet} - N_{H_2,outlet}}{N_{H_2,inlet}} \qquad (7)$$

where $N_{H2,inlet}$ and $N_{H2,outlet}$ are the flow rates of hydrogen into and out of the fuel cell, per unit cross-sectional area of the electrode. If, in addition to hydrogen, CO is also present, the fuel utilization is defined as

$$u_f = \frac{(N_{H_2,inlet} + N_{CO,inlet}) - (N_{H_2,outlet} + N_{CO,outlet})}{(N_{H_2,outlet} + N_{CO,outlet})} \qquad (8)$$

Current density is defined as the current output per unit electrode area, expressed as amperes/cm^2. Drawing more current from the fuel cell stack would increase the current density, which in turn would increase the rate of all the fuel cell reactions – (1) the release of electrons by the carbonate ions at the anode (which also consumes hydrogen) (2) the formation of carbonate ions at the cathode and (3) the water gas shift reaction (eqn.2).

5.2.1 *Relative rates of the various reactions*

An important factor to be noted here is that all the four reactions mentioned above do not take place at the same rate. The slowest reaction, therefore, becomes what is termed as the *rate limiting step*. The water gas shift reaction under the MCFC operating temperatures and in the presence of nickel is very rapid, and can be assumed to be almost instantaneous. Similarly, the electrochemical oxidation of hydrogen into water (on the electrocatalyst – nickel – surface) is also quite fast, compared to the other two reactions involving the carbonate ion

formation and dissociation. Out of these, the cathode reaction to form the carbonate ion is the slowest, and therefore limits the overall rate, and hence, the performance of the fuel cell. Any improvement in the cathode performance, therefore, has an immediate effect on the fuel cell efficiency.

For a given current density and a given flow length for the gases through the gas supply channels in the electrodes, utilization depends on the gas flow rates – it can be seen that increasing the gas flow rate would result in more unconverted fuel (hydrogen) and oxidant ($O_2 + CO_2$) leaving the anode and the cathode, respectively, thus resulting in reduced utilization.

5.2.2 Cell Voltage

The theoretical maximum voltage from a single cell for a given electrochemical reaction is determined by the change in the Gibbs free energy of the reaction at the cell operating temperature. Thus, for the electrochemical oxidation of hydrogen, which is the essence of the fuel cell reaction at 650°C

$$H_2 + \frac{1}{2} O_2 \rightarrow H_2O \qquad (9)$$

the standard cell potential (E^0) is 1.282 V.

The reversible cell potential, which is the voltage measured across the cell under 'no-load' conditions, also called the open circuit voltage (OCV), depends on the gas compositions at the anode and the cathode, and is given by the Nernst equation :

$$V = E^0 + \frac{RT}{nF} \ln \frac{p_{H_2} \, p_{O_2}^{1/2} \, p_{CO_{2(c)}}}{p_{H_2O} \, p_{CO_{2(a)}}} \qquad (10)$$

5.2.3 Voltage losses

When a current is drawn from the fuel cell, the cell voltage drops due to the effects of polarization. The major losses in the cell voltage occur due to what are termed as *concentration polarization* and the *cell internal resistance*. These losses have to be estimated by a combination of experimental and theoretical studies. A set of empirical equations used to estimate the polarization losses are given below:

$$Z_{an} = 2.27 \times 10^{-5} (p_{H_2})^{-0.42} (p_{CO_2})^{-0.17} (p_{H_2O})^{-1.0} \exp\left(\frac{53{,}500}{RT}\right) \qquad (11)$$

$$Z_{ca} = e^{-11.8}(p_{O_2})^{-0.43}(p_{CO_2})^{-0.09}\exp\left(\frac{77,300}{RT}\right) \qquad (12)$$

where Z_{an} and Z_{ca} are respectively the anode and cathode polarizations, expressed in ohms/cm². Similarly, for the cell internal resistance, a value of 0.8Ω/cm² is assumed.

Using the above, the cell voltage under a load (current) is given by

$$V_i = V - iRS_0 - i(Z_{an} + Z_{ca})S_0\,, \qquad (13)$$

where i is the current density, R is the cell internal resistance and S_0 is the cross-sectional area. The power output of the fuel cell is the product of the cell voltage and the current.

5.2.4 Formulation of the model

It can be seen from the preceding discussion that the gas utilization, current density, cell voltage, and the power output are inter-related. Useful information can be derived even from a relatively simple model as that described above by selecting the independent variables and by studying their effect on the cell output, or more importantly, the fuel cell efficiency. The independent variables were identified as follows :

1) By fixing the composition of the fuel that is fed to the anode, it is possible to determine the open circuit voltage. Since the composition of the fuel gas (such as coal gas or reformed natural gas) would depend on the particular fuel processor, it is simpler to treat this as an independent variable. However, it should be noted that in an integrated fuel processor (say, coal gasifier)-fuel cell (MCFC) system, the flow rate of fuel gas (i.e., the output from the fuel processor), would have to be such as to supply adequate hydrogen to the anode reaction, so as to sustain the desired current density (and, in turn, the power output).

2) Depending on the overall process configuration, it is possible to operate the fuel cell system at various utilization levels by varying the flow rates of the anode and cathode inlet gas streams. The fuel utilization, therefore, would be treated as an independent variable. Alternatively, the current density could also be treated as an independent variable.

5.2.5 Execution of the model

The various reactions, as well as the constraints such as the water gas shift equilibrium and the mass balance equations were entered into a spreadsheet (Microsoft Excel). The

spreadsheet software also has a built-in 'Optimizer' that can solve simultaneous equations by using one of the standard numerical methods, such as the Newton method or the conjugate method.

Equilibrium conditions at the fuel cell are sought to be simulated by choosing very small 'step sizes' for the fuel cell reactions. This is explained as follows:
If a fuel utilization factor of 80% is chosen as an independent variable, it means that the output gas composition from the anode must satisfy the equations (8) and (2). Since the water gas shift reaction is faster than the anode reaction, the inlet fuel gas composition is allowed to stabilize first, according to the equilibrium relation. Then a small step of, say, 2% fuel utilization is allowed to proceed, which would result in the consumption of hydrogen, and in the formation of water and CO_2. This would then drive the water gas shift reaction slightly to the 'right', thus consuming CO in the process. The resulting composition then becomes the 'new' anode gas composition, from where the anode reaction would proceed into the next 'step' of 2% utilization, again consuming hydrogen and producing water and CO_2. The cumulative utilization now is 4%. Following another shifting of the water gas equilibrium, the reaction proceeds, until a fuel utilization of 80% is reached.
Note: The 'step size' is arbitrarily chosen, so as to carry out the computations in a reasonable time, and yet result in output compositions that correspond with experimental observations, within a reasonable margin of difference.

5.2.6 *Efficiency*

There are several ways of defining the efficiency of a fuel cell. However, as this study is concerned with the use of coal gas in an MCFC system, the more common definition of efficiency, viz., the electrical power output for a given amount of coal gas would be calculated. This is a simplified form of efficiency calculation, based only on the calorific value of the coal gas and the V-I product of the fuel cell. The efficiency of the coal gasifier is ignored. Other important factors ignored are (1) the waste heat utilization, and (2) the bottoming cycle efficiency involving a steam generation system and a steam turbine. All of these parameters are to be incorporated in a subsequent study.
The efficiency on the basis of the heat of combusiton of the fuel is defined as

$$\eta_{HHV} = \frac{-n\ u_f\ F\ V_i}{\Delta H_{298}} \qquad (14)$$

where n is the number of electrons taking part in the basic electrochemical reaction (=2, for MCFC), u_f is the fuel utilization, F is the Faraday constant (=96490 coulombs/equivalent, or 23.06 kcal/volt), and V_i is the cell voltage under a current load, as defined by equation (13),

and ΔH_{298} is the higher heating (calorific) value of the fuel. It may be noticed that the numerator in eqn.(14) contains an electrical energy term – n and u are dimensionless, and the product of F and V_t is in kilocalories – so that this efficiency term is essentially defined as (electrical output)/(heat input), as is done in conventional power generation systems.

5.2.7 Estimation of material requirements

Typical performance data from BHEL's PEDU system is shown in table 5.1. Assuming that the same gas composition is fed to the fuel cell anode, and assuming a current density of 100mA/cm², and a fuel utilization of 80%, the cell voltage V_t is estimated using the model as 0.43V. From equation (14), this corresponds to an electrical efficiency of 45.2%, using the heating value of coal gas as 813.6 kcal/Nm³ (converted to kcal/mole).

In order to generate, say, 10 kW (= 8612 kcal/h) of power, therefore, the requirement of coal gas would be (8612/813.6)/0.452 = 23.4 Nm³/h. The specific dry gas yield is 2.4 Nm³/kg of coal, which means that the coal requirement would be of the order of 10kg/h.
For gasification, the air requirement is shown in table 5.1 as 2.36 kg/kg of coal, and the corresponding steam requirement as 0.1kg/kg of air. Using these values, the coal requirement for an MCFC stack of 10-kW size, operating at full load would be 23.4/2.4 ≈10kg/h, and the corresponding steam requirement would be about 2.4 kg/h.

The algorithm used in the model is shown on fig. 5.4.

In order to estimate the energy requirements, a number of parameters, apart from the efficiencies of the fuel cell stack and the gasifier have to be known. Some of the important parameters are listed below:
1) the choice, as well as the efficiency of the gas clean up system used,
2) waste heat recovery from the MCFC stack, from both the sensible heat of the exhaust gases, as well as from the combustion of the anode exhaust gas (which contains unconverted fuel),
3) scheme employed for the separation and recycling of carbon dioxide from the anode to the cathode,
4) auxiliary power requirement for the blowers, compressors, pumps, etc.,
5) efficiency of the the boiler for steam generation for gasification, and,
6) if a steam turbine is employed in a bottoming cycle, the efficiencies of such a system including the accessories.
Such a detailed modeling activity is to be undertaken in the next stage, as part of the proposed IGMCFC demonstration project, in collaboration with BHEL's Coal Research group.

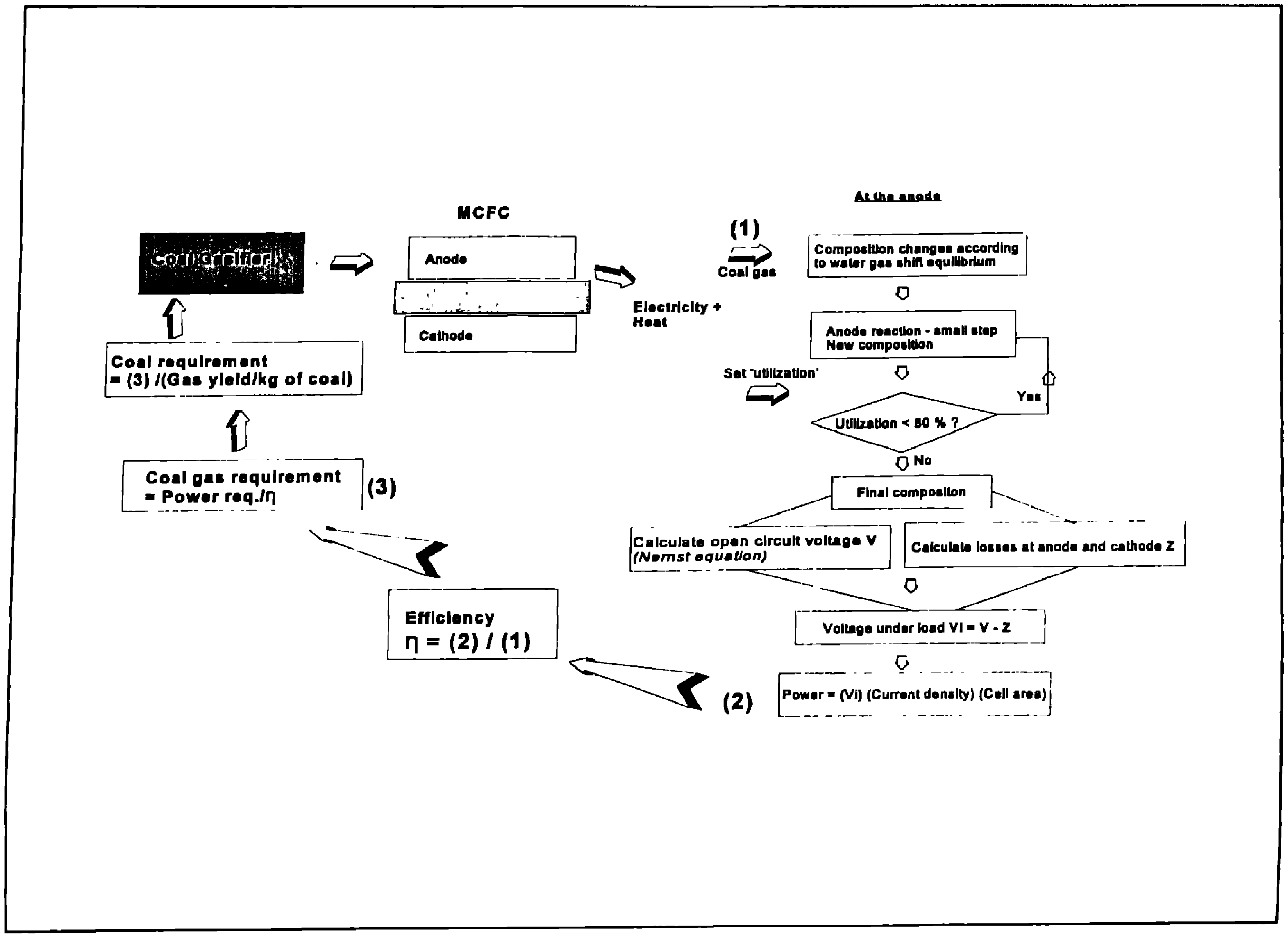


Figure 5.4. Algorithm used in the model

Table 5.1 Sample performance data from BHEL's Process Equipment Design Unit (PEDU)

S.No.		Coal type			
1.	Date of Operation	14/15-11-91	2/7-12-91	11/12-12-91	22-01-92
2.	Coal Type	Singareni	Singareni/NK	NK	NK
3.	Coal Feed Size (mm)	1 - 4	1 - 4	0 -6	0 - 6
4.	Coal Throughput (TPD)	5.64	5.20	9.75	13.08
5.	Steam/Air (kg/kg)	0.10	0.11	0.10	0.10
6.	Air/Coal (kg/kg)	2.36	1.97	1.91	1.97
7.	Operating Pressure (kg/cm² [a])	2.43	2.40	4.00	6.00
8.	Operating Velocity (m/s)	1.61	1.28	1.20	1.16
9.	Bed Temperature (°C)	950/970	890/960	890/960	890/960
10.	Unburnt Carbon in Ash (%/wt)	5.99	5.90	7.95	8.00
11.	Unburnt carbon in Cyclone (%/wt)	16.00	27.00	27.00	25.00
12.	Carbon Conversion (%/wt)	82.60	66.20	65.86	70.61
13.	Cold Gas Efficiency (%)	53.30	41.80	44.90	45.50
14.	Specific Dry Gas Yield (Nm^3/kg Coal)	2.40	1.96	1.87	1.97
15.	Steam Decomposition (%)	49.91	42.30	44.85	43.78
Gas Composition (Vol.%) Dry Basis					
CO_2		13.40	14.00	12.40	13.50
CO		11.20	10.20	12.05	12.10
H_2		12.80	12.87	13.11	12.58
CH_4		0.90	0.87	1.02	1.05
N_2		61.50	62.06	61.41	60.77
O_2		0.20	-	-	-
HCV (kcal/Nm^3)		813.60	782.70	859.20	848.40

NK : North Karanpura
Note: The data is taken from trials conducted during 1991–92. Current performance could be better.

CHAPTER 6

CONCLUSIONS

MCFC technology

(1) MCFC technology appears to be nearing commercialization within the next five years or so. By commercialization, it is meant that fully field-tested systems would be produced at a rate of up to a 100 MW total capacity initially, which would then increase gradually. ERC's 2-MW plant at Santa Clara and MC-Power's 250-kW system at Brea, both in California, USA, are still termed as demonstration plants. It can be said that the operational experience from these plants would decide the pace of future commercialization of MCFC technology.

(2) The development of solid oxide fuel cells (SOFC) and eventual commercialization is expected to lag behind those of MCFC, until certain materials problems associated with the very high temperatures (about 1000 °C) are overcome, or until newer electrolyte materials are discovered which would have ionic conductivity at substantially lower temperatures. It therefore appears logical to proceed with further development and demonstration of coal-based MCFC systems in the country.

(3) Another aspect of continued technology development and demonstration is that when the MCFC technology is sufficiently developed elsewhere, and if available at prices that are affordable, the presence of an existing research and technology background in this field would enable the Indian industry to absorb the imported technology.

Coal gasification

(4) Gasification of coal is an integral part of an IGMCFC system. It appears that in order to effectively use high ash Indian coal, the technology being developed indigenously would form a crucial role. The fuel cell group at TERI therefore plans to work with the Coal Research Group of BHEL to demonstrate the concept of IGMCFC, and to understand the associated engineering problems.

(5) As the coal gasification technology has to be more or less developed within the country because of the nature of Indian coals, any experience in the integration of MCFC systems with a coal gasifier would be invaluable in future projects involving larger, imported MCFC systems.

Gas cleaning

(6) The coal gas exiting the gasifier has to be cleaned in order to remove impurities such as particulates, tar, sulphur, etc. While this is standard practice even in IGCC systems, as

discussed elsewhere, the impurity tolerance limits of MCFC systems are more stringent, and therefore, more work needs to be done on this front in the country. One option is to import such technology during the early stages.

(7) Though system assessment studies done at ECN, Netherlands show that use of a high temperature gas clean up arrangement would increase the overall efficiency of an IGMCFC system, the capability of existing sulphur removal systems to meet MCFC's requirements is not clear, and therefore early demonstration systems of IGMCFC are more likely to use low temperature gas cleaning, with a small penalty in efficiency.

Use of coal gas in MCFC

(8) As evident from our lab-scale, sub-optimal MCFC, use of coal gas as a fuel in MCFC does look promising. The drop in performance while using simulated coal gas, as compared to that while using pure hydrogen as the fuel is nominal.

MCFC work at TERI – follow-up work after this project

(9) The fuel cell group at TERI, based on the experience from this project, has identified major areas where immediate improvement in the MCFC single cell performance can be obtained – these include (1) preparation of better electrolyte matrix, (2) improved gas distribution to the electrodes, (3) minimizing electrical contact resistances in the current collection circuit, apart from continuous improvement in all the aspects.

(10) The group has recently started work on development of a kilowatt-level MCFC stack, in collaboration with the Central Electrochemical Research Institute (CECRI), Karaikudi. Under this project, the main focus of TERI would be in the stack engineering, i.e. fabrication of the bipolar separator plates and other aspects involved in the assembly of the stack components, viz. edge sealing, current collection, heat management, etc. In addition, the selection of better materials to withstand the corrosive environment would also be undertaken.

(11) A major initiative planned is planned to demonstrate the concept of integrated coal gasification-MCFC system, in collaboration with the Coal Research Group of the Bharat Heavy Electricals Limited (BHEL) at Hyderabad. It is proposed to set up a 5–10 kW size MCFC stack, coupled to an experimental coal gasifier at BHEL's Maula Ali site, and this project is expected to provide valuable experience and insight into the actual operation of an IGMCFC system, and in understanding the engineering problems associated with this concept. Among other things, special gas clean up equipment would have to be developed or procured, so as to meet MCFC's tolerance limits.

(12) A very important aspect to be studied is the long-term performance of an MCFC stack that is using coal gas as a fuel. This is possible only by actually coupling an MCFC stack with a coal gasifier, and operating it for a few thousand hours, or by carrying out accelerated testing.

(13) The group also plans to actively explore the possibilities of using gas separation membranes so as to improve the overall efficiency. Two areas that have been identified for the potential application of membrane systems are (1) separation of carbon dioxide from the anode exhaust for recycling to the cathode side, and (2) partial or near-total removal of nitrogen from the following stages – (a) at the air inlet stream to the coal gasifier, so as to feed an oxygen-enriched air for gasification, (b) at the exit of coal gas from the wet gas cleaning section, before feeding to the MCFC stack, and (c) at the cathode inlet stage, again to feed an oxygen-enriched air stream.